

Determinants of Axonal Growth and their Role in the Injured Adult Nervous System

Dissertation

zur

Erlangung der naturwissenschaftlichen Doktorwürde
(Dr. sc. nat.)

vorgelegt der

Mathematisch-naturwissenschaftlichen Fakultät

der

Universität Zürich

von

Stefan Blöchliger

von Goldingen SG

Promotionskomitee

Prof. Dr. Peter Sonderegger (Vorsitz)
Prof. Dr. Martin E. Schwab (Leitung der Dissertation)

Zürich 2005

Table of Contents

Summary	6
Zusammenfassung	8
Chapter 1: Introduction	11
Spinal cord injury – where are we at?	13
Experimental Approaches to Enhance Functional Recovery after Spinal Cord Injury	16
Regulation of Axonal Regeneration and Structural Plasticity by the Myelin-associated inhibitors	18
The Neuron's Intrinsic Growth Capacity and Response to Axotomy	21
Aim of the Present Work	24
References	26
Chapter 2: It Takes More than Two to Nogo	37
References	40
Chapter 3: Neuronal Plasticity and Formation of New Synaptic Contacts Follow Pyramidal Lesions and Neutralization of Nogo-A: A Light and Electron Microscopic Study in the Pontine Nuclei of Adult Rats	42
Abstract	43
Materials and Methods	44
Results	46
Discussion	48
References	52

Chapter 4: Growth and regeneration associated differential gene expression during development and after axonal injury to the peripheral and central nervous system	55
Introduction	56
Methods	58
Results	62
Discussion	78
References	83
 Chapter 5: Dynamic changes in glypican-1 expression in dorsal root ganglion neurons after peripheral and central axonal injury	 91
Abstract	92
Introduction	92
Materials and Methods	93
Results	94
Discussion	99
References	104
 Chapter 6: Axonal injury-dependent induction of the peripheral benzodiazepine receptor in small-diameter adult rat primary sensory neurons	 107
Abstract	108
Introduction	108
Materials and Methods	109
Results	111
Discussion	117
References	118
 Chapter 7: Conclusion and Outlook	 122
References	128
 Curriculum Vitae	 131
 List of Publications	 133
 Acknowledgements	 135

Summary

The clinical consequences of adult central nervous system injuries are extremely severe since there is only a minor capability for functional compensation and an almost complete absence of cell renewal and axonal re-growth and re-connection. The understanding of the developing and adult nervous system is progressing rapidly. In the past decades the growing comprehension has been continuously extended onto neuropathological conditions. We know now that the lack of recovery following injuries of the central nervous system is partly due to environmental, most importantly myelin-associated inhibitory factors, and partly to the inability of injured neurons to mount a gene expression profile that allows axonal growth.

In this thesis determinants of axonal growth are examined and discussed. A way to partially overcome myelin-derived growth inhibition, is to prevent Nogo-A from binding to neuronal receptors by applying monoclonal antibody IN-1. To further investigate the effect of IN-1, rats with unilaterally injured cortical spinal tract were treated with IN-1. This approach was previously shown to enhance structural plasticity and functional recovery in the treated rats. Using light- and electron-microscopy, we show for the first time that outgrowing nerve fibers can form new, ultrastructurally intact synaptic contacts in the adult nervous system following an identical model as described above.

The intracellular mechanisms that enable neurons to grow axons are poorly understood. Microarray analysis offers a way to screen for transcriptional adaptations following axonal injury. We investigate gene expression in lumbar dorsal root ganglia of the adult rat following central or peripheral nerve injury and compare the results with the developmental gene expression in the same population of neurons. Peripheral and central axotomy induce clearly distinguishable cell body responses. For both injury paradigms the expression for more than 50 genes is regulated. The comparison to developmental stages, when axonal outgrowth occurs, reveals that a complete recapitulation of a developmental gene expression pattern is not necessary for the regeneration of peripheral nerves.

We further investigate injury-induced transcriptional and post-transcriptional changes, exemplified by two genes, glypican-1 and the peripheral benzodiazepine receptor (PBR). Our results show that the cell body response to injury is not restricted to changes in transcription

and translation, but also involves post-translational effects, such as protein localization and transport. For glypican-1 the presented results support functions in axonal growth and guidance, e.g. by involvement in slit-robo interactions. We provide a first detailed description of the expression of slit and robo family members in the adult injured and non-injured dorsal root ganglion. Using different histological techniques we show for the first time the induction of the PBR specifically in small-diameter dorsal root ganglion neurons after nerve injury. Ligand binding studies indicate the presence of correctly assembled PBR following injury.

In summary, the results reported in this study show evidence that neurons in the adult nervous system retain capacities for structural reorganization and re-connection following injury if faced with a permissive environment. We characterize the transcriptional cell body response of neurons to injury, an important determinant of the neuronal growth capacity. Additionally, we show that the cell body response is not simply regulated at the level of transcription but is specified by post-transcriptional mechanisms.

Zusammenfassung

Verletzungen des adulten zentralen Nervensystems ziehen schwerwiegende klinische Konsequenzen nach sich, da die Möglichkeiten zur funktionellen Kompensation minimal sind. Auch spontane Zellerneuerung, regeneratives axonales Wachstum und Wiederherstellung von synaptischen Kontakten werden kaum je festgestellt. Das Wissen über das sich entwickelnde und über das adulte Nervensystem wächst rasch, und während der letzten Jahrzehnte hat sich unser Verständnis von Neuropathologie gewandelt. Wir wissen nun, dass die fehlende funktionelle Erholung nach Verletzungen des Zentralnervensystems teilweise von Molekülen abhängt, welche die Nervenzellen umgeben. Dabei sind vor allem die Myelin- assoziierten, inhibierenden Moleküle zu erwähnen. Ausserdem fehlt verletzten Neuronen die Fähigkeit, ein Genexpressionsmuster zu aktivieren, das ihnen erlaubt, Axone zum Wachstum zu veranlassen.

In dieser Dissertation werden bestimmende Faktoren des axonalen Wachstums untersucht und besprochen. Eine Möglichkeit, die mit dem Myelin zusammenhängende Wachstumshemmung teilweise zu überwinden, ist, die Bindung eines inhibitorischen Myelinbestandteils, Nogo-A, an seine neuronalen Rezeptoren zu blockieren, indem ein monoklonaler Antikörper, IN-1, verabreicht wird. Um die Effekte von IN-1 detailliert zu untersuchen, benutzen wir ein Tiermodell bei welchem wir Ratten den Kortikospinaltrakt einseitig durchtrennen. Wie früher gezeigt wurde, verstärken sich dabei strukturelle Plastizität und funktionelle Erholung. Wir zeigen zum ersten Mal auf der elektronenmikroskopischen Ebene, dass neu auswachsende Nervenfasern im verletzten adulten Zentralnervensystem fähig sind, histologisch intakte Synapsen zu bilden. Die intrazellulären Mechanismen, die es Neuronen erlauben, Axone auswachsen zu lassen, werden nach wie vor schlecht verstanden. Wir versuchen hier anhand von Gen-Chip-Analysen einen weiten Überblick über die Anpassung der Transkription nach axonalen Verletzungen zu gewinnen. Wir untersuchen die Genexpression von lumbalen dorsalen Ganglienzellen der adulten Ratte nach Verletzung der peripheren und auch der zentralen Nervenfasern. Die so gewonnenen Resultate vergleichen wir mit der Genexpression derselben Neuronenpopulation während der Embryonalentwicklung. Die periphere und die zentrale Axotomie lösen klar unterscheidbare Antworten im Zellkörper aus. Für beide Verletzungsmuster gilt, dass die Expression von mehr als 50 Genen reguliert wird. Im Vergleich mit der Embryonalentwicklung stellen wir fest, dass für die Regeneration von

peripheren Nerven keine vollständige Rekapitulation des embryonalen Expressionsmusters nötig ist.

Wir untersuchen auch die durch eine Verletzung ausgelösten Änderungen der Gen- und Protein-Expression genauer, dies anhand von zwei Genen, Glypican-1 und dem peripheren Benzodiazepin-Rezeptor (PBR). Unsere Resultate zeigen, dass sich die Antwort des Zellsomas auf Verletzungen nicht nur auf der Ebene der Transkription und Translation zeigt, sondern vielmehr auch in der Lokalisierung und im Transport der Proteine. Im Falle von Glypican-1 legen unsere Resultate nahe, dass dem Protein im Rahmen des axonalen Wachstums und der Richtungszuweisung von auswachsenden Neuriten, zum Beispiel durch die Beeinflussung von Slit-Robo-Interaktionen, eine Rolle zukommt. Wir liefern eine erste detaillierte Beschreibung der Expression der Mitglieder der Slit- und Robo-Familien in verletzten und unverletzten adulten dorsalen Ganglienzellen. Ebenso zeigen wir mit verschiedenen histologischen Techniken zum ersten Mal die Induktion von PBR nach einer Axotomie in dorsalen Ganglien, und zwar spezifisch in kleinkalibrigen Neuronen. Wir demonstrieren das Vorhandensein des intakten PBR mit Hilfe von Liganden-Bindungsversuchen.

Zusammengefasst zeigen die in dieser Dissertation präsentierten Resultate, dass in Neuronen des adulten verletzten Nervensystems die Fähigkeit zur strukturellen Reorganisation und zum Aufbau von synaptischen Verbindungen erhalten bleibt, wenn ihre Umgebung es erlaubt. Wir beschreiben die Genexpression im Zellkörper, welche eine bestimmende Grösse der neuronalen Wachstumskapazität ist, nach neuronalen Verletzungen. Ausserdem zeigen wir, dass diese Antwort nicht auf die Transkription beschränkt bleibt, sondern auch post-transkriptionelle Mechanismen beinhaltet.

Chapter 1

Introduction

The adult mammalian central nervous system (CNS) is known for its inability to spontaneously repair large structural damages in a functionally meaningful way. Therefore extensive injuries to the adult CNS, e.g. spinal cord injury or stroke as well as many degenerative neurological diseases, e.g. Parkinson's disease, Alzheimer's disease or multiple sclerosis, often permanently disable normal functioning of the CNS and may cause maladaptive responses evoking additional severe symptoms.

In marked contrast to the adult CNS, the embryonic and early postnatal developing CNS of higher vertebrates can compensate for structural damage to a high degree, a feature already recognized by Ramón y Cajal in 1928. Neurons of the peripheral nervous system (PNS) retain their regenerative potential throughout development and adulthood.

While the CNS was looked at as a rigid and stable interconnection of neurons during the first half of the last century, it has become more and more clear that the system's plasticity is surprisingly high in terms of normal physiological processing but also in response to pathological conditions including partial, smaller scale injuries. These changes can occur at different levels along the neuraxis, e.g. in the hippocampal formation or in the dorsal horn of the spinal cord. Different domains of a neuron, such as the dendrites, axons or synapses can be altered and the result may be reflected in histological, electrophysiological or behavioral changes. Utilizing the system's intrinsic plastic potential has become an indispensable tool for clinical rehabilitation.

Regardless of local plasticity, the CNS has to ensure that its overall structure and the basic connectivity underlying adequate physiological processing are maintained during the lifetime of an individual. Therefore, cooperative mechanisms are needed to ensure the CNS's stability on the one hand, and to regulate local neuronal plasticity on the other hand, in order to balance the system. Structural alterations of the nervous system by mechanical impact, ischemia or degeneration seem to favor processes that try to preserve the integrity of the spared system rather than allowing extensive adaptations to occur.

Replacing cells that are lost through disease or injury, enhancing the plasticity of the CNS and its compensatory capacity following injury, as well as axonal regeneration, are major goals of today's basic research.

This introduction gives a brief overview about spinal cord injury in humans and about some aspects of its current treatment and rehabilitation. After that, current attempts to promote regeneration and functional recovery in animal models are described. The following section focuses on axonal regeneration and neuronal plasticity in terms of its control by one major myelin-associated growth inhibitor, Nogo-A. Finally, the present understanding of the neuronal response to axotomy is summarized.

Spinal cord injury – where are we at?

At the beginning of the twenty-first century spinal cord injury and injuries to the CNS in general still have devastating consequences for the individual suffering from it. There is no cure, but the knowledge about underlying molecular and cellular processes is growing tremendously fast, giving hope that ways of treating patients can be developed. Current experimental approaches that may lay the basis for effective clinical treatments are discussed in the following section of this chapter.

During the last 20 years the incidence of traumatic spinal cord injuries in industrialized countries (10 - 30 cases per 10⁶ inhabitants and year) has hardly changed (Sett and Crockard, 1991). Between 1997 and 1999, 126 patients suffering from spinal cord injury were treated at the Duke of Cornwall Spinal Treatment Centre, Salisbury District Hospital. 45% of the injuries were due to road traffic accidents, 34% were due to domestic and industrial accidents, 15% to injuries at sports and 6% were caused by self harm and criminal assault. 45% of the patients were hospitalized with cervical injuries, 40% with injuries of the thoracic spinal cord and in 15% the lumbar portion was affected (Grundy and Swain, 2002). In Switzerland the numbers may differ slightly because of a higher incidence of injuries at sports mostly due to skiing accidents. From 123 patients with acute traumatic spinal cord injury treated at the Spinal Cord Injury Centre, University Hospital Balgrist, Zürich, 70% were men and 30% women. Whereas the proportion of accidents between sexes was almost equal for road traffic accidents and injuries at sports, males accounted for 90% of accidents at work whereas women caused 80% of the incidents of self harm. In general more than 50% of the patients are between 16 and 30 years old (Dietz, 2001). The overall mortality after spinal cord trauma was around 13% within the first 7 years following the injury between 1973 and 1980 (DeVivo et al., 1987). Since then life expectancy has increased substantially accompanied by a

significantly better quality of life (Wahle, 1990; DeVivo and Richards, 1992; DeVivo et al., 1999).

For the early clinical assessment and for measuring the clinical outcome of sensory and motor deficits following spinal cord injury the ASIA (American Spinal Injury Association)-scale is internationally accepted, widely used and allows determination of the level of the lesion (Ditunno, 1994; Maynard et al., 1997). In addition, the documentation of functional impairments using the walking index for spinal cord injury (WISCI) and the spinal cord independence measure (SCIM), is crucial to assess remaining nerve functions, to control rehabilitative and therapeutic approaches and to estimate the quality of life of the patient (Ditunno et al., 2000; Itzkovich et al., 2002). A standardized assessment and evaluation protocol for monitoring the extent and characteristics of recovery after spinal cord injury, including clinical tests as well as neurophysiological and neuroradiological techniques, is currently being established and evaluated by five European spinal cord injury centers with the goal to provide a basis for testing and control of new therapeutic interventions (Curt et al., 2004).

The management of spinally injured patients following treatment of immediately life-threatening associated injuries and surgical stabilization of the vertebral column aims at I) the protection from secondary cytotoxic tissue damage, II) preventing complications arising from autonomously controlled organs, from the blood, the skin, joints and limbs, and III) rehabilitation and training of preserved functions and reflexes. In Europe, commonly applied clinical treatments include the infusion of methylprednisolone (within 3 hours after injury: 30mg/kg within 15min i.v. followed by 5.4mg/kg/hour for 23 hours; if commenced 3-8 hours after injury: initial bolus and infusion for 47 hours). Methylprednisolone is a potent anti-inflammatory glucocorticoid with inhibitory effects on lipid peroxidation lowering the production of free radicals following injury (Hall, 1992; Hall et al., 1992). Methylprednisolone was tested in controlled and randomized clinical trials (National Acute Spinal Cord Injury Studies, NASCIS I,II & III) where small but significant neurological improvements were described in patients with complete as well as incomplete spinal cord injury (Bracken et al., 1984; Bracken and Holford, 1993; Bracken et al., 1997). The way methylprednisolone acts, is still very controversial. In animal models no positive effect on secondary cell death of high-dose methylprednisolone treatment after SCI could be found, but a clear reduction in the number of neutrophils and macrophages invading the lesion site was

observed (Bartholdi and Schwab, 1995). The effects of methylprednisolone may also depend on the status of the subject's inflammatory system prior to the injury (L. Schnell, M. Gullo & M.E. Schwab, unpublished data). So far no other drug has been proven clinically helpful in preventing secondary damage following SCI.

Patients with high cervical injuries may need respiratory support. Generally, a central venous catheter is used for several days to supply the body with fluids, electrolytes and human albumin depending on the measured central venous pressure. Whenever the heart rate falls below 50 beats/min, atropine (0.25-0.5mg, s.c., every 8 hours) is used to block parasympathetic suppression of the heart. Anticoagulation should be started within 72 hours after the injury using low molecular weight heparin if there are no medical or surgical contraindications (0.2-0.6ml Fraxiparin® s.c. 1x/day). Due to the risk of acute peptic ulceration proton pump inhibitors or H₂-receptor antagonists are administered starting at the 4th day following the injury. Pain is controlled using morphine analogues, e.g. fentanyl, and in case of missing motility of the bowels neostigmin is a potential drug that can be used. The initial bladder management includes a suprapubic catheter avoiding over-distension of the organ. The patient should be turned every 2 to 3 hours between supine and right and left lateral positions to prevent pressure sores. Daily, joints need to be passively moved to prevent stiffness and contractures. All these early treatment strategies together have strongly improved the outlook for people with SCI. Surgical and medical treatment strategies are discussed in more detail elsewhere (Dietz, 2001; Grundy and Swain, 2002).

In recent years it has become clear that the spinal cord contains capabilities for use-dependent plasticity following injuries. Mostly based on findings in lower vertebrates, rodents, cats and primates, a concept for local spinal circuits controlling locomotion has arisen (for reviews see (Harkema, 2001; Fouad and Pearson, 2004)). Adaptive plasticity in the human spinal cord after spinal cord injury is evident and weight-supported locomotion training on a treadmill has become a promising tool to enhance functional recovery of walking in patients with incomplete injuries. The method consists of partial body-weight support and manual assistance of leg movements providing patterned afferent feedback to the spinal cord. Typically training is carried out for months with gradually reduced weight support and diminished assistance to initiate the swing phase and for stepping. Initial comprehensive studies testing the efficacy of assisted locomotor training revealed sustained stepping movements in acute and chronic clinically incomplete injured patients. The beneficial effects

could be maintained for months or years after completion of training and in cases where self-sustained walking was achieved, no specific training is needed to retain the improvements in everyday life (Wernig et al., 1995; Wernig et al., 1998; Wirz et al., 2001). In contrast to patients with incomplete spinal cord injury, training of patients with complete spinal cord injury did not lead to sustained stepping movements of the legs, possibly because of the total absence of supraspinal input. Treadmill training of patients with complete spinal cord injuries is able though to temporarily alter EMG patterns, i.e. restoring the alternating flexor – extensor and right leg – left leg activation, along with a reduction of spasticity (Dietz et al., 1995). Very recently a robotic device assisting and controlling stepping on a treadmill, named the Lokomat® , was developed (Colombo et al., 2001). It allows better control and reproducibility of assisted leg movements and reduces the number of therapists needed and the physical strain on therapists during the training procedure. Combination of treadmill training with either pharmacological treatment or electrical stimulation has produced first encouraging results but has not yet led to routinely used therapeutic protocols.

Experimental Approaches to Enhance Functional Recovery after Spinal Cord Injury

Based on transplantation experiments showing cortical axons of a rabbit growing into a peripheral nerve transplant, Ramón y Cajal suggested that trophic and tropic factors might be present in substrates permissive for axonal growth. Based on this assumption the lack of supportive factors in the adult CNS was hypothesized (Tello, 1911; Cajal, 1928). Many years later the importance of peripheral nerves as a permissive substrate for axons to regenerate could be demonstrated (Richardson et al., 1980; David and Aguayo, 1981; Schwab and Thoenen, 1985). The use of substrates allowing axonal growth, as peripheral nerve grafts, olfactory ensheathing glial cells, Schwann cells, stem cells and fetal tissue, became one experimental approach to bridge the injured area in the spinal cord of rodents (Paino and Bunge, 1991; Cheng et al., 1996; Xu et al., 1997; Ramon-Cueto et al., 2000; Coumans et al., 2001; Li et al., 2003). Many but not all of these bridging paradigms resulted in enhanced recovery of locomotion (Takami et al., 2002). The use of a polymer scaffold seeded with stem cells was shown to improve open field locomotion (Teng et al., 2002). This experiment combined pure grafting approaches with the idea of providing a microenvironment that actively supports neurite outgrowth and cell survival by trophic signals.

Administration of neurotrophic factors, namely brain-derived neurotrophic factor (BDNF) and neurotrophin-3 (NT-3), was tested successfully in a variety of spinal cord injury models. Neurotrophic factors were delivered via mini-osmotic pumps, a tool that can also be used in human patients, or by transplanting genetically modified cells or more recently viral vectors (Kobayashi et al., 1997; Zhou et al., 2003). Depending on the experimental model, treatment with neurotrophic factors resulted in enhanced sprouting and regeneration of descending motor tracts, partial functional recovery or decreased cell death of axotomized neurons (Schnell et al., 1994; Grill et al., 1997; Shibayama et al., 1998).

Earlier this year two research groups succeeded in reducing secondary apoptotic cell death following spinal cord injury and in promoting locomotor recovery by pharmacologically blocking P2X7 purine receptors or by neutralizing the pro-apoptotic CD95 ligand by applying CD95 ligand specific antibodies (Demjen et al., 2004; Wang et al., 2004).

Many extracellular matrix constituents influence axonal outgrowth, either in a supportive or repressive way. Following spinal cord injury the environment at the site of injury changes profoundly, leading among other changes to elevated expression of chondroitin sulphate proteoglycans (CSPGs), that can effectively inhibit axonal re-growth into the site of injury, and to the build-up of the glial scar (for reviews see (Rhodes and Fawcett, 2004; Silver and Miller, 2004)). Breaking down the glycosaminoglycan side chains of CSPGs by injections of chondroitinase ABC was demonstrated to enhance regeneration of descending motor as well as ascending sensory fiber tracts and to result in some improvement of locomotor and proprioceptive behavior (Bradbury et al., 2002). The inhibition of intracellular PKC- γ enabled dorsal root ganglion (DRG) neurons to partially overcome CSPG- and myelin-induced inhibition in the dorsal columns following spinal cord injury (Sivasankaran et al., 2004).

Another promising approach originated in findings from culture experiments where it was shown that in the presence of optimal concentrations of NGF, axons of PNS neurons heavily grew into explants derived from the sciatic nerve but not into optic nerve explants (Schwab and Thoenen, 1985), leading to the assumption that specific neurite growth inhibitors must be associated with CNS tissues. Following experiments localized the inhibitory action to mature, differentiated oligodendrocytes in the CNS, consistent with results that showed strong inhibition of axon outgrowth on CNS white matter (Schwab and Caroni, 1988). By partial purification and biochemical characterization of rat myelin two protein fractions with

inhibitory action were isolated with molecular weights of 35 and 250 kDa, subsequently called NI-35 and NI-250 (Caroni and Schwab, 1988b). Later the same components were found in CNS material from many other mammals including humans. In 2000 the full length cDNA of rat NI-250 and the human homologue were cloned and named Nogo-A (Spillmann et al., 1997; Spillmann et al., 1998; Chen et al., 2000; GrandPre et al., 2000; Prinjha et al., 2000). Disinhibition of axonal growth by interfering with the action of Nogo-A in the CNS offers possibilities to learn about CNS plasticity, regeneration and development. The major findings involving Nogo-A are further discussed in the next section and in chapter 2.

Regulation of Axonal Regeneration and Structural Plasticity by Myelin-associated inhibitors

Kennard reported the ability of monkeys with cortical lesions at early postnatal stages to develop motor skills, whereas adult monkeys with similar cortical lesions suffered from a permanent loss of motor function. Therefore, the *Kennard Principle*, states that functional recovery critically depends on the age of the animal subjected to an injury (Kennard, 1936, 1938; Teuber, 1974).

Pioneering work on the corticobulbar and corticospinal tract of the hamster provided an anatomical correlate for the observation that functional recovery and compensation were more pronounced the younger the animal. Unilateral injury of the corticospinal tract (CST) at the level of the medulla oblongata (pyramidotomy) in the adult hamster led to nerve fiber degeneration and retraction rostrally and caudally from the site of lesion with no axonal re-growth. In the infant hamster though, if the same operation was performed, severed axons re-grew via a new pathway to their appropriate target sites in the medulla oblongata and spinal cord (Kalil and Reh, 1979). A more detailed study of re-growing CST axons revealed that re-growing axons did not make their way through the site of the lesion but crossed to the contralateral brainstem rostrally from it, that they formed a compact bundle of fibers and grew caudally for 6-7mm. Although following an aberrant trajectory, the pattern of termination in the dorsal column nuclei and the dorsal horn of the cervical spinal cord seemed normal. Synapse formation by re-growing axons was confirmed by electron microscopy. The speed of axonal growth was determined to be around 1mm/day, which is somewhat slower than during normal development of the CST (2-4mm/day). This response was most pronounced at 4-8

days of age whereas no fiber growth was observed if the lesion was performed twenty or more days postnatally (Kalil and Reh, 1982). A few years later it could be shown that unilateral pyramidotomy in immature hamsters not only evoked a growth response in injured CST axons but also in the contralateral intact CST. At local spinal levels, but not in the brainstem, collaterals of the uninjured CST sprouted into the denervated side in a topographically meaningful way such that axons originating in the somatosensory cortex connected to dorsal horn neurons whereas those of the motor cortex terminated primarily in the ventral horn. For compensatory axonal growth of the uninjured CST and for axonal re-growth to occur, similar permissive time frames were found (Kuang and Kalil, 1990a, b).

The developmental stage of the CNS therefore controls the capacity of axonal growth in response to injury, a feature strongly correlated with the progressive myelination of developing fiber tracts. The closure of the time window for axonal growth can be delayed by X-irradiation of the developing spinal cord, abolishing myelin formation and oligodendrocyte maturation, a procedure that allowed long-distance re-growth of injured CST axons and compensatory sprouting of intact CST neurite following partial spinal cord injury and pyramidotomy respectively in the rat (Savio and Schwab, 1990; Vanek et al., 1998).

Since the description of NI-35 and NI-250, several additional constituents of myelin apart from Nogo-A have been found with inhibitory effects on axonal outgrowth, namely myelin-associated glycoprotein (MAG) and oligodendrocyte-myelin glycoprotein (OMgp), semaphorin 4D, ephrin B3, netrin-1 and the proteoglycans V2 and brevican (McKerracher et al., 1994; Wang et al., 2002). Interestingly, Nogo-A, MAG and OMgp partially share receptors and intracellular signaling pathways, including a very recently identified co-receptor, LINGO-1 (Mi et al., 2004). The issue of receptors and downstream signaling components is further discussed in chapter 2.

A monoclonal IgM antibody, mAb IN-1, was raised, recognizing rat NI-250, later cloned as Nogo-A (Caroni and Schwab, 1988a). mAb IN-1 proved to be a powerful tool in overcoming myelin-derived inhibition in the central nervous system. The application of mAb IN-1, by implanting hybridoma cells that produce the antibody into the lateral ventricle of the brain following dorsal hemisection of the spinal cord, allowed massive sprouting of injured CST fibers rostral to the lesion and more importantly long distance regenerative axonal growth up to 11mm beyond the site of injury, an observation that was never observed in control rats

(Schnell and Schwab, 1990). In the following years locomotor recovery following partial SCI and treatment with mAb IN-1 was reported from various experiments (Bregman et al., 1995; Merkler et al., 2001). Currently the effect of a new generation of monoclonal IgG antibodies recognizing a specific sequence of Nogo-A is under investigation. The influence of new anti-Nogo-A antibodies roughly mimicks the effects observed with IN-1, even though the new antibodies are applied intrathecally by mini-osmotic pumps (unpublished results, L. Schnell, T. Liebscher & M.E. Schwab).

Apart from inducing long-distance axonal regeneration, the action of mAb IN-1 substantially enhanced structural plasticity in the adult CNS of the rat contributing to partial recovery of fine motor movements following unilateral pyramidotomy, a finding similar to the results obtained from experiments in immature hamsters discussed in preceding sections. The injured CST established bilateral projections at different levels of the brainstem, including the red nucleus, basilar pontine and the dorsal column nuclei and showed enhanced regenerative sprouting (Raineteau et al., 1999). Additionally, sprouting of the non-injured CST to the denervated side in the spinal cord was observed, resembling structural plasticity found in the immature rat CNS (Thallmair et al., 1998; Z'Graggen et al., 1998; Z'Graggen et al., 2000). Subsequent experiments showed that the action of mAb IN-1 was not restricted to the CST, rather other descending motor systems as the rubrospinal tract participated in reorganizing the injured motor system (Raineteau et al., 2001). Compensatory sprouting and re-organization can therefore be enhanced by counteracting Nogo-A, an intervention that is followed by improved functional recovery. Spontaneous structural re-organization can occur in the cortico-proprio-spinal systems following spinal cord injury. These alterations likely account for some of the spontaneous recovery of function seen in injured animals (Bareyre et al., 2004).

The discovery of receptors and downstream signalling components for myelin-associated growth inhibitors offers possibilities to interfere with the inhibitors' effects at sites different from the epitope recognized by mAb IN-1 (see chapter 2). The identification of Nogo-66, one of three domains inhibitory for neurite outgrowth, and its receptor NgR, led to the development of a peptide, NEP1-40, that competitively antagonized Nogo-66 binding to NgR and that was demonstrated to improve functional recovery following spinal cord injury in rats (GrandPre et al., 2000; Fournier et al., 2001; GrandPre et al., 2002; Li and Strittmatter, 2003;

Oertle et al., 2003). Pharmacological interference with Rho-kinase, a downstream effector of NgR produced similar results (Dergham et al., 2002; Fournier et al., 2003).

Surprisingly, constitutive Nogo-A knock-out mice showed different regenerative responses to spinal cord injury, depending on the strategy used to get rid of Nogo-A, Nogo-A/-B or Nogo-A/-B and -C. One research group found some regenerative axonal growth in a selective Nogo-A knock-out mouse line that showed compensatory up-regulation of Nogo-B (Simonen et al., 2003). Another group reported massive regeneration in a Nogo-A/-B knock-out approach, whereas a third group didn't observe any regenerative reaction in Nogo-A/-B or Nogo-A/-B/-C knock-out mice (Kim et al., 2003; Zheng et al., 2003). Further characterization, analyses and inducible knock-out systems may provide better insight into the specific role of the Nogo proteins. As with the Nogo knock-out animals, the gross anatomy of the brain seemed normal in NgR knock-out mice, in which a reactive over-expression of Nogo-A was found. Behaviorally this knock-out mouse displayed hypoactivity and motor impairments. Following spinal cord injury CST axons did not regenerate, an unexpected result comparable though to results obtained from MAG-deficient mice, whereas raphe- and rubrospinal tract partially regenerated and helped functional recovery (Bartsch et al., 1995; Kim et al., 2004).

The Neuron's Intrinsic Growth Capacity and Response to Axotomy

During the development of the nervous system a series of events need to occur in a precisely defined temporal and spatial frame. Neurons and glial cells are generated from multipotent precursors. Cells move to their final location within the CNS by radial and tangential migration. These processes are paralleled and followed by axonal outgrowth and guidance leading to target selection and synapse formation. Neurons that actively grow neurites during development are characterized by the specific array of proteins they express which allows them to elongate (Fawcett, 1992). Classically these proteins comprise cytoskeletal proteins such as actins, neurofilaments, tubulins and microtubule-associated proteins, the proteins encoded by certain immediate early genes, and the prototypical growth associated protein GAP-43 which is strongly expressed in neurons along the growing axon as well as in the growth cone. Neuronal GAP-43 expression decreases when connections with target cells are established during maturation of the corticospinal tract and in dorsal root ganglion (DRG) neurons (Fitzgerald et al., 1991; Karimi-Abdolrezaee et al., 2002). GAP-43 expression

therefore correlates with the intrinsic capacity of neurons to extend axons during development. Constitutive GAP-43 knock-out mice reveal pathfinding defects whereas the neurite growth rate seems normal (Strittmatter et al., 1995). When maturation of the nervous system is complete, GAP-43 expression is very low, but can still be detected in specific areas of the CNS known for their plastic potential such as the olfactory bulb, the hippocampal formation and the superficial laminae of the dorsal horn (Kapfhammer and Schwab, 1994).

Cutting the sciatic nerve in the adult rat leads to major changes in gene expression with hundreds of genes being up- or down-regulated. Microarray analysis is a powerful tool to detect changes in mRNA expression in the DRG following sciatic nerve transection (Costigan et al., 2002; Xiao et al., 2002). Overall cellular changes after axotomy are called the *cell body response* to injury (Lieberman, 1971). This cell body response allows DRG neurons to re-grow their peripheral axons and to re-innervate target structures following axotomy of their peripheral branch. In contrast to injury to the peripheral branch, the cell body reaction is much more moderate after injury to the central branch as in the case of dorsal rhizotomy or spinal cord injury. For example, the regeneration associated protein GAP-43 is not induced following dorsal rhizotomy whereas it is re-expressed at high levels following peripheral axotomy in DRG neurons (Woolf et al., 1990; Chong et al., 1992; Chong et al., 1994). This observation fits well with the fact that central processes of DRG neurons are not regenerating through the dorsal root entry zone into the spinal cord, putting GAP-43 forth as a marker for cells in a growing state. Transgenic over-expression of GAP-43 induces spontaneous sprouting along the axon of axotomized Purkinje cells and co-over-expression of GAP-43 and CAP-23, another major growth-associated protein, strongly increases axonal regeneration in spinal cord injured mice (Buffo et al., 1997; Bomze et al., 2001).

The discrepancy of the cell body response between centrally or peripherally injured DRG neurons led to the hypothesis that only peripheral injury leads to a full blown cell body response, enabling the neuron to regain regenerative axonal growth. On the other hand, the neuron displays an abortive reaction to injury of its central branch and fails to induce a growth program. Previously, peripherally injured DRG neurons were rendered capable to regenerate their central axon into a peripheral nerve graft in the spinal cord (Richardson and Issa, 1984). In addition, sciatic nerve transection one week prior to a partial dorsal spinal cord injury enabled injured proprioceptive neurites to regenerate across the site of injury in the spinal cord (Neumann and Woolf, 1999). Peripheral axotomy alone can induce sprouting of the

central branch of injured DRG neurons in the dorsal horn of the spinal cord (Woolf et al., 1992). The extent of the cell body response of long projection neurons depends critically on how far away from the cell body the injury occurs whereas the probability that a neuron dies following axotomy is inversely related to the distance between the site of injury and the cell body, as specified for retinal ganglion cells (Richardson et al., 1984; Aguayo et al., 1991; Berkelaar et al., 1994).

The factors responsible to elicit the cell body response are not well defined. The family of neurotrophic factors, including NGF, BDNF, NT-3 and NT-4 in higher vertebrates and their receptors, trkA, trkB, trkC, p75, and the more recently identified co-receptor sortilin, likely play a key role in inducing and maintaining the cell body response by retrograde transport (for review see (Verge et al., 1996); (Schwab, 1977; Nykjaer et al., 2004)). Nerve growth factor (NGF), glial-derived neurotrophic factor (GDNF) and NT-3 promoted axonal re-growth and synaptic reconnection of specific subpopulations of dorsal root ganglion neurons following dorsal rhizotomy (Ramer et al., 2000).

Some immediate early genes are rapidly induced following axotomy and as inducible transcription factors, c-jun, JunB, JunD and c-fos may serve as initial regulators of axonal re-growth. In severed DRG neurons for example, c-jun is only up-regulated following peripheral nerve injury but not following dorsal rhizotomy. If the injured central branch of DRG neurons is provided with a growth permissive environment that some axonal regeneration can occur, c-Jun expression is concomitantly induced in those neurons (Broude et al., 1997). When provided with a growth permissive graft, neuronal subpopulations, e.g. neurons of the inferior olive, neurons giving rise to mossy fibers and neurons in the deep cerebellar nuclei, were enabled to elongate their axons into the graft, in clear contrast to Purkinje cell axons (Dooley and Aguayo, 1982; Rossi et al., 1995; Buffo et al., 1997). c-Jun, JunD and GAP-43 were up-regulated in all classes of neurons showing axonal growth, whereas their expression failed to be induced in most of the injured Purkinje cells, controlled by retrogradely transported signals along the axon that can be inhibited by the application of mAb IN-1 (Zagrebelsky et al., 1998). The application of mAb IN-1 was able to induce c-Jun and JunD expression in injured Purkinje cells and enabled sprouting of uninjured Purkinje cell axons (Buffo et al., 2000). Over-expression of GAP-43 selectively in Purkinje cells can partially override myelin-derived inhibition of neuronal growth (Gianola and Rossi, 2004).

These results show evidence that the cell response following injury is regulated both by inhibitory, myelin-associated signals as well as inductive signals, e.g. neurotrophic factors. The expression of some transcription factors and of GAP-43 can correlate with the ability for axonal growth, and their regulation depends on the neuronal subpopulation, the developmental stage and the location within the nervous system.

Aim of the present work

Myelin-associated inhibitors are mediators of complex signals regulating axonal growth (Chapter 2). Their importance becomes apparent relatively late in CNS development, when myelination of projecting nerve fiber tracts is established. They play a role in terminating the growth-permissive period in early postnatal life during which higher vertebrates can more successfully compensate following injuries to the CNS than adults. The presence of myelin-associated inhibitors in the adult partially explains the lack of regenerative axonal growth and restricted compensatory adaptations. In the laboratory of M.E. Schwab, antibodies blocking some of the inhibitory activity of Nogo-A were raised and their application led to promising results enhancing axonal regeneration and locomotor recovery after partial SCI. In a model of unilateral CST lesions, the influence of Nogo-A on structural plasticity and compensatory sprouting was examined in great detail. M.E. Schwab and colleagues succeeded in inducing structural adaptations and improved voluntary fine movements in adult rats by applying antibodies recognizing Nogo-A. On the histological level, fibers of the injured CST established bilateral projections at the level of the red nucleus, the basilar pontine nuclei and the dorsal column nuclei. The uninjured CST in turn sent sprouts to the denervated side of the spinal cord. We want to study whether sprouting CST fibers are actually able to build new synaptic contacts following unilateral CST lesions and treatment with anti-Nogo-A antibody by carefully analyzing new projections in the basilar pons of adult rats (Chapter 3). Anti-Nogo-A antibody injections into the cerebellum can induce spontaneous sprouting of Purkinje cells, an effect that is paralleled by changes in gene expression in the targeted neurons (Buffo et al., 2000). Similar results were obtained by applying IN-1 to intact adult rats where the antibodies led to increased numbers of aberrant projections from the CST in parallel with increased expression of growth-associated genes, e.g. GAP-43, and transcription factors (Bareyre et al., 2002). Therefore, Nogo-A likely participates in regulating the cell body response following axotomy in CNS neurons. Except for the regulation of a few genes, e.g.

GAP-43 and c-jun, the cell body response to axotomy is not well understood. We aim to compare cell body responses of DRG neurons following axotomy of the peripheral versus the central branch in more detail. These injury-induced changes are then compared to the developmental gene expression pattern in DRG neurons, in order to investigate whether a recapitulation of developmental gene expression profiles is necessary for successful regeneration or structural reorganization in the spinal cord, as it is seen following peripheral axotomy (Chapter 4). Furthermore, we want to identify differentially expressed genes in the adult DRG in response to different types of axonal injury, including neuropathic pain models. The regulation of a protein's activity can happen during transcriptional, translational or post-translational steps. In addition to changes in gene transcription levels we aim to detect post-transcriptional regulation and pharmacological interactions of selected injury-regulated genes (Chapter 5 and 6).

References

- Aguayo AJ, Rasminsky M, Bray GM, Carbonetto S, McKerracher L, Villegas-Perez MP, Vidal-Sanz M, Carter DA (1991) Degenerative and regenerative responses of injured neurons in the central nervous system of adult mammals. *Philos Trans R Soc Lond B Biol Sci* 331:337-343.
- Bareyre FM, Haudenschild B, Schwab ME (2002) Long-lasting sprouting and gene expression changes induced by the monoclonal antibody IN-1 in the adult spinal cord. *J Neurosci* 22:7097-7110.
- Bareyre FM, Kerschensteiner M, Raineteau O, Mettenleiter TC, Weinmann O, Schwab ME (2004) The injured spinal cord spontaneously forms a new intraspinal circuit in adult rats. *Nat Neurosci* 7:269-277.
- Bartholdi D, Schwab ME (1995) Methylprednisolone inhibits early inflammatory processes but not ischemic cell death after experimental spinal cord lesion in the rat. *Brain Res* 672:177-186.
- Bartsch U, Bandtlow CE, Schnell L, Bartsch S, Spillmann AA, Rubin BP, Hillenbrand R, Montag D, Schwab ME, Schachner M (1995) Lack of evidence that myelin-associated glycoprotein is a major inhibitor of axonal regeneration in the CNS. *Neuron* 15:1375-1381.
- Berkelaar M, Clarke DB, Wang YC, Bray GM, Aguayo AJ (1994) Axotomy results in delayed death and apoptosis of retinal ganglion cells in adult rats. *J Neurosci* 14:4368-4374.
- Bomze HM, Bulsara KR, Iskandar BJ, Caroni P, Skene JH (2001) Spinal axon regeneration evoked by replacing two growth cone proteins in adult neurons. *Nat Neurosci* 4:38-43.
- Bracken MB, Holford TR (1993) Effects of timing of methylprednisolone or naloxone administration on recovery of segmental and long-tract neurological function in NASCIS 2. *J Neurosurg* 79:500-507.
- Bracken MB, Collins WF, Freeman DF, Shepard MJ, Wagner FW, Silten RM, Hellenbrand KG, Ransohoff J, Hunt WE, Perot PL, Jr. (1984) Efficacy of methylprednisolone in acute spinal cord injury. *Jama* 251:45-52.
- Bracken MB, Shepard MJ, Holford TR, Leo-Summers L, Aldrich EF, Fazl M, Fehlings M, Herr DL, Hitchon PW, Marshall LF, Nockels RP, Pascale V, Perot PL, Jr., Piepmeyer J, Sonntag VK, Wagner F, Wilberger JE, Winn HR, Young W (1997) Administration of methylprednisolone for 24 or 48 hours or tirilazad mesylate for 48 hours in the

- treatment of acute spinal cord injury. Results of the Third National Acute Spinal Cord Injury Randomized Controlled Trial. National Acute Spinal Cord Injury Study. *Jama* 277:1597-1604.
- Bradbury EJ, Moon LD, Popat RJ, King VR, Bennett GS, Patel PN, Fawcett JW, McMahon SB (2002) Chondroitinase ABC promotes functional recovery after spinal cord injury. *Nature* 416:636-640.
- Bregman BS, Kunkel-Bagden E, Schnell L, Dai HN, Gao D, Schwab ME (1995) Recovery from spinal cord injury mediated by antibodies to neurite growth inhibitors. *Nature* 378:498-501.
- Broude E, McAtee M, Kelley MS, Bregman BS (1997) c-Jun expression in adult rat dorsal root ganglion neurons: differential response after central or peripheral axotomy. *Exp Neurol* 148:367-377.
- Buffo A, Zagrebelsky M, Huber AB, Skerra A, Schwab ME, Strata P, Rossi F (2000) Application of neutralizing antibodies against NI-35/250 myelin-associated neurite growth inhibitory proteins to the adult rat cerebellum induces sprouting of uninjured purkinje cell axons. *J Neurosci* 20:2275-2286.
- Buffo A, Holtmaat AJ, Savio T, Verbeek JS, Oberdick J, Oestreicher AB, Gispén WH, Verhaagen J, Rossi F, Strata P (1997) Targeted overexpression of the neurite growth-associated protein B-50/GAP-43 in cerebellar Purkinje cells induces sprouting after axotomy but not axon regeneration into growth-permissive transplants. *J Neurosci* 17:8778-8791.
- Cajal Ry (1928) Degeneration and regeneration of the nervous system, reprint 1959 Edition. New York: Hafner.
- Caroni P, Schwab ME (1988a) Antibody against myelin-associated inhibitor of neurite growth neutralizes nonpermissive substrate properties of CNS white matter. *Neuron* 1:85-96.
- Caroni P, Schwab ME (1988b) Two membrane protein fractions from rat central myelin with inhibitory properties for neurite growth and fibroblast spreading. *J Cell Biol* 106:1281-1288.
- Chen MS, Huber AB, van der Haar ME, Frank M, Schnell L, Spillmann AA, Christ F, Schwab ME (2000) Nogo-A is a myelin-associated neurite outgrowth inhibitor and an antigen for monoclonal antibody IN-1. *Nature* 403:434-439.
- Cheng H, Cao Y, Olson L (1996) Spinal cord repair in adult paraplegic rats: partial restoration of hind limb function. *Science* 273:510-513.

- Chong MS, Fitzgerald M, Winter J, Hu-Tsai M, Emson PC, Wiese U, Woolf CJ (1992) GAP-43 mRNA in Rat Spinal Cord and Dorsal Root Ganglia Neurons: Developmental Changes and Re-expression Following Peripheral Nerve Injury. *Eur J Neurosci* 4:883-895.
- Chong MS, Reynolds ML, Irwin N, Coggeshall RE, Emson PC, Benowitz LI, Woolf CJ (1994) GAP-43 expression in primary sensory neurons following central axotomy. *J Neurosci* 14:4375-4384.
- Colombo G, Wirz M, Dietz V (2001) Driven gait orthosis for improvement of locomotor training in paraplegic patients. *Spinal Cord* 39:252-255.
- Costigan M, Befort K, Karchewski L, Griffin RS, D'Urso D, Allchorne A, Sitarski J, Mannion JW, Pratt RE, Woolf CJ (2002) Replicate high-density rat genome oligonucleotide microarrays reveal hundreds of regulated genes in the dorsal root ganglion after peripheral nerve injury. *BMC Neurosci* 3:16.
- Coumans JV, Lin TT, Dai HN, MacArthur L, McAtee M, Nash C, Bregman BS (2001) Axonal regeneration and functional recovery after complete spinal cord transection in rats by delayed treatment with transplants and neurotrophins. *J Neurosci* 21:9334-9344.
- Curt A, Schwab ME, Dietz V (2004) Providing the clinical basis for new interventional therapies: refined diagnosis and assessment of recovery after spinal cord injury. *Spinal Cord* 42:1-6.
- David S, Aguayo AJ (1981) Axonal elongation into peripheral nervous system "bridges" after central nervous system injury in adult rats. *Science* 214:931-933.
- Demjen D, Klussmann S, Kleber S, Zuliani C, Stieltjes B, Metzger C, Hirt UA, Walczak H, Falk W, Essig M, Edler L, Krammer PH, Martin-Villalba A (2004) Neutralization of CD95 ligand promotes regeneration and functional recovery after spinal cord injury. *Nat Med* 10:389-395.
- Dergham P, Ellezam B, Essagian C, Avedissian H, Lubell WD, McKerracher L (2002) Rho signaling pathway targeted to promote spinal cord repair. *J Neurosci* 22:6570-6577.
- DeVivo MJ, Richards JS (1992) Community reintegration and quality of life following spinal cord injury. *Paraplegia* 30:108-112.
- DeVivo MJ, Krause JS, Lammertse DP (1999) Recent trends in mortality and causes of death among persons with spinal cord injury. *Arch Phys Med Rehabil* 80:1411-1419.
- DeVivo MJ, Kartus PL, Stover SL, Rutt RD, Fine PR (1987) Seven-year survival following spinal cord injury. *Arch Neurol* 44:872-875.

- Dietz V (2001) Klinik der Rückenmarkschädigung, 1. Auflage Edition. Stuttgart: Kohlhammer.
- Dietz V, Colombo G, Jensen L, Baumgartner L (1995) Locomotor capacity of spinal cord in paraplegic patients. *Ann Neurol* 37:574-582.
- Ditunno JF, Jr. (1994) American spinal injury standards for neurological and functional classification of spinal cord injury: past, present and future. 1992 Heiner Sell Lecture of the American Spinal Injury Association. *J Am Paraplegia Soc* 17:7-11.
- Ditunno JF, Jr., Ditunno PL, Graziani V, Scivoletto G, Bernardi M, Castellano V, Marchetti M, Barbeau H, Frankel HL, D'Andrea Greve JM, Ko HY, Marshall R, Nance P (2000) Walking index for spinal cord injury (WISCI): an international multicenter validity and reliability study. *Spinal Cord* 38:234-243.
- Dooley JM, Aguayo AJ (1982) Axonal elongation from cerebellum into peripheral nervous system grafts in the adult rat. *Ann Neurol* 12:221.
- Fawcett JW (1992) Intrinsic neuronal determinants of regeneration. *Trends Neurosci* 15:5-8.
- Fitzgerald M, Reynolds ML, Benowitz LI (1991) GAP-43 expression in the developing rat lumbar spinal cord. *Neuroscience* 41:187-199.
- Fouad K, Pearson K (2004) Restoring walking after spinal cord injury. *Prog Neurobiol* 73:107-126.
- Fournier AE, GrandPre T, Strittmatter SM (2001) Identification of a receptor mediating Nogo-66 inhibition of axonal regeneration. *Nature* 409:341-346.
- Fournier AE, Takizawa BT, Strittmatter SM (2003) Rho kinase inhibition enhances axonal regeneration in the injured CNS. *J Neurosci* 23:1416-1423.
- Gianola S, Rossi F (2004) GAP-43 overexpression in adult mouse Purkinje cells overrides myelin-derived inhibition of neurite growth. *Eur J Neurosci* 19:819-830.
- GrandPre T, Li S, Strittmatter SM (2002) Nogo-66 receptor antagonist peptide promotes axonal regeneration. *Nature* 417:547-551.
- GrandPre T, Nakamura F, Vartanian T, Strittmatter SM (2000) Identification of the Nogo inhibitor of axon regeneration as a Reticulon protein. *Nature* 403:439-444.
- Grill R, Murai K, Blesch A, Gage FH, Tuszynski MH (1997) Cellular delivery of neurotrophin-3 promotes corticospinal axonal growth and partial functional recovery after spinal cord injury. *J Neurosci* 17:5560-5572.
- Grundy D, Swain A (2002) ABC of Spinal Cord Injury, 4th edition Edition. London: BMJ Books.

- Hall ED (1992) The neuroprotective pharmacology of methylprednisolone. *J Neurosurg* 76:13-22.
- Hall ED, Braughler JM, McCall JM (1992) Antioxidant effects in brain and spinal cord injury. *J Neurotrauma* 9 Suppl 1:S165-172.
- Harkema SJ (2001) Neural plasticity after human spinal cord injury: application of locomotor training to the rehabilitation of walking. *Neuroscientist* 7:455-468.
- Itzkovich M, Tripolski M, Zeilig G, Ring H, Rosentul N, Ronen J, Spasser R, Gepstein R, Catz A (2002) Rasch analysis of the Catz-Itzkovich spinal cord independence measure. *Spinal Cord* 40:396-407.
- Kalil K, Reh T (1979) Regrowth of severed axons in the neonatal central nervous system: establishment of normal connections. *Science* 205:1158-1161.
- Kalil K, Reh T (1982) A light and electron microscopic study of regrowing pyramidal tract fibers. *J Comp Neurol* 211:265-275.
- Kapfhammer JP, Schwab ME (1994) Inverse patterns of myelination and GAP-43 expression in the adult CNS: neurite growth inhibitors as regulators of neuronal plasticity? *J Comp Neurol* 340:194-206.
- Karimi-Abdolrezaee S, Verge VM, Schreyer DJ (2002) Developmental down-regulation of GAP-43 expression and timing of target contact in rat corticospinal neurons. *Exp Neurol* 176:390-401.
- Kennard MA (1936) Age and other factors in motor recovery from precentral lesions in monkeys. *Am J Physiol* 115:138-146.
- Kennard MA (1938) Reorganization of motor function in the cerebral cortex of monkeys deprived of motor and premotor areas in infancy. *J Neurophysiol* 1:477-496.
- Kim JE, Liu BP, Park JH, Strittmatter SM (2004) Nogo-66 receptor prevents raphespinal and rubrospinal axon regeneration and limits functional recovery from spinal cord injury. *Neuron* 44:439-451.
- Kim JE, Li S, GrandPre T, Qiu D, Strittmatter SM (2003) Axon regeneration in young adult mice lacking Nogo-A/B. *Neuron* 38:187-199.
- Kobayashi NR, Fan DP, Giehl KM, Bedard AM, Wiegand SJ, Tetzlaff W (1997) BDNF and NT-4/5 prevent atrophy of rat rubrospinal neurons after cervical axotomy, stimulate GAP-43 and α -tubulin mRNA expression, and promote axonal regeneration. *J Neurosci* 17:9583-9595.
- Kuang RZ, Kalil K (1990a) Specificity of corticospinal axon arbors sprouting into denervated contralateral spinal cord. *J Comp Neurol* 302:461-472.

- Kuang RZ, Kalil K (1990b) Branching patterns of corticospinal axon arbors in the rodent. *J Comp Neurol* 292:585-598.
- Li S, Strittmatter SM (2003) Delayed systemic Nogo-66 receptor antagonist promotes recovery from spinal cord injury. *J Neurosci* 23:4219-4227.
- Li Y, Decherchi P, Raisman G (2003) Transplantation of olfactory ensheathing cells into spinal cord lesions restores breathing and climbing. *J Neurosci* 23:727-731.
- Lieberman AR (1971) The axon reaction: a review of the principal features of perikaryal responses to axon injury. *Int Rev Neurobiol* 14:49-124.
- Maynard FM, Jr., Bracken MB, Creasey G, Ditunno JF, Jr., Donovan WH, Ducker TB, Garber SL, Marino RJ, Stover SL, Tator CH, Waters RL, Wilberger JE, Young W (1997) International Standards for Neurological and Functional Classification of Spinal Cord Injury. American Spinal Injury Association. *Spinal Cord* 35:266-274.
- McKerracher L, David S, Jackson DL, Kottis V, Dunn RJ, Braun PE (1994) Identification of myelin-associated glycoprotein as a major myelin-derived inhibitor of neurite growth. *Neuron* 13:805-811.
- Merkler D, Metz GA, Raineteau O, Dietz V, Schwab ME, Fouad K (2001) Locomotor recovery in spinal cord-injured rats treated with an antibody neutralizing the myelin-associated neurite growth inhibitor Nogo-A. *J Neurosci* 21:3665-3673.
- Mi S, Lee X, Shao Z, Thill G, Ji B, Relton J, Levesque M, Allaire N, Perrin S, Sands B, Crowell T, Cate RL, McCoy JM, Pepinsky RB (2004) LINGO-1 is a component of the Nogo-66 receptor/p75 signaling complex. *Nat Neurosci* 7:221-228.
- Neumann S, Woolf CJ (1999) Regeneration of dorsal column fibers into and beyond the lesion site following adult spinal cord injury. *Neuron* 23:83-91.
- Nykjaer A, Lee R, Teng KK, Jansen P, Madsen P, Nielsen MS, Jacobsen C, Kliemann M, Schwarz E, Willnow TE, Hempstead BL, Petersen CM (2004) Sortilin is essential for proNGF-induced neuronal cell death. *Nature* 427:843-848.
- Oertle T, van der Haar ME, Bandtlow CE, Robeva A, Burfeind P, Buss A, Huber AB, Simonen M, Schnell L, Brosamle C, Kaupmann K, Vallon R, Schwab ME (2003) Nogo-A inhibits neurite outgrowth and cell spreading with three discrete regions. *J Neurosci* 23:5393-5406.
- Paino CL, Bunge MB (1991) Induction of axon growth into Schwann cell implants grafted into lesioned adult rat spinal cord. *Exp Neurol* 114:254-257.
- Prinjha R, Moore SE, Vinson M, Blake S, Morrow R, Christie G, Michalovich D, Simmons DL, Walsh FS (2000) Inhibitor of neurite outgrowth in humans. *Nature* 403:383-384.

- Raineteau O, Z'Graggen WJ, Thallmair M, Schwab ME (1999) Sprouting and regeneration after pyramidotomy and blockade of the myelin-associated neurite growth inhibitors NI 35/250 in adult rats. *Eur J Neurosci* 11:1486-1490.
- Raineteau O, Fouad K, Noth P, Thallmair M, Schwab ME (2001) Functional switch between motor tracts in the presence of the mAb IN-1 in the adult rat. *Proc Natl Acad Sci U S A* 98:6929-6934.
- Ramer MS, Priestley JV, McMahon SB (2000) Functional regeneration of sensory axons into the adult spinal cord. *Nature* 403:312-316.
- Ramon-Cueto A, Cordero MI, Santos-Benito FF, Avila J (2000) Functional recovery of paraplegic rats and motor axon regeneration in their spinal cords by olfactory ensheathing glia. *Neuron* 25:425-435.
- Rhodes KE, Fawcett JW (2004) Chondroitin sulphate proteoglycans: preventing plasticity or protecting the CNS? *J Anat* 204:33-48.
- Richardson PM, Issa VM (1984) Peripheral injury enhances central regeneration of primary sensory neurones. *Nature* 309:791-793.
- Richardson PM, McGuinness UM, Aguayo AJ (1980) Axons from CNS neurons regenerate into PNS grafts. *Nature* 284:264-265.
- Richardson PM, Issa VM, Aguayo AJ (1984) Regeneration of long spinal axons in the rat. *J Neurocytol* 13:165-182.
- Rossi F, Jankovski A, Sotelo C (1995) Differential regenerative response of Purkinje cell and inferior olivary axons confronted with embryonic grafts: environmental cues versus intrinsic neuronal determinants. *J Comp Neurol* 359:663-677.
- Savio T, Schwab ME (1990) Lesioned corticospinal tract axons regenerate in myelin-free rat spinal cord. *Proc Natl Acad Sci U S A* 87:4130-4133.
- Schnell L, Schwab ME (1990) Axonal regeneration in the rat spinal cord produced by an antibody against myelin-associated neurite growth inhibitors. *Nature* 343:269-272.
- Schnell L, Schneider R, Kolbeck R, Barde YA, Schwab ME (1994) Neurotrophin-3 enhances sprouting of corticospinal tract during development and after adult spinal cord lesion. *Nature* 367:170-173.
- Schwab ME (1977) Ultrastructural localization of a nerve growth factor-horseradish peroxidase (NGF-HRP) coupling product after retrograde axonal transport in adrenergic neurons. *Brain Res* 130:190-196.
- Schwab ME, Thoenen H (1985) Dissociated neurons regenerate into sciatic but not optic nerve explants in culture irrespective of neurotrophic factors. *J Neurosci* 5:2415-2423.

- Schwab ME, Caroni P (1988) Oligodendrocytes and CNS myelin are nonpermissive substrates for neurite growth and fibroblast spreading in vitro. *J Neurosci* 8:2381-2393.
- Sett P, Crockard HA (1991) The value of magnetic resonance imaging (MRI) in the follow-up management of spinal injury. *Paraplegia* 29:396-410.
- Shibayama M, Hattori S, Himes BT, Murray M, Tessler A (1998) Neurotrophin-3 prevents death of axotomized Clarke's nucleus neurons in adult rat. *J Comp Neurol* 390:102-111.
- Silver J, Miller JH (2004) Regeneration beyond the glial scar. *Nat Rev Neurosci* 5:146-156.
- Simonen M, Pedersen V, Weinmann O, Schnell L, Buss A, Ledermann B, Christ F, Sansig G, van der Putten H, Schwab ME (2003) Systemic deletion of the myelin-associated outgrowth inhibitor Nogo-A improves regenerative and plastic responses after spinal cord injury. *Neuron* 38:201-211.
- Sivasankaran R, Pei J, Wang KC, Zhang YP, Shields CB, Xu XM, He Z (2004) PKC mediates inhibitory effects of myelin and chondroitin sulfate proteoglycans on axonal regeneration. *Nat Neurosci* 7:261-268.
- Spillmann AA, Amberger VR, Schwab ME (1997) High molecular weight protein of human central nervous system myelin inhibits neurite outgrowth: an effect which can be neutralized by the monoclonal antibody IN-1. *Eur J Neurosci* 9:549-555.
- Spillmann AA, Bandtlow CE, Lottspeich F, Keller F, Schwab ME (1998) Identification and characterization of a bovine neurite growth inhibitor (bNI-220). *J Biol Chem* 273:19283-19293.
- Strittmatter SM, Fankhauser C, Huang PL, Mashimo H, Fishman MC (1995) Neuronal pathfinding is abnormal in mice lacking the neuronal growth cone protein GAP-43. *Cell* 80:445-452.
- Takami T, Oudega M, Bates ML, Wood PM, Kleitman N, Bunge MB (2002) Schwann cell but not olfactory ensheathing glia transplants improve hindlimb locomotor performance in the moderately contused adult rat thoracic spinal cord. *J Neurosci* 22:6670-6681.
- Tello F (1911) La influencia del neurotropismo en la regeneracion de los nerviosos. *Trab Lab Invest Biol* 9:123-159.
- Teng YD, Lavik EB, Qu X, Park KI, Ourednik J, Zurakowski D, Langer R, Snyder EY (2002) Functional recovery following traumatic spinal cord injury mediated by a unique

- polymer scaffold seeded with neural stem cells. *Proc Natl Acad Sci U S A* 99:3024-3029.
- Teuber HL (1974) Recovery of function after lesions of the central nervous system: history and prospects. *Neurosci Res Prog Bull* 12:197-209.
- Thallmair M, Metz GA, Z'Graggen WJ, Raineteau O, Kartje GL, Schwab ME (1998) Neurite growth inhibitors restrict plasticity and functional recovery following corticospinal tract lesions. *Nat Neurosci* 1:124-131.
- Vanek P, Thallmair M, Schwab ME, Kapfhammer JP (1998) Increased lesion-induced sprouting of corticospinal fibres in the myelin-free rat spinal cord. *Eur J Neurosci* 10:45-56.
- Verge VM, Gratto KA, Karchewski LA, Richardson PM (1996) Neurotrophins and nerve injury in the adult. *Philos Trans R Soc Lond B Biol Sci* 351:423-430.
- Wahle H (1990) [10-year follow-up of occupational integration of 50 patients with complete paraplegia]. *Rehabilitation (Stuttg)* 29:112-120.
- Wang KC, Koprivica V, Kim JA, Sivasankaran R, Guo Y, Neve RL, He Z (2002) Oligodendrocyte-myelin glycoprotein is a Nogo receptor ligand that inhibits neurite outgrowth. *Nature* 417:941-944.
- Wang X, Arcuino G, Takano T, Lin J, Peng WG, Wan P, Li P, Xu Q, Liu QS, Goldman SA, Nedergaard M (2004) P2X7 receptor inhibition improves recovery after spinal cord injury. *Nat Med* 10:821-827.
- Wernig A, Nanassy A, Muller S (1998) Maintenance of locomotor abilities following Laufband (treadmill) therapy in para- and tetraplegic persons: follow-up studies. *Spinal Cord* 36:744-749.
- Wernig A, Muller S, Nanassy A, Cagol E (1995) Laufband therapy based on 'rules of spinal locomotion' is effective in spinal cord injured persons. *Eur J Neurosci* 7:823-829.
- Wirz M, Colombo G, Dietz V (2001) Long term effects of locomotor training in spinal humans. *J Neurol Neurosurg Psychiatry* 71:93-96.
- Woolf CJ, Shortland P, Coggeshall RE (1992) Peripheral nerve injury triggers central sprouting of myelinated afferents. *Nature* 355:75-78.
- Woolf CJ, Reynolds ML, Molander C, O'Brien C, Lindsay RM, Benowitz LI (1990) The growth-associated protein GAP-43 appears in dorsal root ganglion cells and in the dorsal horn of the rat spinal cord following peripheral nerve injury. *Neuroscience* 34:465-478.

- Xiao HS, Huang QH, Zhang FX, Bao L, Lu YJ, Guo C, Yang L, Huang WJ, Fu G, Xu SH, Cheng XP, Yan Q, Zhu ZD, Zhang X, Chen Z, Han ZG (2002) Identification of gene expression profile of dorsal root ganglion in the rat peripheral axotomy model of neuropathic pain. *Proc Natl Acad Sci U S A* 99:8360-8365.
- Xu XM, Chen A, Guenard V, Kleitman N, Bunge MB (1997) Bridging Schwann cell transplants promote axonal regeneration from both the rostral and caudal stumps of transected adult rat spinal cord. *J Neurocytol* 26:1-16.
- Zagrebelsky M, Buffo A, Skerra A, Schwab ME, Strata P, Rossi F (1998) Retrograde regulation of growth-associated gene expression in adult rat Purkinje cells by myelin-associated neurite growth inhibitory proteins. *J Neurosci* 18:7912-7929.
- Z'Graggen WJ, Metz GA, Kartje GL, Thallmair M, Schwab ME (1998) Functional recovery and enhanced corticofugal plasticity after unilateral pyramidal tract lesion and blockade of myelin-associated neurite growth inhibitors in adult rats. *J Neurosci* 18:4744-4757.
- Z'Graggen WJ, Fouad K, Raineteau O, Metz GA, Schwab ME, Kartje GL (2000) Compensatory sprouting and impulse rerouting after unilateral pyramidal tract lesion in neonatal rats. *J Neurosci* 20:6561-6569.
- Zheng B, Ho C, Li S, Keirstead H, Steward O, Tessier-Lavigne M (2003) Lack of enhanced spinal regeneration in Nogo-deficient mice. *Neuron* 38:213-224.
- Zhou L, Baumgartner BJ, Hill-Felberg SJ, McGowen LR, Shine HD (2003) Neurotrophin-3 expressed in situ induces axonal plasticity in the adult injured spinal cord. *J Neurosci* 23:1424-1431.

Chapter 2

It Takes More Than Two to Nogo

Clifford J. Woolf and Stefan Bloechlinger

Science, Vol. 297, pp. 1132-1134, 2002

to-second pulse trains was reported by Papadogiannis *et al.* (8). Last year, de Paul *et al.* measured a train of 250-as pulses directly in the time domain (9).

Can such pulse trains be used for time-resolved attosecond spectroscopy? Salières *et al.* proposed in 1996 to use them for monitoring processes that occur with the period $T_L/2$ of the train. Candidates for such processes are harmonic generation itself or above threshold ionization (2), a laser-induced ionization process in which electrons absorb more photons than they need to be released. All of these processes can be described by "simple man's models" (10). Unfortunately, today's attosecond pulses are not sufficiently intense to realize time-resolved attosecond spectroscopy of these processes.

Although HHG is now an established source for attosecond pulse trains, it has one major limitation. Applications of time-resolved spectroscopy to dynamics that do not occur with the $T_L/2$ period require single isolated attosecond pulses. But there may be a way around this problem. For laser pulses shorter than 10 fs, the resulting individual harmonics fall below the femtosecond limit. Because the laser pulse lasts for only a few T_L , the harmonics cannot develop; instead, a soft x-ray attosecond pulse should be generated.

Krausz and co-workers (11) generated such an isolated attosecond x-ray pulse ($\lambda \approx 14$ nm) by irradiating a very short laser

pulse ($\lambda \approx 750$ nm) of ~ 5 -fs duration on a krypton gas sample, and filtering the outgoing radiation to a 5-eV range around 90 eV. They then irradiated the target krypton sample simultaneously with the x-ray pulse and a laser pulse of visible light of a few laser cycles duration. The x-ray pulse ionized the krypton atoms. The energy spectrum of the photoelectrons depended on the phase of the laser pulse at the moment of the electron's detachment. When the authors changed the relative delay between the laser and the soft x-ray pulse, a modulation of the spectral width appeared, allowing the duration of the x-ray pulse to be estimated as ~ 650 as.

Krausz and co-workers now describe (1) the first genuine application of isolated attosecond pulses for time-resolved attosecond spectroscopy. They study the absorption and emission of laser photons by electronic wavepackets created by soft x-ray radiation. Normally, the photoelectron energy spreads as a result of the photon absorption or emission (12). If, however, the emitted electron wavepacket is temporally confined to a fraction of T_L , its energy spectrum may be up- or down-shifted by several laser photon energies without broadening. The laser light can then "steer" the electron wavepacket like a classical particle. The results of such "steering" depend on the timing of the attosecond x-ray pulse relative to the absolute phase of the laser (see the figure), offering

a simple, single-shot tool for time-resolved attosecond spectroscopy.

Attophysics has moved from dream to reality. One can expect fruitful applications of time-resolved attosecond spectroscopy to HHG or to above threshold ionization processes induced by ultrashort laser pulses, in which the absolute phase of the laser pulse plays a crucial role (13). Attosecond spectroscopy will provide diagnostics and perhaps new ways of controlling these processes, in particular to obtain better ways of short x-ray coherent pulse generation.

References and Notes

1. R. Kienberger *et al.*, *Science* **297**, 1144 (2002); published online 11 July 2002 (*Science* 10.1126/science.1073866).
2. C. J. Joachain, M. Dörr, N. Kylstra, *Adv. Atom. Mol. Opt. Phys.* **42**, 225 (2000).
3. Ch. Spielmann *et al.*, *Science* **278**, 661 (1997).
4. P. B. Corkum, *Phys. Rev. Lett.* **71**, 1994 (1993).
5. K. C. Kulander, K. J. Schafer, J. L. Krause, in *Super-Intense Laser-Atom Physics*, B. Piraux, A. L'Huillier, K. Rzażewski, Eds. (Plenum, New York, 1993).
6. M. Lewenstein *et al.*, *Phys. Rev. A* **49**, 2117 (1994).
7. P. Antoine, A. L'Huillier, M. Lewenstein, *Phys. Rev. Lett.* **77**, 1234 (1996).
8. N. Papadogiannis *et al.*, *Phys. Rev. Lett.* **83**, 4289 (1999).
9. P. M. Paul *et al.*, *Science* **292**, 1689 (2001).
10. P. Salières *et al.*, *Science* **292**, 902 (2001).
11. M. Hentschel *et al.*, *Nature* **414**, 509 (2001).
12. N. M. Kroll, K. M. Watson, *Phys. Rev. A* **8**, 804 (1973).
13. G. G. Paulus *et al.*, *Nature* **414**, 182 (2001).
14. I thank the Deutsche Forschungsgemeinschaft, Alexander von Humboldt-Foundation, the VolkswagenStiftung, the ESF, and European Union Research Training Network "Cold Quantum Gases."

PERSPECTIVES: NEUROSCIENCE

It Takes More Than Two to Nogo

Clifford J. Woolf and Stefan Bloechlinger

The environment of the adult mammalian central nervous system (CNS) is hostile to the growth of axons and is a major contributor to the inability of injured neurons to regenerate. Much of this inhibition is caused by myelin, the insulating lipid and protein material that is wrapped around axons, ensuring rapid transmission of electrical signals along central nerve fibers. In the CNS, myelin is produced by supporting glial cells called oligodendrocytes. These cells also make growth-inhibitory proteins that become embedded within the myelin sheath.

Injured nerve fibers that make contact with CNS myelin cease to regenerate. At least three growth-inhibitory proteins have been identified so far: Nogo-A, named for its inhibitory action on axonal growth; myelin-associated glycoprotein (MAG); and oligodendrocyte myelin glycoprotein (OMgp). Although Nogo-A is known to bind to the Nogo receptor (NgR), the receptors for MAG and OMgp have remained elusive. Now, in an extraordinary and unexpected convergence reported by several groups including Liu *et al.* (1) on page 1190 of this issue, all three molecules appear to bind to the same receptor, NgR (2–4). This discovery opens up exciting new possibilities for overcoming axonal growth inhibition, a vital step in neuronal regrowth after brain or spinal cord injury.

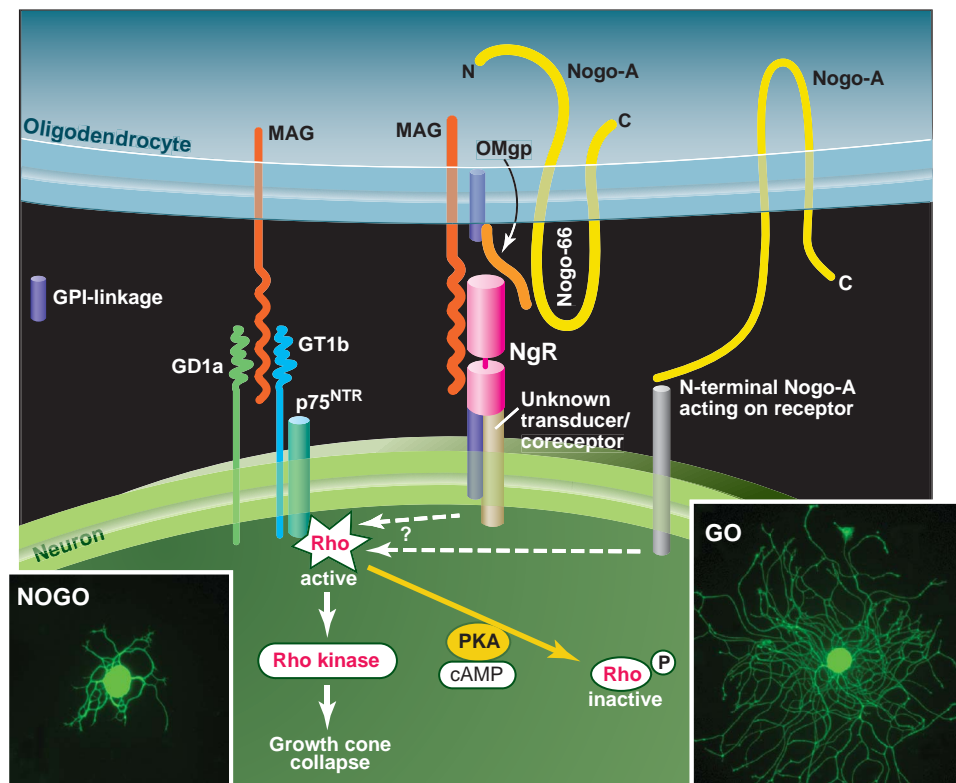
During the development of the nervous system and in neurons grown in culture, the extension of axons from the cell body

begins with the formation of small processes whose active tips have a specialized structure called the axonal growth cone. The growth cone interacts with the environment to determine the direction and rate of axon elongation. When the growth cone contacts CNS myelin, its cytoskeletal structure is altered, causing it to collapse and resulting in cessation of axonal growth. Nogo-A, MAG, and OMgp all contribute to the inhibitory action of CNS myelin on axonal growth and regeneration.

Nogo-A, a member of the reticulon family of proteins, has two inhibitory domains: a cell surface domain called Nogo-66 (5), and a long amino-terminal region (6) (see the figure). The Nogo-66 domain on the oligodendrocyte surface binds to NgR, a leucine-rich repeat protein that is attached to the extracellular surface of the neuronal membrane by glycosylphosphatidylinositol (GPI) (4). The location of the inhibitory amino-terminal domain of Nogo-A may be cytoplasmic, although this remains unclear (5, 6). If this is the case, then the amino-terminal domain of Nogo-A can inhibit axonal growth only when myelin is disrupted by injury. No receptor

Enhanced online at
www.sciencemag.org/cgi/
content/full/297/5584/1132

The authors are in the Neural Plasticity Research Group, Department of Anesthesia, Massachusetts General Hospital and Harvard Medical School, Boston, MA 02129, USA. E-mail: woolf.clifford@mgh.harvard.edu



Blocking axonal growth. Three growth-inhibitory molecules—MAG (red), OMgp (orange), and the extracellular Nogo-66 domain of Nogo-A (yellow)—are produced by oligodendrocytes in the CNS. These growth-inhibitory proteins become embedded in the myelin sheath that surrounds axons, and they block the regeneration of nerve fibers. They all bind to the same neuronal receptor NgR (pink), resulting in the activation of signaling pathways that block axonal growth and induce growth cone collapse. NgR may require a coreceptor to transduce intracellular signals via molecules such as the Rho GTPase, but this putative coreceptor has not been identified. Activation of PKA leads to inactivation of Rho and prevents growth cone collapse. In addition to binding to NgR, MAG also interacts with a complex between the gangliosides GT1b and GD1a and the neurotrophin receptor p75, resulting in activation of Rho. The photomicrographs depict primary adult dorsal root ganglion neurons grown either on a laminin substrate that is permissive for growth (right) or on a CNS myelin substrate that prevents growth (left).

for the Nogo-A amino-terminal domain has been reported so far. Competitive inhibition of the binding of Nogo-66 to NgR by an antagonistic peptide, NEP1-40, overcomes all of the inhibitory action of Nogo-66 and much but not all of the inhibitory action of CNS myelin on cultured neurons (7). In vivo studies reveal similar effects on regenerative neural growth after spinal cord injury for both NEP1-40 (7) and IN-1, a monoclonal antibody that recognizes Nogo-A (8). IN-1 antibody treatment also causes rearrangement of intact fiber tracts, which suggests that Nogo-A tonically suppresses neural growth in the adult CNS (9).

MAG is a sialic acid-binding protein of the SIGLEC (sialic acid-dependent immunoglobulin-like family member lectin) group. It inhibits axonal growth in multiple in vitro assays, although, surprisingly, deleting the *MAG* gene does not promote neuronal regeneration in mice (10). OMgp is a GPI-anchored protein that was recently found to potentially inhibit neurite outgrowth

in culture (3). Both MAG and OMgp, like Nogo-66, bind to NgR with high affinity (1, 3). Although the NgR binding sites for OMgp and Nogo-66 appear to overlap, MAG and Nogo-66 bind to different sites on NgR (1). Removal of NgR by cleaving its GPI membrane anchor results in loss of the growth-inhibitory action of all three proteins. In contrast, introduction of exogenous NgR into neurons that are unresponsive to the growth-inhibitory proteins renders them responsive (1–4). NgR is therefore a promiscuous receptor binding to multiple inhibitory myelin proteins, and it appears to act as the major convergence point on the surface of growth cones for detecting many of the inhibitory influences of CNS myelin.

NgR has no transmembrane or intracytoplasmic domains and so must produce inhibition by binding to a membrane-bound coreceptor that transduces the extracellular signal and activates intracellular signaling cascades that lead to the collapse of the

growth cone. Apparently, MAG binds not only to NgR (1) but also to the gangliosides GD1a and GT1b at least in some (11), but not all (1), assays. This ganglioside action requires the low-affinity nonselective neurotrophin receptor p75, which forms a complex with GT1b that binds to MAG (12). Thus, like Nogo-A, MAG seems to have two independent receptors.

Which signaling molecules downstream of NgR or the GT1b/p75 complex transduce the activation signals of Nogo-A, MAG, and OMgp that result in growth cone collapse? One possibility is Rho, a small membrane-bound guanine triphosphatase (GTPase). Neurons expressing dominant-negative Rho, which cannot transduce signals, are not responsive to the growth-inhibitory properties of MAG. Blocking Rho-GTPase activity with the *Clostridium botulinum* enzyme C3 allows neurites to grow on MAG substrates in vitro (13). Inhibition of Rho-kinase (a downstream target of Rho that interacts with the cytoskeleton) overcomes GT1b-mediated blockade of axonal elongation. In addition, cyclic adenosine monophosphate (cAMP) blocks MAG-induced inhibition by activating protein kinase A (PKA), which inactivates Rho through phosphorylation (14). Recently, it has been shown that cAMP promotes neurite growth after spinal cord injury in vivo (15, 16).

The convergence of inhibitory influences at the level of both cell surface receptors and intracellular signaling could be the reason for the devastating suppression of neuronal growth by CNS myelin after spinal cord injury. This convergence could explain the powerful independent effects of Nogo-A, MAG, and OMgp, as well as the modest increase in regeneration that is produced by blocking the activity of each individual growth-inhibitory protein. Neuronal regeneration is likely to be improved by targeting NgR or Rho rather than by targeting Nogo-A, MAG, or OMgp independently. However, one major concern with this type of treatment is that it may enable maladaptive sprouting and growth of noninjured neurons, which could disrupt the highly organized connectivity of the CNS established during development. Indeed, the function of Nogo-A, MAG, or OMgp may be related more to preservation of the wiring of the CNS than to suppression of neuronal regeneration. In any case, myelin inhibition is not the only factor responsible for the lack of regeneration. Astrocytes, another type of CNS glial cell, also produce inhibitory molecules, including tenascin and chondroitin sulfate proteoglycan. In addition, overcoming inhibition is only half the story; an increase in the intrinsic growth capacity of the injured neurons is also re-

quired (17). Nonetheless, the new reports identifying the importance of NgR in preventing neuronal regeneration represent a big step forward in our understanding of the molecular pathways that impede regeneration in the CNS. The fact that these reports provide a point of convergence—and therefore a potential reduction in the number of interventions necessary to promote nerve regeneration—is also good news.

PERSPECTIVES: ASTRONOMY

The Secrets Behind Supernovae

H.-Th. Janka

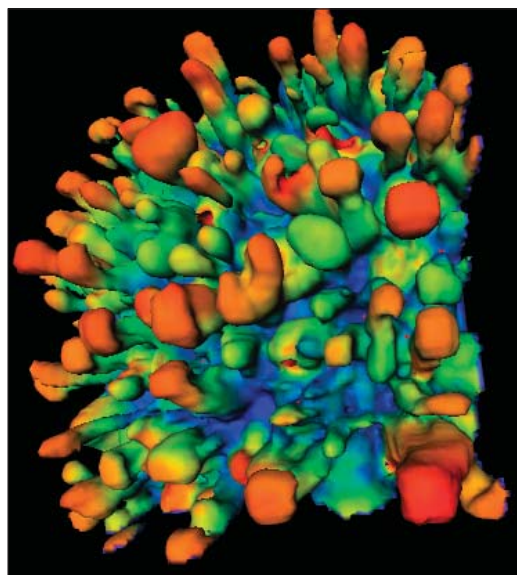
Once every second, somewhere in the universe a massive star is disrupted in a supernova explosion. Visible even at cosmic distances, these stellar catastrophes provide valuable information about the history of star formation in the universe. Ejecting several solar masses of stellar debris, they enrich the interstellar medium with heavy elements from millions of years of quiescent nuclear burning, and with radioactive nuclei that are freshly synthesized during the star's violent death.

As brilliant as it may be, a supernova explosion is only a weak side effect of a much more energetic event. Theory suggests that as the iron core of the exploding star collapses to form a neutron star or black hole, most of the gravitational binding energy is carried away by neutrinos. This prediction was confirmed by the detection of two dozen of the 10^{58} neutrinos from Supernova 1987A in the underground experiments of Kamiokande, Irvine-Michigan-Brookhaven, and Baksan. Typically, only 1% of the released energy goes into kinetic energy of the ejecta, and only a small fraction of this energy is converted to electromagnetic radiation.

How is energy transferred from the collapsing compact remnant to the matter that gets ejected? Understanding this driving force of the explosion is crucial for predicting remnant masses, explosion energies, and nucleosynthetic yields. It is thus essential for establishing the theoretical link between the properties of massive stars and the observables of supernova explosions. Unfortunately, observations have

References

1. B. P. Liu, A. Fournier, T. GrandPré, S. M. Strittmatter, *Science* **297**, 1190 (2002); published online 27 June 2002 (10.1126/science.1073031).
2. M. Domeniconi *et al.*, *Neuron* **35**, 283 (2002).
3. K. C. Wang *et al.*, *Nature* **417**, 941 (2002).
4. A. E. Fournier, T. GrandPré, S. M. Strittmatter, *Nature* **409**, 341 (2001).
5. T. GrandPré, F. Nakamura, T. Vartanian, S. M. Strittmatter, *Nature* **403**, 439 (2000).
6. M. S. Chen *et al.*, *Nature* **403**, 434 (2000).
7. T. GrandPré, S. Li, S. M. Strittmatter, *Nature* **417**, 547 (2002).
8. B. S. Bregman *et al.*, *Nature* **378**, 498 (1995).
9. M. Thallmair *et al.*, *Nature Neurosci.* **1**, 124 (1998).
10. U. Bartsch *et al.*, *Neuron* **15**, 1375 (1995).
11. A. A. Vyas *et al.*, *Proc. Natl. Acad. Sci. U.S.A.* **99**, 8412 (2002).
12. T. Yamashita, H. Higuchi, M. Tohyama, *J. Cell Biol.* **157**, 565 (2002).
13. M. Lehmann *et al.*, *J. Neurosci.* **19**, 7537 (1999).
14. P. Lang *et al.*, *EMBO J.* **15**, 510 (1996).
15. J. Qiu *et al.*, *Neuron* **34**, 895 (2002).
16. S. Neumann, F. Bradke, M. Tessier-Lavigne, A. I. Basbaum, *Neuron* **34**, 885 (2002).
17. S. Neumann, C. J. Woolf, *Neuron* **23**, 83 (1999).



Three-dimensional supernova simulation. The perspective image shows convective mixing in a newly formed neutron star. The mushroom-shaped structures are a result of hydrodynamic instabilities (19). The colors represent different fluid entropy values (blue, low; red, high) on a surface of constant proton-to-neutron ratio. [Adapted from (19)]

so far been unable to constrain the processes that take place in the collapsed core of a star.

Future measurement platforms may provide the required data by allowing thousands of neutrinos and possibly gravitational waves to be measured in a future supernova in our Galaxy. But current knowledge is based mainly on numerical simulations and analytic analysis. Despite more than 30 years of research and increasingly detailed computer models, there is still no satisfactory understanding of the start of the explosion.

Stellar iron cores become gravitationally unstable when energetic photons begin to split iron-group nuclei into α particles and free nucleons (protons and neutrons). At the same time, electrons are captured by nuclei and free protons, thereby reducing the pres-

sure even more and producing large numbers of electron neutrinos. The latter can leave the star unhindered until they get trapped as the density grows. Within less than a second, the inner part of the core collapses to nuclear densities and then resists further compression due to the onset of nucleon degeneracy and repulsive nuclear forces.

At this moment, a hydrodynamical shock wave is launched and propagates outward through the still supersonically infalling outer core. There is general agreement that this shock cannot cause an explosion directly. It suffers from severe energy losses by photodisintegration of iron nuclei and neutrino emission and therefore stalls at a radius of 100 to 200 km.

But just fractions of a second later, the situation has changed. The temperature behind the standing shock has dropped so much that energetic neutrinos, which leave the hot, nascent neutron star in large fluxes, are readily absorbed by free nucleons in the postshock layer (the layer right behind the supernova shock). If this energy deposition is large enough, it can revive the stalled shock and lead to a successful "delayed" explosion (1, 2). Because the ultimate fate of the shock is determined by a delicate rivalry between competing processes, detailed computer models are needed to answer the question of whether the energy transfer to the shock by neutrinos is sufficient to lead to an explosion.

Wilson and Mayle (3) have successfully simulated such neutrino-driven explosions by making two assumptions, which are, however, not generally accepted. They assumed that convective mixing by neutron-finger instabilities (4) in the neutron star boosts neutrino emission. Moreover, they considered high densities of pions (strongly interacting elementary particles that are built from a quark and an antiquark) in the neutron star medium to obtain explosion energies in the observed range (5). Both assumptions favor an explosion because the energy transfer by neutrinos increases sensitively with higher neutrino luminosities and energies.

But important other physics was missing from the models of Wilson and colleagues, as suggested by spectral observations of

The author is at the Max-Planck-Institut für Astrophysik, Karl-Schwarzschild-Strasse 1, 85741 Garching, Germany. E-mail: thj@mpa-garching.mpg.de

Chapter 3

Neuronal Plasticity and Formation of New Synaptic Contacts Follow Pyramidal Lesions and Neutralization of Nogo-A: A Light and Electron Microscopic Study in the Pontine Nuclei of Adult Rats

Stefan Blöchliger, Oliver Weinmann, Martin E. Schwab and Michaela Thallmair

Neuronal Plasticity and Formation of New Synaptic Contacts Follow Pyramidal Lesions and Neutralization of Nogo-A: A Light and Electron Microscopic Study in the Pontine Nuclei of Adult Rats

STEFAN BLÖCHLINGER, OLIVER WEINMANN, MARTIN E. SCHWAB, AND
MICHAELA THALLMAIR*

Brain Research Institute, University of Zurich and Swiss Federal Institute of Technology-
Zurich, CH-8057 Zurich, Switzerland

ABSTRACT

Regeneration and compensatory sprouting are limited after lesions in the mature mammalian central nervous system in contrast to the developing central nervous system (CNS). After neutralization of the growth inhibitor Nogo-A, however, massive sprouting and rearrangements of fiber connections occurred after unilateral pyramidal tract lesions in adult rats: Corticofugal fibers from the lesioned side crossed the midline of the brainstem and innervated the contralateral basilar pontine nuclei. To determine whether these newly sprouted fibers formed synaptic contacts, we analyzed the corticofugal fibers in the basilar pontine nuclei contralateral to the lesion by light and electron microscopy 2 weeks after pyramidotomy and treatment with the Nogo-A-inhibiting monoclonal antibody IN-1 (mAb IN-1). The mAb IN-1, but not a control antibody, led to structural changes in the basilar pons ipsilateral and contralateral to the lesion site. Fibers sprouted across the pontine midline and terminated topographically. They established asymmetric synaptic contacts with the characteristics of normal corticopontine terminals. These results show that adult CNS fibers are able to sprout and to form new synaptic contacts after a lesion when a growth-permissive microenvironment is provided. *J. Comp. Neurol.* 433:426–436, 2001. © 2001 Wiley-Liss, Inc.

Indexing terms: compensatory sprouting; neutralizing antibody; basilar pons; synapse; axotomy; ultrastructure

Regenerative and compensatory plastic fiber growth after lesions is restricted to short distances in the adult mammalian central nervous system (CNS). CNS tract lesions, therefore, lead to permanent functional impairment. This limited anatomical and functional repair in the mature CNS contrasts with the situation in the immature CNS, in which regeneration and compensatory sprouting of lesioned and unlesioned fibers can take place, and functional deficits are small (Kennard, 1936, 1938; Kalil and Reh, 1982; Kartje-Tillotson et al., 1986; Whishaw and Kolb, 1988; Barth and Stanfield, 1990; Kuang and Kalil, 1990).

The importance of myelin and the myelin-associated neurite growth inhibitor Nogo-A in preventing regenerative and compensatory fiber growth in the adult mammalian CNS has been well described (Caroni and Schwab, 1988a,b; Schwab et al., 1993; Kapfhammer, 1997; Chen et

al., 2000). After corticospinal tract (CST) lesions, neutralization of Nogo-A by the monoclonal inhibitor-neutralizing antibody 1 (mAb IN-1) enhanced long-distance regeneration of adult corticospinal axons and recovery of locomotor functions (Schnell and Schwab, 1990, 1993; Bregman et

Grant sponsor: Swiss National Science Foundation; Grant numbers: 31-45549.95/2 and 4038-43918.95/2; Grant sponsor The Spinal Cord Consortium of the Christopher Reeve Paralysis Foundation; Grant sponsor: The International Research Institute for Paraplegia; Grant sponsor: The Velux Foundation; Grant sponsor: The Biotechnology Program of the European Union; Grant sponsor: Mr. Joachim Huber (private donation).

*Correspondence to: Dr. Michaela Thallmair, Laboratory of Genetics, The Salk Institute for Biological Studies, 10010 North Torrey Pines Road, La Jolla, CA 92037. E-mail: thallmair@salk.edu

Received 14 July 2000; Revised 14 November 2000; Accepted 12 February 2001

al., 1995). In addition, compensatory sprouting of lesioned axons and of corresponding unlesioned neurites after a unilateral pyramidotomy in adult rats treated with mAb IN-1 was observed in several studies (Thallmair et al., 1998; Z'Graggen et al., 1998; Raineteau et al., 1999). Nogo antibody-induced sprouting is thought to play an important role for the functional recovery seen in these animals (Thallmair et al., 1998; Z'Graggen et al., 1998). Anatomically, sprouting fibers from the lesioned pyramidal tract were seen to cross the midline and innervate the contralateral basilar pons and red nucleus in a topographically specific pattern (Thallmair et al., 1998; Z'Graggen et al., 1998). This finding is of special interest, because the newly formed projections innervate a region that was not denervated by the lesion and, thus, contained no vacant synaptic sites. Here, we show by electron microscopy that these sprouted, midline-crossing fibers established synapses with the typical characteristics of corticopontine synaptic terminals.

MATERIALS AND METHODS

Animals and surgery

Unilateral lesions of the CST at the level of the medulla oblongata (pyramidotomy) were performed in male Lewis rats at 8–10 weeks of age. The animals were divided into the following experimental groups: 1) tracing only ($n = 3$ rats), 2) lesion only ($n = 2$ rats), 3) lesion and anti-horseradish peroxidase (anti-HRP) antibody treatment ($n = 3$ rats), and 4) lesion and IN-1 antibody treatment ($n = 6$ rats). Rats were anesthetized by an intraperitoneal (i.p.) injection of Hypnorm (0.3 mg/kg body weight; Janssen, Buckinghamshire, England) and Dormicum (0.6 mg/kg body weight; Roche, Reinach, Switzerland). The medullary pyramids were exposed by a ventral approach through an opening of the occipital bone, as described earlier (Thallmair et al., 1998). The left CST was transected rostral to the decussation using a fine tungsten needle with the basilar artery serving as a landmark for the midline. During the same operation, rats were injected in the cortex/hippocampus contralateral to the lesion with hybridoma cells secreting either mAb IN-1 or anti-HRP as a control antibody. Cyclosporin A (1 mg/100 g body weight, i.p.; Sandimmun; Novartis, Basel, Switzerland) was given daily by intraperitoneal injection during the first 7 days postoperatively to allow the transplants to grow. The control group 2—without transplant—received cyclosporin as well. The sensorimotor cortex of the lesioned CST was injected on the day of operation with the anterograde tracer biotin dextran amine (BDA) by pressure injection (10% BDA in 0.1 M phosphate buffer, pH 7.2; Molecular Probes, Eugene, OR; 2.5 μ l into three or four injection sites, mainly in the forelimb area) using a 5- μ l Hamilton syringe (Hamilton, Reno, NV). Figure 1A shows a scheme of the experimental design. After surgery and the following day, animals were injected with caprofen (5 mg/kg body weight, subcutaneously; Rimadyl; Pfizer AG, Zurich, Switzerland) as a painkiller and Ringer's solution (i.p.). All experiments were approved by the institution's animal care and use committee (Kantonales Veterinäramt Zürich) and conformed to National Institutes of Health guidelines.

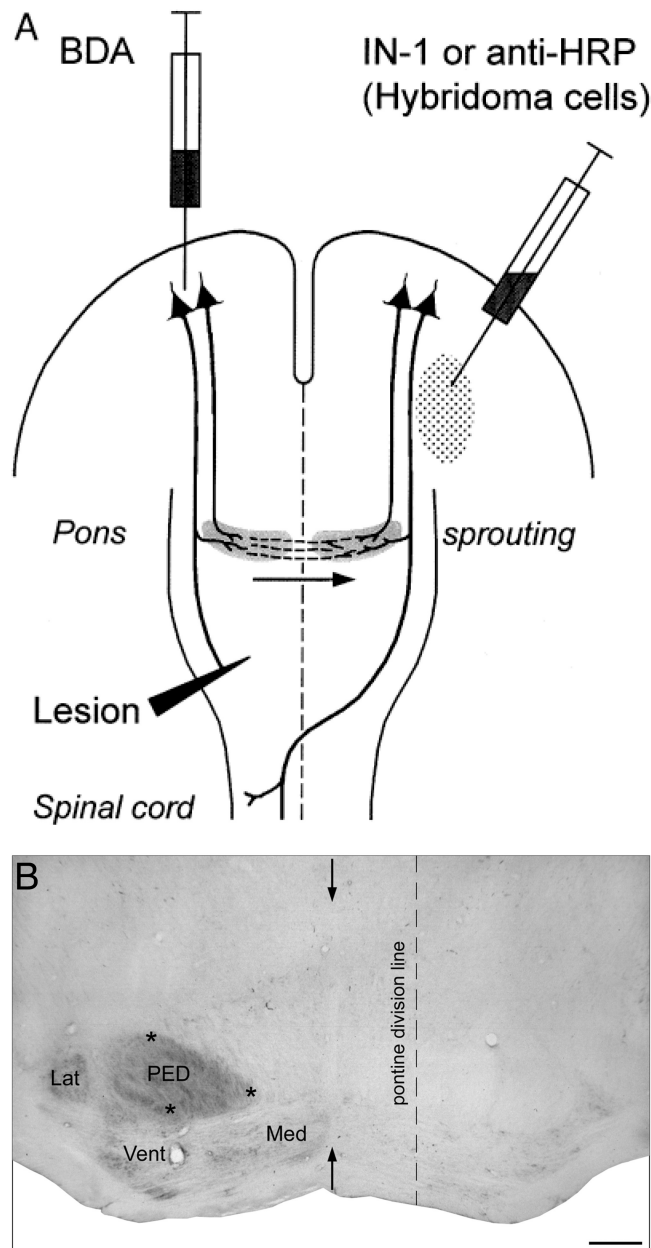


Fig. 1. **A:** Schematic illustration of the experimental design. The corticospinal tracts, the unilateral lesion site, and the injection sites for the tracer biotinylated dextran amine (BDA) and the hybridoma cells are depicted. BDA was injected into the motor cortex ipsilateral to the lesion site to label lesioned corticospinal tract (CST) fibers. The hybridoma cells were injected into the hippocampal region close to the lateral ventricle, contralateral to the tracer and the lesion site, where they form a graft of antibody-producing cells. The dashed lines represent newly sprouted fibers in the pons after the CST lesion and inhibitor-neutralizing antibody 1 (IN-1) application. The arrow indicates the growth direction of the new fibers. Anti-HRP, anti-horseradish peroxidase. **B:** Transverse section containing the basilar pontine nuclei (lateral, Lat; ventral, Vent; medial, Med) and the cerebral peduncle (PED). The midline is indicated by arrows. The pontine division line is taken parallel to the midline and separates the lateral and ventral pontine nucleus from the medial pontine nucleus. This line crosses the medialmost part of the cerebral peduncle that serves as an anatomical landmark. Asterisks in the cerebral peduncle represent the location of the squares where labeled, corticofugal fibers were counted. Scale bar = 360 μ m.

Histochemistry

Fourteen days after the BDA injections, all animals were deeply anesthetized with pentobarbital (450 mg/kg, i.p.; Nembutal, Abbott Laboratories, Cham, Switzerland) and perfused transcardially with 100 ml of 0.5 M phosphate buffer (PB), pH 7.4, containing 0.9% NaCl [phosphate-buffered saline (PBS), pH 7.4] and 50,000 UE heparin (Liquemin; Roche, Reinach, Switzerland) followed by 1,000 ml of the fixative (4% paraformaldehyde, 0.1% glutaraldehyde, and 0.2% picric acid in 0.125 M PB, pH 7.4). The brains and spinal cords were removed and post-fixed overnight in the same fixative at 4°C. The following day, the pons was removed and embedded in a gelatin-chicken albumin solution polymerized with 25% glutaraldehyde. The tissue was cut on a Vibratome into 50- μ m-thick cross sections that were collected in 0.1 M PB and serially mounted on Superfrost-slides (Menzel-Gläser, Germany) according to the semifree-floating technique of Herzog and Brösamle (1997). The sections were washed and incubated overnight at 4°C with an avidin-biotin-peroxidase complex (ABC; Elite kit; 1:100 in 0.1 M PB; Vector Laboratories, Burlingame, CA). The next day, the sections were washed three times for 10 minutes each in 0.1 M PB followed by a 5-minute wash in 0.05 M Tris buffer, pH 8.0. The sections were reacted in 0.05% 3,3'-diaminobenzidine (DAB; Sigma, Buchs, Switzerland) and 0.003% H₂O₂ in 0.05 M Tris buffer, pH 8.0, for about 16 minutes. The process was stopped by washing in 0.1 M PBS, pH 7.4. After three washes in 0.1 M PBS, the sections that were used for light microscopic evaluation were air dried, dehydrated, and coverslipped with Eukitt (Kandler, Freiburg, Germany).

Tissue processing for the electron microscope

After the DAB reaction, sections were postfixed for 1 hour in 2.5% glutaraldehyde in 0.1 M cacodylate buffer, pH 7.4, and subsequently washed in 0.1 M cacodylate buffer. Regions with sprouted fibers were cut out with a razor blade, postfixed for 20 minutes in 2% OsO₄ in cacodylate buffer, and dehydrated in an ascending series of ethanol. A contrast enhancement with 1% uranyl acetate in 70% ethanol was integrated during the dehydration. The tissue was flat embedded in Epon-Araldite (Serva, Heidelberg, Germany). After polymerization at 60°C for 72 hours, the blocks were trimmed, and semithin sections were examined for the presence of labeled axons. Ultrathin sections were cut on an LKB Ultratome (Bromma, Sweden), collected on Pioloform-coated nickel grids (Stork Veco B.V., Eerbeek, Netherlands), and contrasted with Reynold's lead-citrate solution. The sections were air dried and examined in a Zeiss EM 902, electron microscope (EM). Pictures were taken on Scientia EM films (Agfa-Gevaert N.V., Brussels, Belgium) and with a Gatan 792 MultiScan Camera (Pleasanton, CA).

Neuroanatomical analysis

For the light microscopic neuroanatomical analysis, three transverse sections of the basilar pons from each animal were chosen. The most rostral section was taken at the level where the lateral pontine nucleus appears. At an intermediate pontine level, a section was chosen that contained the ventromedial cluster of pontine neurons. The level of the third, more caudally located section was de-

fined by the absence of the ventromedial cluster of pontine neurons and by the appearance of decussating fibers of the trapezoid body. The basilar pons and the cerebral peduncle were outlined, and the midline was indicated using a camera lucida attached to an Olympus microscope (Tokyo, Japan). A vertical line parallel to the midline that divided the basilar pons into a medial part and a lateral part was drawn to anatomically separate the ventral pontine nucleus from the medial pontine nucleus. This pontine division line always crossed the medialmost part of the cerebral peduncle that served as an anatomical landmark and was always located medial to the dense pontine innervation area seen in unilaterally pyramidotomized and IN-1 antibody-treated animals contralateral to the lesion site. The distance between the midline and the pontine division line was about one-third of the distance between the midline and the lateral border of the cerebral peduncle (Fig. 1B). This division is similar to that proposed by Mihailoff et al. (1981). The medial part contained the medial pontine nucleus, and the lateral part contained most of the ventral and lateral pontine nuclei (Fig. 1B).

The cross-sectioned area of the cerebral peduncle was measured using the NeuroLucida program (version 2.1; MicroBrightField, Inc., Colchester, VT). Square areas of 29.4 μ m \times 29.4 μ m each were selected at three different locations within the cerebral peduncle (Fig. 1B, asterisks), all labeled corticofugal fibers in these three areas were counted at \times 400 magnification, and the total number of labeled fibers per peduncle was calculated. To evaluate the innervation pattern of the basilar pons contralateral to the tracer injection, we evaluated three main features. First, all labeled fibers crossing the midline were counted in all three selected sections and divided by the total number of labeled fibers of the cerebral peduncle for each animal: This value was called the *crossing fiber index*. Second, we counted all of the fibers that crossed the medial-ventral pontine dividing line ventral to the cerebral peduncle. Third, the area with the highest density of labeled fibers in the lateral part of the contralateral basilar pons was selected, a square of 23.5 μ m \times 23.5 μ m was placed in the center of this area, and all labeled axonal structures crossing the borders of this square were counted at a \times 1,000 magnification. All results of these three evaluations were normalized for interanimal tracing variability to the number of labeled cerebral peduncle axons, as described above. To examine possible changes in the ipsilateral innervation, the most lateral, ipsilateral innervation field in the ventral pontine nucleus was chosen, and, again, all labeled axonal structures crossing the borders of a square (23.5 μ m \times 23.5 μ m) were counted at \times 1,000 magnification. In addition, all bouton-like swellings of the fibers that were located within the square and had a diameter greater than twice the fiber diameter were counted to estimate the number of boutons formed per fiber. The number of boutons on those fibers was divided by the total number of fibers crossing the borders of the square, resulting in a boutons per fiber index (*boutons/fiber index*).

Statistical evaluation

To test the data for significant differences, the two-sample *t*-test assuming unequal variances was used. All data are presented as mean values \pm the standard error of the mean (S.E.M.).

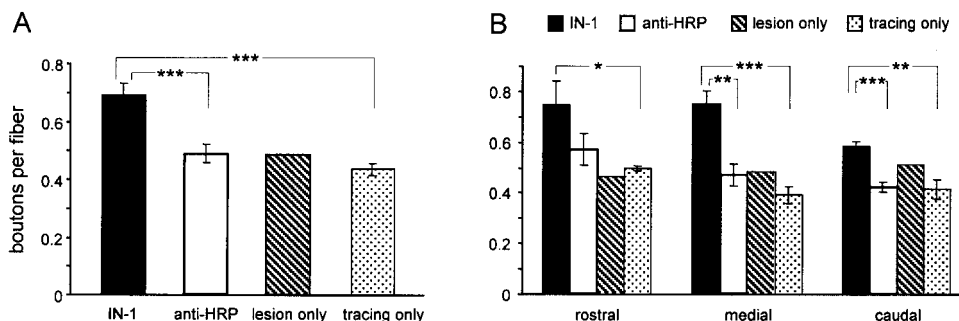


Fig. 2. Quantification of the innervation density in the most lateral corticopontine termination field in the ventral nucleus ipsilateral to the tracer injection and lesion. **A:** Animals that underwent a unilateral pyramidal lesion and received the monoclonal antibody (mAb) IN-1 showed a 40% higher boutons per fiber index than the control

groups. **B:** Rostrocaudal distribution of the boutons per fiber index. The significant increase in bouton-like structures in animals in the lesion and mAb IN-1 treatment group was found at all pontine levels. Asterisks indicate significance: single asterisk, $P < 0.05$; double asterisks, $P < 0.01$; triple asterisks, $P < 0.001$.

Figure preparation

Images were assembled in Photoshop software (version 5.5; Adobe Systems, Mountain View, CA). Contrast and brightness levels were adjusted when necessary.

RESULTS

Light microscopic studies

In all groups of animals, the tracer injection was centered in the forelimb area of the motor cortex. To account for interanimal differences in tracing, the number of BDA-positive neurites in the rostral cerebral peduncle was determined for each rat, as described in Materials and Methods. The average number of labeled fibers was not significantly different between the various experimental groups: $9,285 \pm 589$ axons in the anatomical control group ($n = 3$ rats; tracing only), $12,180$ axons in the group of lesioned animals ($n = 2$ rats), $13,620 \pm 1,342$ axons in the lesioned group that was treated with anti-HRP antibody ($n = 3$ rats), and $11,147 \pm 1,176$ axons in the group of lesioned animals with IN-1 antibody treatment ($n = 6$ rats).

Corticopontine innervation: Lesioned side

General innervation pattern. All experimental groups showed an ipsilateral pontine innervation pattern, as in several previous studies (Mihailoff et al., 1978; Wiesendanger and Wiesendanger, 1982; Panto et al., 1995; Z'Graggen et al., 1998). In animals with sharp and exclusive forelimb motor cortex labeling, a single central innervation field was observed at rostral pontine levels within the ventral nucleus; more caudally, an additional small innervation area in the medial part of the pons was found. At caudal pontine levels, the innervation areas were enlarged further, spreading over lateral, ventral, and medial aspects of the basilar pons. These anatomical findings were not influenced by the lesion location or the type of antibody treatment.

Fiber and bouton density. Slight and variable changes in the density of corticopontine fibers in the ventral nucleus of the pons on the side of the CST lesion could be observed after a unilateral CST lesion and antibody treatment; however, this did not reach significance (tracing only group: 0.38; $n = 3$ rats; lesion only group: 0.72;

$n = 2$ rats; lesion and anti-HRP antibody group: 0.58; $n = 3$ rats; lesion and IN-1 antibody group: 0.68; $n = 6$ rats).

The number of bouton-like structures along labeled fibers innervating the ventral pontine nuclei was determined and expressed as the boutons/fiber index (see Materials and Methods). Whereas the lesioned animals showed at best a trend for an increase, animals with CST lesion and IN-1 antibody treatment showed a robust increase of about 40% in the boutons/fiber index at all levels of the pons (Fig. 2). Control antibody-treated rats never showed such an effect.

Corticopontine fibers crossing the midline: Innervation of the contralateral pons

General innervation pattern. In normal adult rats, only a very minor group of corticopontine fibers projects to the contralateral basilar pontine nuclei, mainly at mid-pontine and caudal levels (Wiesendanger and Wiesendanger, 1982; Panto et al., 1995; Z'Graggen et al., 1998). Unilateral pyramidotomy combined with IN-1 antibody treatment resulted in changes of the contralateral basilar pontine nuclei innervation: An increased number of fibers crossing the midline and a dense contralateral innervation of the ventral pontine nucleus were found (Fig. 3D–F). This contralateral projection was distributed to the mirror image location of the typical corticopontine projection zones. The density of this new contralateral innervation, however, was always less than the ipsilateral innervation of the corresponding area. In the animals that received unilateral pyramidotomy alone or with anti-HRP antibody treatment, sprouting of some fibers that projected to the contralateral medial pontine nucleus and innervation of a zone near the midline at a very low density were observed (Fig. 3A–C). To investigate this compensatory sprouting after a unilateral pyramidotomy in more detail, we quantified the number of midline-crossing corticopontine fibers, their spread to the ventral pontine nucleus, and the density of the terminal plexus formed.

Midline-crossing corticopontine fibers. Corticopontine fibers from the lesioned side of the brain crossed the midline either at the level of the ventral part of the pons (white matter, where axons of pontine neurons cross to the contralateral side before they ascend as mossy fibers to

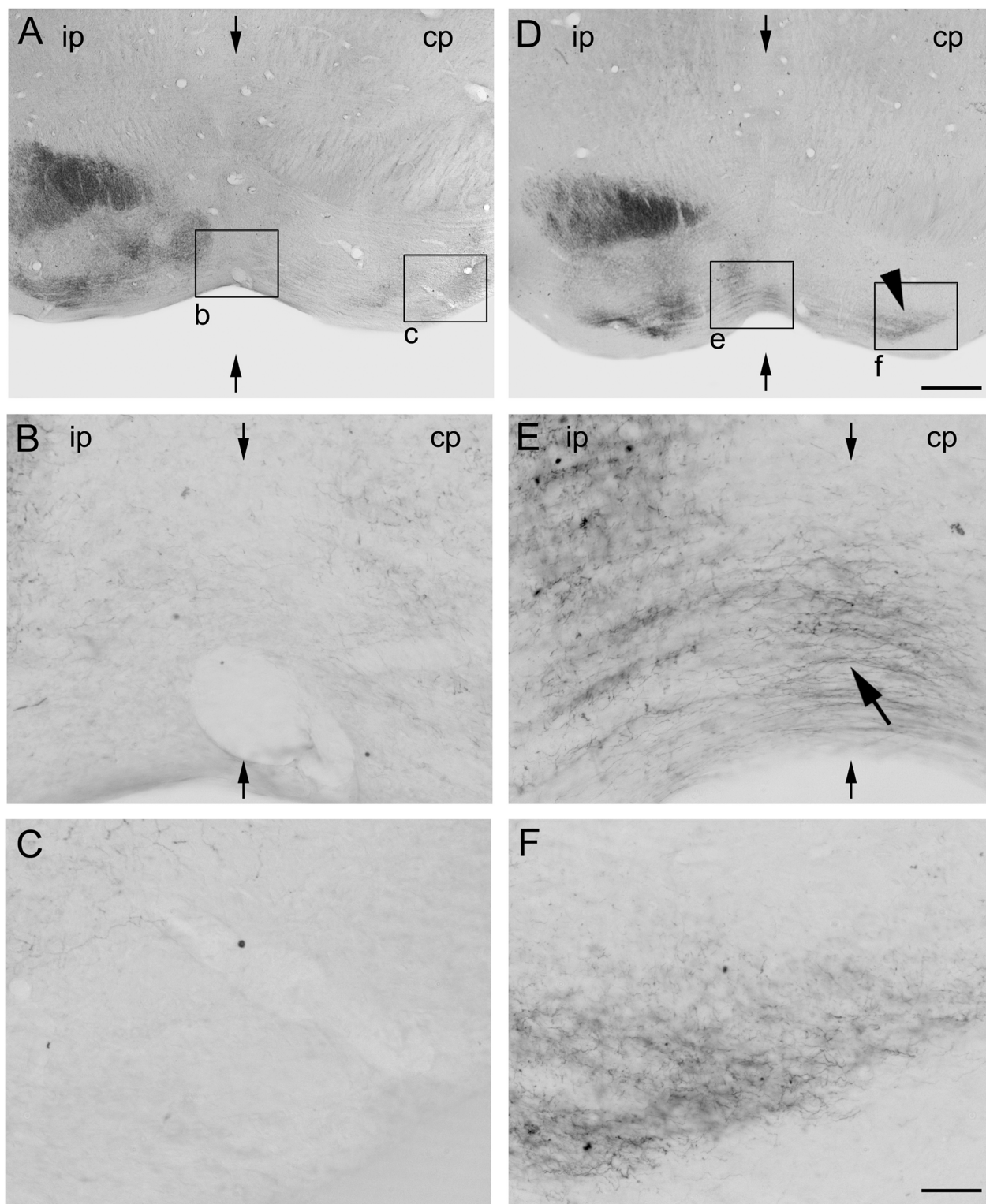


Fig. 3. Cross sections through the basilar pontine nuclei. Photomicrographs on the left (A–C) show BDA-labeled corticofugal fibers from lesioned animals that received a control antibody (anti-HRP), and photomicrographs on the right (D–F) show sections with traced fibers from lesioned, mAb IN-1-treated animals. Enlargements of the areas boxed (b, c, e, and f) are shown in B, E (midline), C, and F (ventral pontine nucleus of the contralateral pons). A–C: In lesioned, anti-HRP-treated animals, only very few fibers innervate the contralateral pons (cp; right lower half of A). Crossing fibers are rare in the midline

(B) and in the ventral pontine nuclei of the contralateral pons (C). D–F: Lesioned animals that received mAb IN-1 showed an increased projection from the ipsilateral pons (ip) to the contralateral pons (cp; arrowhead). At higher magnification, the midline-crossing fibers (E, large arrow) and the contralateral innervation field in the ventral pontine nucleus (F) 2 weeks after IN-1 treatment and unilateral pyramidotomy are seen. Arrows indicate the midline. Scale bars = 360 μ m in D (also applies to A); 60 μ m in F (also applies to B, C, E,).

the cerebellum) or directly between the basilar pontine nuclei (gray matter). Normal animals, rats with CST lesion alone, or lesioned, control antibody-treated rats had only very few corticopontine fibers crossing the midline (Figs. 3C, 5A,B). In the pons of lesioned animals that were treated with IN-1, however, about three times more corticopontine fibers crossing the midline were found (Figs. 3E, 4C, 5A). Similar to what was seen in normal rats, the number of crossing fibers increased from rostral to caudal pontine levels (Fig. 5B). The few crossing fibers in the lesioned, anti-HRP antibody-treated and the lesion-only group ended in an area close to the midline. All labeled fibers in this area were very thin, forming a diffuse innervation field of very low density. In lesioned, IN-1-treated animals, this innervation area also was present, but many labeled fibers projected straight and laterally through this area to arborize and terminate in more lateral regions (ventral pontine nucleus; Fig. 3F).

Crossed fiber projection to the lateral part of the pons. To examine which parts of the contralateral pons were reached by the midline-crossing fibers, a vertical line was drawn separating the medial part from the more lateral parts of the nuclear complex (Fig. 1B). All labeled fibers crossing this pontine division line were counted at the three pontine levels. Fibers crossing this line reached at least the ventral pontine nucleus and also may project to more lateral regions. In normal animals, only very few fibers were seen to cross the medial-lateral division line, even at most caudal pontine levels. Pyramidotomy, especially when combined with a control antibody-secreting hybridoma transplant, showed a small increase in the number of laterally growing fibers (Fig. 5C). The lesioned, IN-1 antibody-treated animals had about twice as many fibers crossing the medial-lateral division line; this increase was significant at all pontine levels and increased from rostral levels to caudal levels (Fig. 5C,D).

Innervation density of contralateral pontine nuclei. In each examined cross section, the area in the lateral part of the pons that contained the densest innervation by crossing corticopontine fibers was evaluated quantitatively for fiber density (see Materials and Methods, above). There were no significant differences between normal animals, pyramidotomy alone animals, and lesioned, control (anti-HRP) antibody-treated rats at rostral levels (Fig. 5F). At midpontine and caudal levels, the lesioned control groups had slightly higher fiber densities (Fig. 5F). The innervation index of the lesioned, IN-1 antibody-treated group, in which the highest labeling density was always located in the lateral part of the ventral pontine nucleus, was at least two times higher than in the other groups (Fig. 5E). An example of the innervation density in a lesioned, IN-1 antibody-treated animal is shown in Figure 4A (ipsilateral to the lesion) and Figure 4B (contralateral to the lesion). This increase of innervation density showed a rostral-to-caudal gradient, similar to the number of midline-crossing fibers (Fig. 5F).

Ultrastructural studies

General findings. At the ultrastructural level, BDA labeling was characterized by the presence of an electron-dense DAB reaction product filling the entire cytoplasm of the labeled axons or terminals (Fig. 6). Cell organelles, such as mitochondria, endoplasmic reticulum, and synaptic vesicles, remained free of label. Ultrathin sections of the pons showed the known distribution of fibers and

neuronal somata (Mihailoff et al., 1981). At the ventral border, bundles of strongly myelinated fibers, the *fibrae transversae*, formed the efferent system of the pons that projects as mossy fibers to the contralateral cerebellar hemisphere. Between the cerebral peduncle and this ventral white matter, clusters of pontine neurons alternated with bundles of fibers, most of them myelinated. Within the clusters of these pontine neurons, unmyelinated axonal and dendritic profiles were present. Synaptic profiles that were found in the pons were asymmetric and contained round vesicles of various sizes.

Labeled axonal and presynaptic structures. The lateral part of the ventral pontine nuclei contralateral to the pyramidal lesion and the tracer injection was analyzed for labeled axons and synapses in mAb IN-1-treated animals. Most of these labeled, crossed corticopontine axons were of small diameter (from 0.04 μm up to 0.29 μm ; most were between 0.15 μm and 0.25 μm if no mitochondrial profiles were present, whereas neurites containing mitochondria had diameters up to 0.53 μm). It is noteworthy that none of the labeled axons was myelinated (consistently in five animals; approximately ten labeled fibers per section), in contrast to many labeled myelinated axons in pontine innervation fields ipsilateral to the tracer injection (data not shown). Vesicle-like structures that were seen in the labeled axons often were round and had the same size as the vesicles seen in labeled synapses.

Labeled synapses, frequently in the vicinity of labeled axonal profiles, showed a high variability in size and often very irregular shapes (Fig. 6). Most of them were large, and they contained up to six mitochondrial profiles. Compared with neighboring, unlabeled presynaptic structures, the number of mitochondria in these labeled, presumably newly formed synapses appeared to be increased. The synaptic vesicles were homogeneous in size (25–40 μm) and round in shape. All examined labeled boutons formed asymmetric synaptic contacts on dendritic processes, often on dendritic spines (Fig. 6). Axosomatic contacts on basilar pontine neurons were not found. Labeled synapses were found almost exclusively in lesioned, mAb IN-1-treated animals; about ten labeled fibers and three or four synapses were found per EM section (0.5 mm \times 0.5 mm) of the lateral pons of mAb IN-1-treated animals ($n = 5$ rats).

DISCUSSION

In this report, we provide evidence for lesion-induced sprouting of corticopontine fibers after mAb IN-1 treatment in adult rats. The fibers sprouted across the pontine midline and established new synapses contralateral to the lesion and tracer injection site. The novel synapses showed the same ultrastructural characteristics that are seen in normal corticopontine synaptic endings.

A unilateral pyramidotomy in adult mammals leads to long-lasting functional impairments of fine motor control of the forelimbs, as shown in previous studies. No functional recovery of precision movements and little or no anatomical plasticity were found after such lesions in mature animals (Kuang and Kalil, 1990). Masking of the myelin-associated neurite growth inhibitor Nogo-A by mAb IN-1 resulted in major structural rearrangements and an almost complete functional recovery in several behavioral tasks (Thallmair et al., 1998; Z'Graggen et al., 1998).

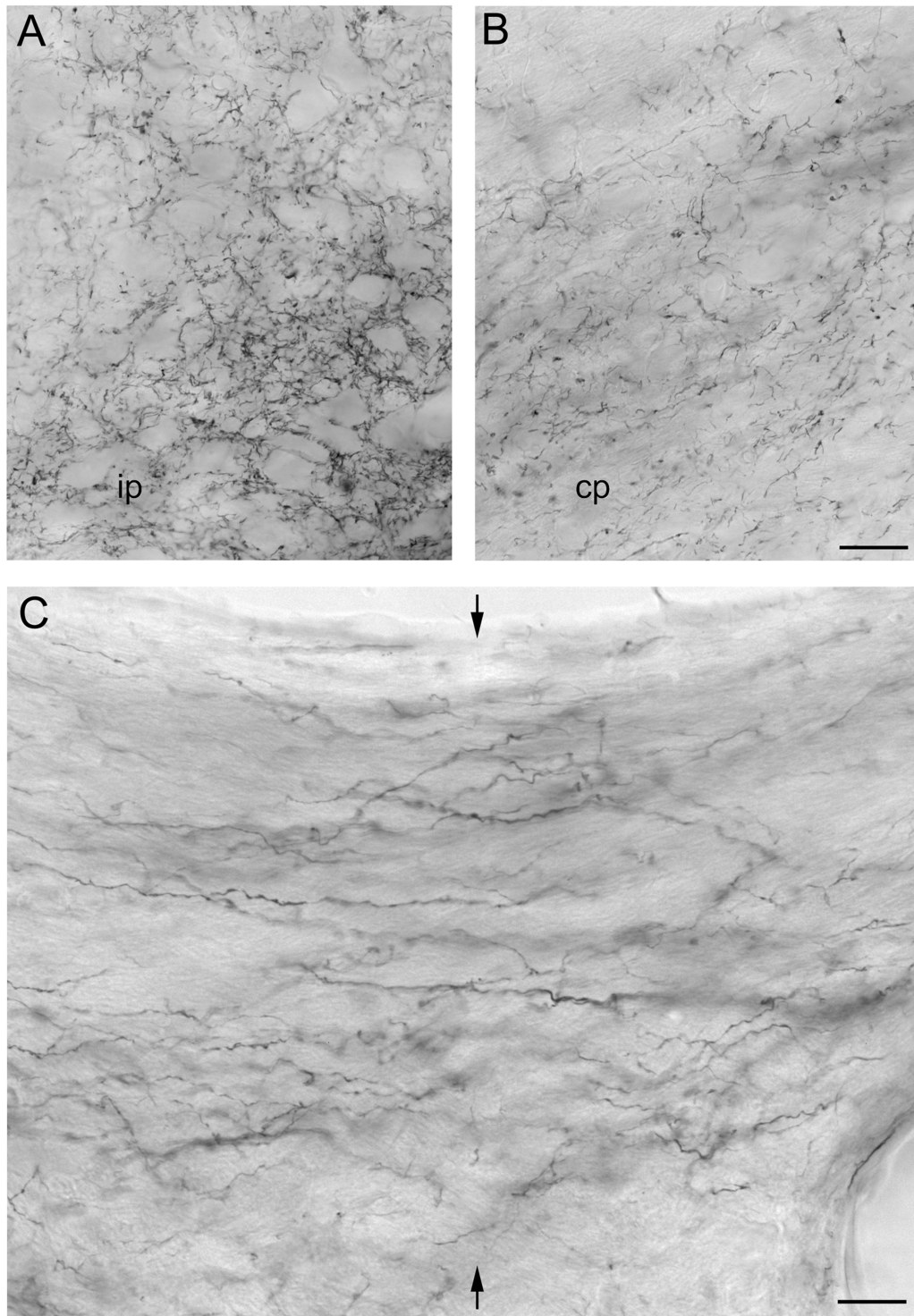


Fig. 4. **A,B:** High magnification views of cross sectional areas of the ipsilateral pontine (ip; A) and the contralateral pontine (cp; B) innervation zone in the ventral pontine nucleus in an IN-1 antibody-treated, lesioned animal. **C:** Midline-crossing fibers. Arrows indicate the midline. Scale bars = 60 μm in B (also applies to A); 20 μm in C.

The treatment with the IN-1 antibody resulted in an increase of the midline-crossing fibers, of fibers growing to more lateral regions of the contralateral pons, and of the

contralateral pontine innervation density. This new contralateral innervation resembled the innervation of the ipsilateral basilar pons, which is organized somatotopi-

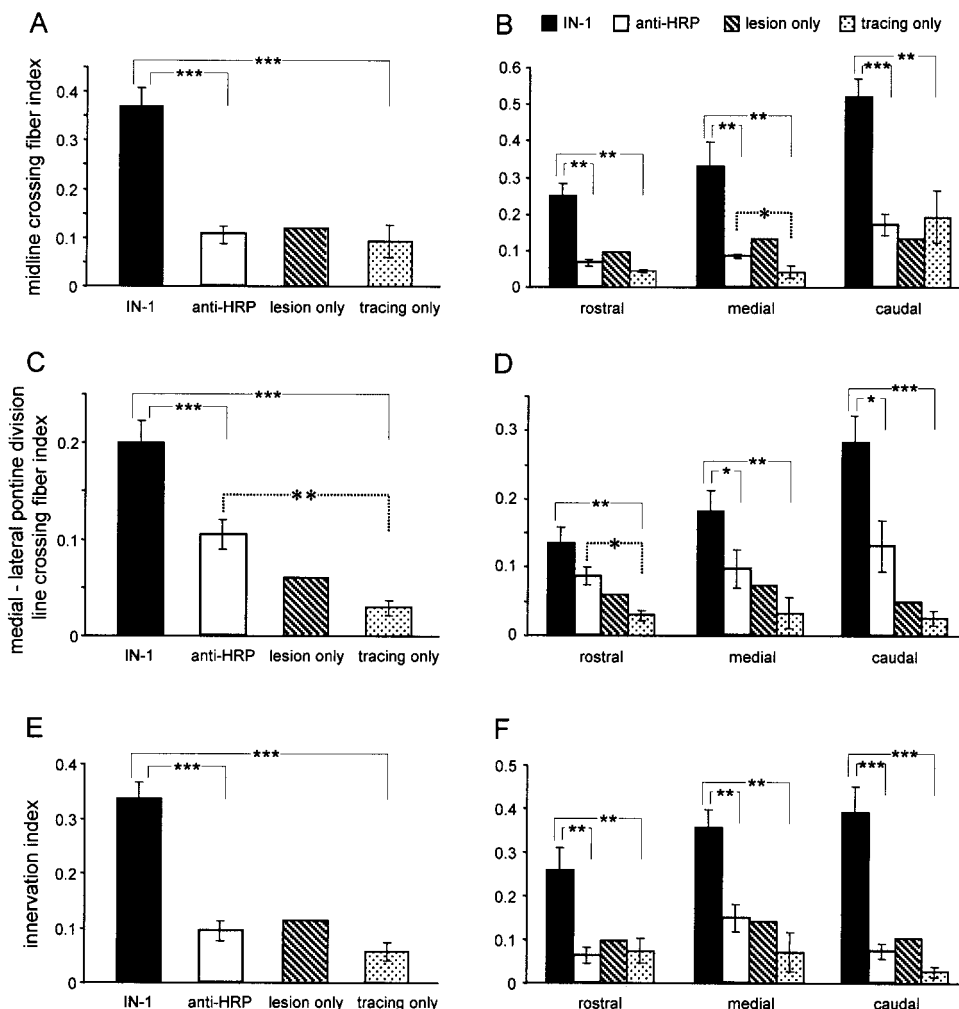


Fig. 5. Three main features were evaluated to quantify the innervation of the basilar pons contralateral to the lesion and the tracer injection site. **A:** Quantification of pontine midline-crossing fibers. In mAb IN-1-treated animals, a three-fold increase of midline-crossing fibers was found, whereas the anti-HRP-treated and lesion-only animals showed values similar to those found in normal rats (tracing only). **B:** Like the normal animals, the number of midline-crossing fibers increased from rostral to caudal pontine levels. At every pontine level, the IN-1 group showed significantly more midline-crossing fibers than the control groups. **C:** To determine which parts of the contralateral pons were reached by the midline-crossing fibers, all axons crossing the pontine division line were counted. The unilateral pyramidal lesion, especially when combined with an anti-HRP antibody treatment, resulted in a small increase in the number of laterally

growing fibers. The lesioned, IN-1 antibody-treated animals, however, showed almost twice as many fibers crossing this lateral line. **D:** The number of fibers crossing the pontine division line increased from rostral to caudal, similar to the number of midline-crossing fibers. This increase was significant for the mAb IN-1-treated and anti-HRP-treated animals at all pontine levels. **E:** Pyramidotomy in combination with IN-1 antibody treatment led to an at least two-fold increase in the innervation index, whereas there were no significant differences between the control groups. **F:** The innervation index was significantly enhanced in mAb IN-1-treated animals at all pontine levels, with a slight trend toward higher values from rostral to caudal. Asterisks indicate significance: single asterisk, $P < 0.05$; double asterisks, $P < 0.01$; triple asterisks, $P < 0.001$ (t test).

cally (Mihailoff et al., 1978; Wiesendanger and Wiesendanger, 1982; Panto et al., 1995). Animals that showed such structural plasticity in the pons and sprouting in the cervical spinal cord recovered almost completely in a food-pellet reaching paradigm, a behavioral task that required fine motor control (Z'Graggen et al., 1998).

The new BDA-labeled axons and terminals contralateral to the lesion and tracer injection site most likely represent sprouted corticofugal fibers; such fibers were virtually absent in normal and lesioned control animals. However, we cannot exclude the possibility that some of the labeled fibers and boutons in the contralateral basilar

pontine nuclei may represent the normal crossed corticopontine projection, which is very small (Wiesendanger and Wiesendanger, 1982; Panto et al., 1995; Z'Graggen et al., 1998). In addition, we showed fibers and boutons in regions of the pons that typically do not receive the normal crossed projection. Thus, we suggest that normal crossed projections play a minor role in the expansion of the contralateral terminal fields after lesion and IN-1 antibody treatment. The increase of midline-crossing fibers in the pons may be derived from fibers that are redirected to the contralateral pons or from neurites that formed new collaterals to innervate the contralateral pontine nuclei.

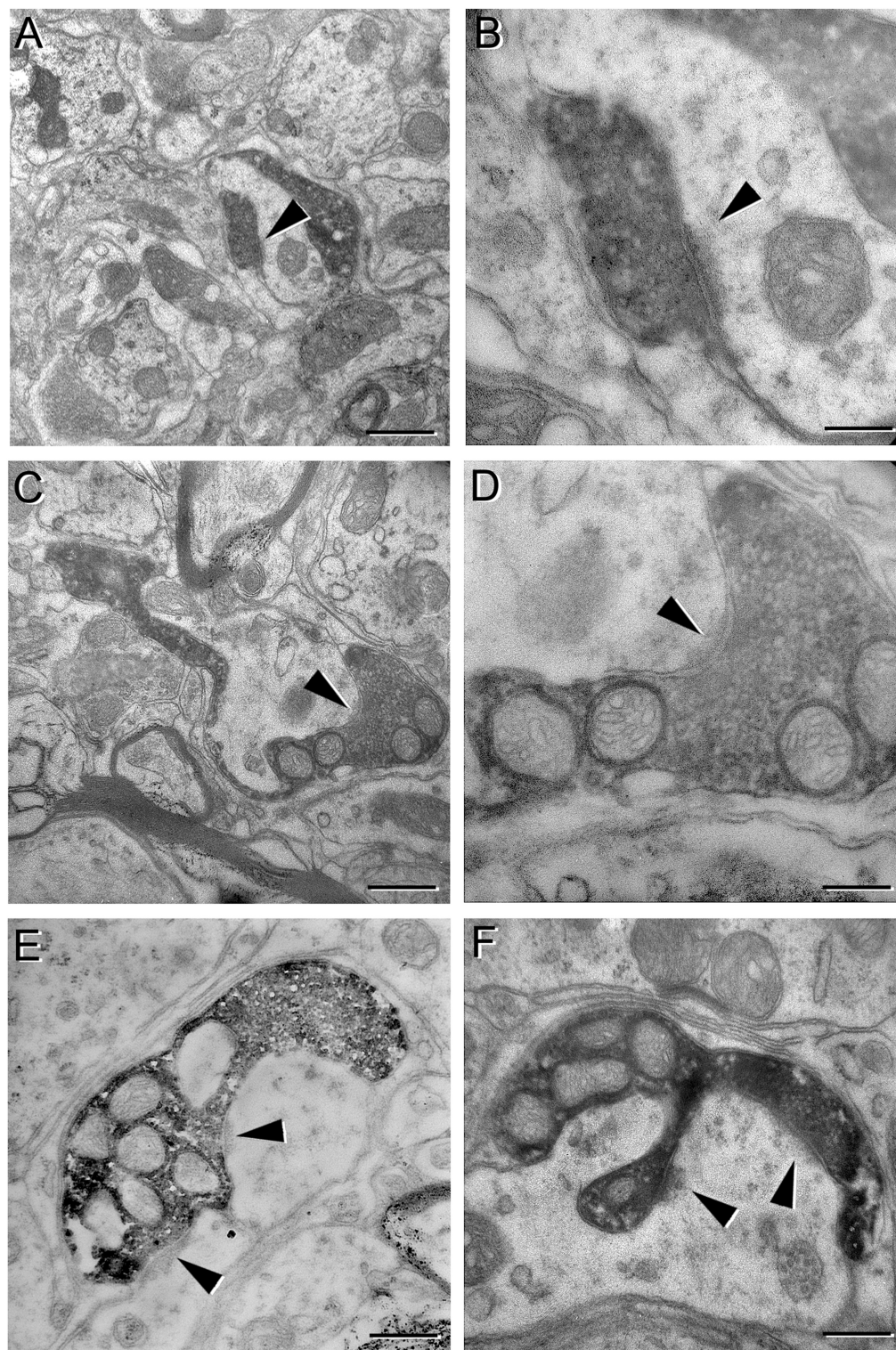


Fig. 6. Representative examples of boutons filled with 3,3'-diaminobenzidine (DAB) reaction product located in the ventral pontine nucleus contralateral to the lesion and the tracer injection site in IN-1 antibody-treated animals. All boutons contained round vesicles. They formed asymmetric synaptic sites (arrowheads) and contacted dendritic processes. **A:** Overview of a region in the ventral pontine nucleus with a labeled synapse. **B:** Higher magnification of the syn-

apse depicted in A. **C:** Unmyelinated axon filled with DAB reaction product with terminal synaptic site. **D:** Higher magnification of the synapse depicted in C. The synaptic cleft, the electron-dense active zone, and the round vesicles are illustrated. **E,F:** Note the irregular shapes of these synapses, both of which show two active sites and contain several mitochondrial profiles. Scale bars = 2.5 μm in A; 0.7 μm in B; 1.6 μm in C; 0.6 μm in D; 1.1 μm in E; 0.4 μm in F.

The new midline-crossing fibers terminated topographically in the contralateral basilar pontine nuclei, and the EM results showed that the synapses formed by these midline-crossing fibers had the typical structural characteristics of corticopontine boutons (Mihailoff and McArdle, 1981). The synaptic contacts were asymmetric (Gray's type I; Gray, 1959) and the boutons contained round vesicles (rat: Mihailoff and McArdle, 1981; cat: Holländer et al., 1969). Considering these structural characteristics, we suggest that the new synapses belong to Mihailoff and McArdle's (1981) category 1 of pontine terminal endings. The finding of new synapses with the typical characteristics of corticopontine presynaptic profiles in the contralateral pons after a unilateral lesion corroborates earlier EM reports in which axonal sprouting in the corticopontine system was described after neonatal cortical lesions (Leong, 1976; Mihailoff and Castro, 1981). The new synapses terminated exclusively on dendrites, as described previously for normal synaptic contacts of the same category (Brodal, 1968; Holländer et al., 1969; Mihailoff and McArdle, 1981).

Neutralization of the myelin-associated neurite growth inhibitor Nogo-A also resulted in some lesion-induced changes in the ipsilateral pons. In the ipsilateral medial pontine nuclei, the fiber density showed a small and variable increase after lesion alone and in combination with antibody treatment. A similar weak increase in fiber density has been found in the ipsilateral pons after a unilateral pyramidotomy in the neonatal and adult rat in a previous report (Z'Graggen et al., 2000). In our study, however, we found a significantly enhanced bouton/fiber index in the ipsilateral pons in mAb IN-1-treated animals after a unilateral pyramidal lesion, reflecting sprouting and possibly reinforcement of ipsilateral corticopontine connections.

The lesion-induced changes of the corticopontine innervation described here probably are due to and influenced by a variety of factors in addition to the neutralization of the neurite growth inhibitor Nogo-A. Functional imbalance of the motor and sensory systems caused by the lesion may lead to an up-regulation of growth-promoting, guidance, and survival factors (Wizenmann et al., 1993; Thoenen, 1995). The nature of these factors in the corticopontine system is not known at the moment. The information for the formation of new, characteristic corticopontine synapses also must be present or reexpressed in these adult animals.

The anatomical results presented here were obtained 2 weeks after the lesion and implantation of the antibody-secreting hybridoma cells. Thus, the structural changes occurred rapidly, and, most likely, these rearrangements remain stable over time, as shown in a previous study from our laboratory (Z'Graggen et al., 1998). The precise time course of sprouting, synapse formation, and possibly also retraction phenomena is not known. Corticopontine fibers may be rerouted or may give rise to new collaterals. When new synapses are formed, a phase of activity-driven refinement may follow and, finally, the elimination of exuberant or wrong connections. Some of the fibers terminating in the pons are collaterals of corticospinal fibers (Ugolini and Kuypers, 1986; Akintunde and Buxton, 1992). The transection of these fibers by the pyramidal lesion may lead to a compensatory sprouting across the pontine midline (Sabel and Schneider, 1988; "pruning effect"). In addition, the unilateral pyramidal lesion denervates

half of the spinal cord and the dorsal column nuclei ipsilateral to the lesion, which may cause a functional imbalance of the motor and sensory systems. Activity-driven up-regulation of neurotrophic or growth-promoting factors may induce the formation of new collaterals, enhanced terminal arborizations, and new synapses in the pontine nuclei.

Recently, a new additional role of Nogo-A has been found (Zagrebelsky et al., 1998): Myelin-associated neurite growth inhibitors seem to actively suppress the expression of growth-associated genes in adult central neurons. Thus, the application of neutralizing antibodies not only may provide a growth-permissive microenvironment by locally masking the myelin-associated neurite growth inhibitor Nogo-A but also may lead to an up-regulation of growth-associated gene expression in the cell body.

In a previous study, we showed that a very high degree of functional recovery takes place after unilateral pyramidotomy and treatment with mAb IN-1 (Z'Graggen et al., 1998). The sprouted fibers and the new synapses described here in the pons, as well as other plastic rearrangements in the brainstem, brain, and spinal cord (Thallmair et al., 1998), probably contribute and collaborate to restore fine movements in these unilaterally lesioned, anti-Nogo-A antibody-treated adult animals.

LITERATURE CITED

- Akintunde A, Buxton DF. 1992. Origins and collateralization of corticospinal, corticopontine, corticorubral and corticostriatal tracts: a multiple retrograde fluorescent tracing study. *Brain Res* 586:208–218.
- Barth TM, Stanfield BB. 1990. The recovery of forelimb-placing behavior in rats with neonatal unilateral cortical damage involves the remaining hemisphere. *J Neurosci* 10:3449–3459.
- Bregman BS, Kunkel-Bagden E, Schnell L, Dai HN, Gao D, Schwab ME. 1995. Recovery from spinal cord injury mediated by antibodies to neurite growth inhibitors. *Nature* 378:498–501.
- Brodal P. 1968. The corticopontine projection in the cat. I. Demonstration of a somatotopically organized projection from the primary sensorimotor cortex. *Exp Brain Res* 5:210–234.
- Caroni P, Schwab ME. 1988a. Antibody against myelin-associated inhibitor of neurite growth neutralizes nonpermissive substrate properties of CNS white matter. *Neuron* 1:85–96.
- Caroni P, Schwab ME. 1988b. Two membrane protein fractions from rat central myelin with inhibitory properties for neurite growth and fibroblast spreading. *J Cell Biol* 106:1281–1288.
- Chen MS, Huber AB, van der Haar ME, Frank M, Schnell L, Spillmann AA, Christ F, Schwab ME. 2000. Nogo-A is a myelin-associated neurite outgrowth inhibitor and an antigen for monoclonal antibody IN-1. *Nature* 403:434–439.
- Gray EG. 1959. Axo-somatic and axo-dendritic synapses of the cerebral cortex: electron microscope study. *J Anat* 93:420–433.
- Herzog A, Brösamle C. 1997. Semifree-floating treatment—a simple and fast method to process consecutive sections for immunohistochemistry and neuronal tracing. *J Neurosci Methods* 72:57–63.
- Holländer H, Brodal P, Walberg F. 1969. Electron microscopic observations on the structure of the pontine nuclei and the mode of termination of the corticopontine fibers. An experimental study in the cat. *Exp Brain Res* 7:95–110.
- Kalil K, Reh T. 1982. A light and electron microscopic study of regrowing pyramidal tract fibers. *J Comp Neurol* 211:265–275.
- Kapfhammer JP. 1997. Restriction of plastic fiber growth after lesions by central nervous system myelin-associated neurite growth inhibitors. *Adv Neurol* 73:7–27.
- Kartje-Tillotson G, Neafsey EJ, Castro AJ. 1986. Topography of corticopontine remodelling after cortical lesions in newborn rats. *J Comp Neurol* 250:206–214.
- Kennard MA. 1936. Age and other factors in motor recovery from precentral lesions in monkeys. *Am J Physiol* 115:138146.
- Kennard MA. 1938. Reorganization of motor function in the cerebral cortex

- of monkeys deprived of motor and premotor areas in infancy. *J Neurophysiol* 1:477–496.
- Kuang RZ, Kalil K. 1990. Specificity of corticospinal axon arbors sprouting into denervated contralateral spinal cord. *J Comp Neurol* 302:461–472.
- Leong SK. 1976. A qualitative electron microscopic investigation of the anomalous corticofugal projections following neonatal lesions in the albino rats. *Brain Res* 107:1–8.
- Mihailoff GA, Castro AJ. 1981. Autoradiographic and electron microscopic degeneration evidence for axonal sprouting in the rat corticopontine system. *Neurosci Lett* 21:267–273.
- Mihailoff GA, McArdle CB. 1981. The cytoarchitecture, cytology, and synaptic organization of the basilar pontine nuclei in the rat. II. Electron microscopic studies. *J Comp Neurol* 195:203–219.
- Mihailoff GA, Burne RA, Woodward DJ. 1978. Projections of the sensorimotor cortex to the basilar pontine nuclei in the rat: an autoradiographic study. *Brain Res* 145:347–354.
- Mihailoff GA, McArdle CB, Adams CE. 1981. The cytoarchitecture, cytology, and synaptic organization of the basilar pontine nuclei in the rat. I. Nissl and Golgi studies. *J Comp Neurol* 195:181–201.
- Panto MR, Cicirata F, Angaut P, Parenti R, Serapide F. 1995. The projection from the primary motor and somatic sensory cortex to the basilar pontine nuclei. A detailed electrophysiological and anatomical study in the rat. *J Hirnforsch* 36:7–19.
- Raineteau O, Z'Graggen WJ, Thallmair M, Schwab ME. 1999. Sprouting and regeneration after pyramidotomy and blockade of the myelin-associated neurite growth inhibitors NI 35/250 in adult rats. *Eur J Neurosci* 11:1486–1490.
- Sabel BA, Schneider GE. 1988. The principle of “conservation of total axonal arborizations”: massive compensatory sprouting in the hamster subcortical visual system after early tectal lesions. *Exp. Brain Res* 73:505–518.
- Schnell L, Schwab ME. 1990. Axonal regeneration in the rat spinal cord produced by an antibody against myelin-associated neurite growth inhibitors. *Nature* 343:269272.
- Schnell L, Schwab ME. 1993. Sprouting and regeneration of lesioned corticospinal tract fibres in the adult rat spinal cord. *Eur J Neurosci* 5:1156–1171.
- Schwab ME, Kapfhammer JP, Bandtlow CE. 1993. Inhibitors of neurite growth. *Annu Rev Neurosci* 16:565–595.
- Thallmair M, Metz GAS, Z'Graggen WJ, Raineteau O, Kartje GL, Schwab ME. 1998. Neurite growth inhibitors restrict plasticity and functional recovery following corticospinal tract lesions. *Nat Neurosci* 1:124–131.
- Thoenen H. 1995. Neurotrophins and neuronal plasticity. *Science* 270:593–598.
- Ugolini G, Kuypers HG. 1986. Collaterals of corticospinal and pyramidal fibres to the pontine grey demonstrated by a new application of the fluorescent fibre labelling technique. *Brain Res* 365:211–227.
- Whishaw IQ, Kolb B. 1988. Sparing of skilled forelimb reaching and corticospinal projections after neonatal motor cortex removal or hemidecortication in the rat: support for the Kennard doctrine. *Brain Res* 451:97–114.
- Wiesendanger R, Wiesendanger M. 1982. The corticopontine system in the rat. II. The projection pattern. *J Comp Neurol* 208:227–238.
- Wizenmann A, Thies E, Klostermann S, Bonhoeffer F, Bahr M. 1993. Appearance of target-specific guidance information for regenerating axons after CNS lesions. *Neuron* 11:975–983.
- Zagrebelsky M, Buffo A, Skerra A, Schwab ME, Strata P, Rossi F. 1998. Retrograde regulation of growth-associated gene expression in adult rat Purkinje cells by myelin-associated neurite growth inhibitory proteins. *J Neurosci* 18:7912–7929.
- Z'Graggen WJ, Metz GAS, Kartje GL, Thallmair M, Schwab ME. 1998. Functional recovery and enhanced corticofugal plasticity after unilateral pyramidal tract lesion and blockade of myelin-associated neurite growth inhibitors in adult rats. *J Neurosci* 18:4744–4757.
- Z'Graggen WJ, Fouad K, Raineteau O, Metz GAS, Schwab ME, Kartje GL. 2000. Compensatory sprouting and impulse rerouting after unilateral pyramidal tract lesion in neonatal rats. *J Neurosci* 20:6561–6569.

Chapter 4

Growth and regeneration associated differential gene expression during development and after axonal injury to the peripheral and central nervous system

Stefan Bloechlinger, Laurie A. Karchewski, Michael Costigan and Clifford J. Woolf

Introduction

The ability of neurite extension and axonal growth within the nervous system of mammals varies strongly with age and between the central and peripheral nervous systems. In the embryonic and early postnatal stage the nervous system's plasticity is enormous, serving to build up the appropriate connections among nerve cells as well as their non-neuronal targets. In the early postnatal stage, the central nervous system (CNS) can restore damage to a high degree and, in parallel with maturation of the CNS, its growth capacity is reduced after birth prohibiting uncontrolled axonal growth in the adult (Cai *et al.*, 2001; Kapfhammer & Schwab, 1994). This lack of axonal growth capacity becomes apparent after injuries to the brain or spinal cord because the loss in function cannot be restored by regeneration of nerve cells and their lost interactions (Schwab, 2004; Schwab & Bartholdi, 1996). In comparison to the adult CNS, the peripheral nervous system (PNS) allows neuronal re-growth after nerve damage, resulting in partial target re-innervation and recovery of lost function (Bray *et al.*, 1981; Rhodes & Fawcett, 2004; Schmitt *et al.*, 2003; Schwab & Bartholdi, 1996).

It is believed that in order to grow successfully, neurons require a favorable environment and the activation of a growth program to do so. Myelin-associated molecules (Nogo, MAG, OMgp) which strongly inhibit axonal growth *in vitro* and *in vivo* are responsible for a great proportion of regenerative failure in the adult CNS (Chen *et al.*, 2000; GrandPré *et al.*, 2000; McKerracher *et al.*, 1994; Schwab, 2004; Wang *et al.*, 2002). Besides inhibitory extracellular cues, the growth capacity of a neuron is crucial, determined by its transcriptional and translational apparatus supplying the cell with structural elements and membrane- and intracellular receptors (Chong *et al.*, 1996; Neumann & Woolf, 1999; Richardson & Issa, 1984; Schreyer & Skene, 1993). It is known that embryonic neurons possess a far greater intrinsic potential for regenerative axonal growth after injury. Therefore,

regenerative axonal growth in the adult nervous system has been attributed to the manifestation of an embryonic-like neuronal phenotype (Cai *et al.*, 2001; Chong *et al.*, 1996; Neumann & Woolf, 1999). A number of intrinsic neuronal molecules have been identified as favorable for neuronal growth, for instance those belonging to the GAP-43-like family (for review see (Bomze *et al.*, 2001; Caroni, 2001; Skene, 1989). GAP-43 (growth-associated protein 43) is widely seen as a typical growth-related protein because of its high expression during embryonic and early postnatal development, its strong induction in dorsal root ganglion (DRG) neurons after injury to the peripheral nerve and its correlation to a growing phenotype (Aigner *et al.*, 1995; Aigner & Caroni, 1993; Chong *et al.*, 1994; Frey *et al.*, 2000; Schreyer & Skene, 1991). Other molecules have been identified and suggested to contribute to axonal growth. Their expression patterns during development and after neural injury in the adult are often not well characterized. It is not clear for most of these genes whether their expression pattern mimics that of GAP-43 and therefore supports the theory of the recapitulation of a developmental transcriptional program after nerve injury in the adult.

In our study we performed microarray analysis on rat DRG and found more than 120 differentially regulated genes during development and following injury. Based on this, we profile the expression of five genes during development and after injury to the peripheral and the central nervous system and compare them to the expression of GAP-43 to test the hypotheses that growth-associated genes are regulated in primary sensory neurons after peripheral axotomy in order to mount a growing phenotype seen during the development of the nervous system. We show that genes regulated after injury do not necessarily recapitulate developmental expression and that some of the examined genes are, in contrast to GAP-43, also regulated by axotomy of their central axons.

Methods

Surgery and tissue collection

Adult male Sprague Dawley rats (200-250g) and rat embryos were used in this study and all procedures were performed in accordance with the Massachusetts General Hospital Animal Research regulations. For surgery, the animals were anesthetized with isoflurane (inhalation induction, 4%; maintenance, 2.5%) and underwent either a unilateral sciatic nerve transection (SNT), a unilateral dorsal rhizotomy (DR) or a bilateral lesion of the dorsal funiculus (DCL) including the ascending dorsal column fibers and the dorsal part of the corticospinal tract (dCST) at thoracic level T6/7. For DR and DCL the spinal cord was exposed by either a hemi- or total laminectomy. The dorsal roots of L4, L5 and L6 (DR) or the dorsal funiculus (DCL), were cut using fine micro-scissors. For SNT, the left sciatic nerve was exposed at midthigh, ligated and transected distal to the ligation. The wound was carefully sutured and animals were kept alive for the indicated numbers of days. Animals were terminally anesthetized by CO₂, decapitated and exsanguinated. The sciatic nerve was exposed and traced to L4 and L5 DRGs. L4 and L5 DRGs were bilaterally removed, followed by dissection of the spinal cord. The dissection of the brain was simultaneously performed by a second person, in order to quickly collect fresh tissue. DRGs and the area of the cerebral cortex including the sensory-motor hindlimb area were removed bilaterally and immediately frozen in tubes on dry ice or, for *in situ* hybridization, embedded in OCT compound (Tissue Tek) and frozen on dry ice. Tissue was stored at -80°C until use.

Microarray Analysis

Total RNA was extracted from homogenized DRG samples using acid phenol extraction (TRIzol reagent, Gibco-BRL). RNA concentration was evaluated by A₂₆₀ measurement, and quality was assessed by electrophoresis on a 1.5% agarose gel. Each RNA

sample used for hybridization of each array was extracted from rat L4 and L5 DRGs (10 ganglia pooled from 5 animals, per sample).

Affymetrix rat genome U34A oligonucleotide microarrays, representing 8799 known transcripts and expressed sequence tags (ESTs), were used (Santa Clara, CA <http://www.affymetrix.com>). Oligonucleotides are arranged in pairs corresponding to different regions of the target mRNA with multiple probe pairs. Each probe pair consists of a 25 nucleotide perfect match (PM) to the target region coupled with a 25-mer with a single mismatch (MM) at the 13th nucleotide. Transcript abundance is estimated by analysis of signal intensity of the PM/MM pairs. The arrays are hybridized with biotin-labeled cRNA, prepared as per standard Affymetrix protocol. Briefly, total RNA (8 µg) from DRGs was reverse transcribed using an oligo-dT primer coupled to a T7 RNA polymerase binding site. Double-stranded cDNA was made and biotinylated-cRNA synthesized using T7 polymerase. The cRNA was hybridized for 16 hours to an array, followed by binding with a streptavidin-conjugated fluorescent marker, and then incubated with a polyclonal anti-streptavidin antibody coupled to phycoerythrin as an amplification step. Following washing, the chips were scanned with a Hewlett-Packard GeneArray laser scanner and data analyzed using GeneChip software. External standards were included to control for hybridization efficiency and sensitivity.

Hybridization levels for each species of mRNA detected on the arrays are expressed by intensity (signal) and as present (P), marginal (M) or absent (A) calls, calculated by Affymetrix software (MAS 5.0, $\alpha_1 = 0.04$ $\alpha_2 = 0.06$). To normalize the array data standard Affymetrix protocols were used, each array was scaled to a target signal of 2500 across all probe sets (MAS 5.0). Genes with A calls or intensity levels < 1000 at every time-point examined were excluded. Genes included into table 1 or 2 show a fold difference ≥ 1.4 or ≤ -1.4 at any one of the investigated experimental conditions, the result obtained for the 3d SNT time-point corresponds to the previously published triplicate chip analysis for that time-point

(cut-off ≥ 1.4 , ≤ -1.4 fold change respectively) and their developmental expression profile and mRNA expression in response to injury has not been well described yet (Costigan *et al.*, 2002).

Isotopic In Situ Hybridization

In situ hybridization was carried out as described previously (Karchewski et al., 1999) using 48 base pair oligonucleotide probes complementary to and selective for the following mRNAs: GAP-43 (Accession #M16228), α -internexin (Accession #M73049), glypican-1 (Accession # NM_030828), α -fodrin (Accession #AF084186), osteopontin (Accession #M146656), α 7-integrin (Accession #X65036). Oligonucleotide probes (80 ng) were labeled using terminal transferase with either α -[³⁵S]dATP or α -[³³P]dATP (NEN, MA, USA) and purified through a spin column (Qiagen, CA, USA). Specific activities ranged from 2.0-5.2 x 10⁶ cpm/ng oligonucleotide.

Slides were hybridized at 43°C for 14-18 hours in a buffer containing 50% formamide, 4x SSC, 1x Denhardt's solution, 1% sarcosyl, 0.02 M phosphate buffer (pH 7.0), 10% dextran sulphate, 500 mg/ml heat-denatured salmon sperm, 200 mM DTT and 10⁷ cpm/ml of radiolabeled oligonucleotide probe. Slides were washed 4 x 15 minutes in 1x SSC at 55°C, brought to room temperature, dipped twice in dH₂O, dehydrated in ascending alcohols, and air-dried. The hybridization stringency conditions used require homologies greater than 90% for retention of the transcripts following the washes (Dagerlind et al., 1992). Slides were stored at 4°C until processed by emulsion autoradiography.

The specificity of hybridization signal for each probe was ascertained by hybridization of adjacent sections with labeled probe, labeled probe with a 1000-fold excess of cold probe, or labeled probe with a 1000-fold excess of another, dissimilar cold probe of the same length and similar G-C content.

Emulsion Autoradiography

Under safelight conditions, slides were dipped in NTB-2 nuclear track emulsion (Kodak) (1:1 in dH₂O) dried and stored in lightproof slide boxes with desiccant at 4°C. The sections were exposed for 1-12 weeks before being developed and fixed. For viewing under darkfield conditions using a fiber-optic darkfield stage adapter (MVI, MA, USA), slides were left unstained and coverslipped using glycerol. For viewing under the brightfield microscope, slides were counterstained with 0.5% Toluidine blue (pH 4-4.5), differentiated and coverslipped using Permount (Fisher). Photographs were taken using a Spot camera (Diagnostic Instruments Inc., MVI, MA, USA).

Slot blotting

Slot blots were produced as described previously (Costigan *et al.*, 2002). Briefly total RNA (1.25 µg) was directly transferred to Hybond N+ nylon membrane under vacuum. The slot blots were produced in batches of six. Each tissue type RNA sample was applied from a master mix ensuring equal loading across all of the blots. Gene specific probes between 200-500 bp were produced using RT-PCR. PCR was performed on cDNA reverse transcribed from total RNA, extracted from lumbar DRGs, using poly-dT as a primer. Primers were designed using the Primer3 software (<http://www-genome.wi.mit.edu/>) from the 1000 most 3' nucleotides within each accession sequence. These fragments were subsequently cloned into the PCRII vector (TA cloning Kit, Invitrogen) and the identity of each was confirmed by sequencing. These cDNAs were gel-purified and used to produce ³²P-labeled cDNA probes (Prime-It kit, Stratagene).

Results

Growth-related genes have distinct expression patterns in the DRG of the developing CNS.

Chip analysis from lumbar DRG reveals the characteristic expression of growth-associated protein-43 (GAP-43), a crucial protein determining axonal growth processes, during CNS development (Donovan *et al.*, 2002; Frey *et al.*, 2000; Karimi-Abdolrezaee *et al.*, 2002). High levels of GAP-43 mRNA are detected in DRG at time-points E15, E18, E20 until P0 followed by a significant decrease in GAP-43 expression in the adult animal (2.4 fold change P0 vs. adult, Figure 1A). α -internexin, the earliest intermediate filament expressed during embryonic development (Ching & Liem, 1991; Chiu *et al.*, 1989; Fliegner *et al.*, 1990; Kaplan *et al.*, 1990; Pachter & Liem, 1985), shares the property of high expression in DRG early in development at E15 and declining levels of detectable mRNA towards adulthood (Figure 1B). In contrast to GAP-43 mRNA levels of α -internexin rapidly decrease after E15 and show a slower reduction between E18 and P0. GAP-43 and α -internexin represent genes with strong expression during embryonic development of the CNS when neural cell migration, proliferation and differentiation, as well as neuritogenesis occur and both are genes with moderate to low levels of mRNA in the adult DRG. Although α -internexin was attributed an absent (A) call in the adult DRG, *in-situ* hybridization and slot-blot analysis clearly detect α -internexin mRNA in the adult DRG (Figure 1B, 2B and 3B).

In general we have observed two other major developmental expression patterns for growth-related genes in the rat lumbar DRG. Glypican-1, a glycosyl phosphatidyl inositol (GPI) – anchored heparan sulphate proteoglycan (for reviews see Bandtlow & Zimmermann, 2000; Fransson, 2003), and α -fodrin, a member of the spectrin superfamily of submembranous cytoskeletal proteins (Hartwig, 1995; Ursitti *et al.*, 2001), are both expressed at high levels in the embryo and expression levels remain stable in the adult DRG, revealing relatively constant gene expression in the developing as well as in the mature rat DRG (Figure

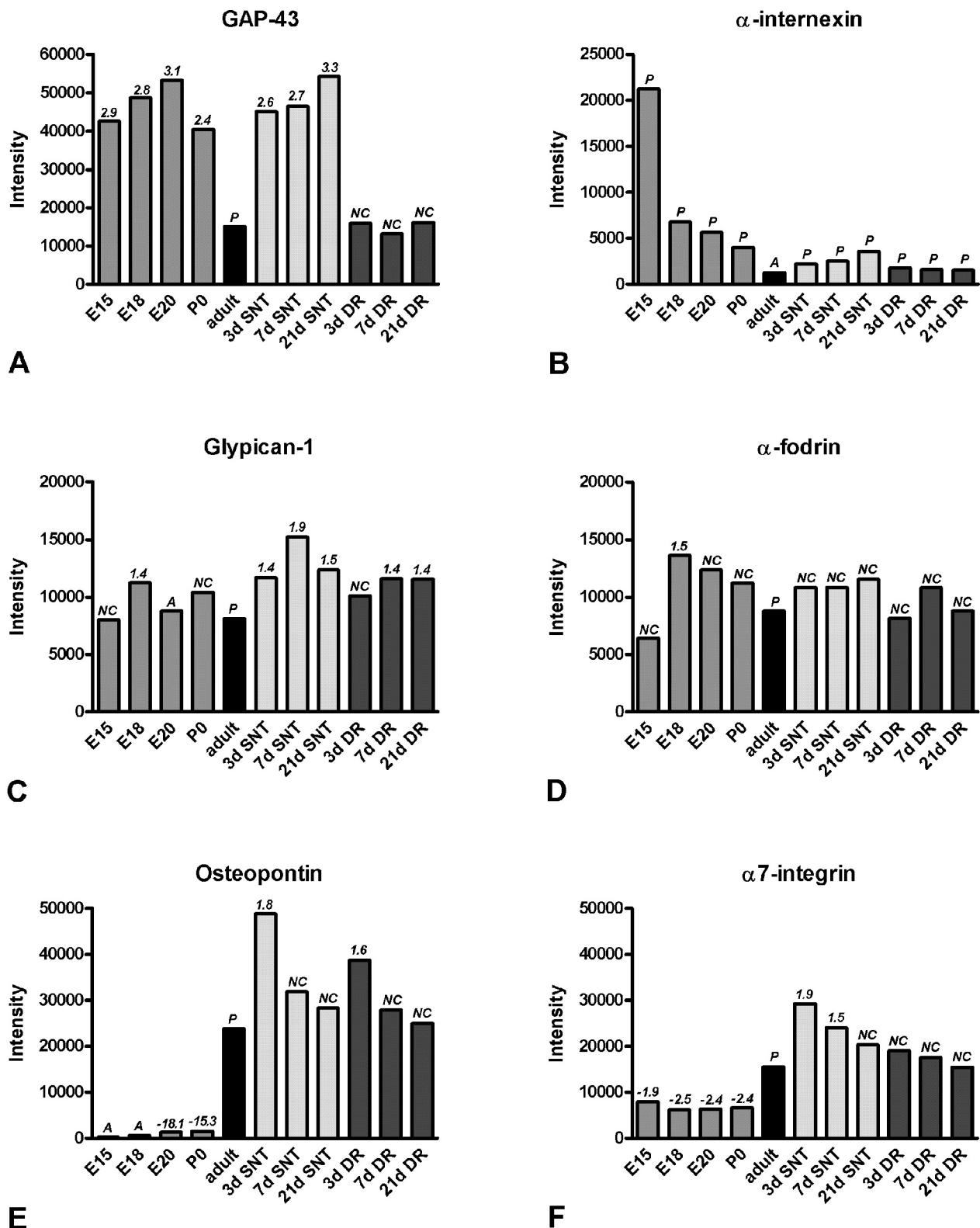


Figure 1

Bar graph revealing data obtained from microarrays showing the developmental expression-intensity of six selected genes in lumbar DRGs at embryonic days 15, 18 and 20, as well as at postnatal day 0 and in the adult. Included is the comparison of the expression pattern following peripheral (SNT; sciatic nerve transection) or central (DR, dorsal rhizotomy) axotomy to the non-injured (naïve) in the adult lumbar DRG at day 3, 7 and 21 post-injury. (A): absent call by Affymetrix; (P): present call by Affymetrix; (NC): no change. Values above bars represent the fold difference compared to adult.

1C and 1D). Osteopontin, a glycoprotein with diverse functions in cell adhesion and cellular activation, chemoattraction and immunomodulation (for review see (Denhardt & Guo, 1993; Denhardt *et al.*, 2001; Wang *et al.*, 1998), is detected at very low levels in E15 and E18 DRG (absent (A) call by Affymetrix). Slightly higher levels of mRNA are detected by chip analysis in the DRG at E20 and P0 (present (P) call, Figure 1E). In the adult rat DRG, osteopontin mRNA expression is increased 15.3 fold compared to P0 (Figure 1E). The $\alpha 7$ -integrin subunit of the laminin-1/-2 receptive molecule $\alpha 7/\beta 1$ -integrin (Hammarberg *et al.*, 2000; Yao *et al.*, 1996) shows moderate levels of mRNA at embryonic stages, with a substantial increase of mRNA levels in the adult DRG (adult vs. P0 2.4 fold increase, Figure 1F). Together, these two genes show highest mRNA expression in the adult DRG, whereas lower levels of mRNA are detected in the embryo.

We find 116 genes that showed significant developmental regulation in DRGs falling into different categories including genes coding for structural and signaling molecules as well as proteins involved in cell metabolism (Table 1). Many ribosomal components are found to be strongly expressed early in development showing generally slightly lower but still elevated expression levels around P0 compared to adult (Table 2).

Sciatic nerve transection (SNT) dynamically up- or down-regulates neural growth-related genes in adult DRG neurons.

Affymetrix gene chip analysis performed with mRNA from adult lumbar L4 and L5 DRG compares the expression of the above mentioned genes between uninjured animals and animals that underwent a SNT either 3 days, 7 days or 21 days prior to mRNA preparation. SNT is known to cut approximately 60% of the axons of L4 and L5 lumbar DRG neurons. Here we show that GAP-43 mRNA expression is induced as early as 3 days post-SNT (2.6 fold increase) and mRNA levels increase over the whole time-course examined (21d SNT vs. adult 3.3 fold, Figure 1A). α -internexin, dramatically down-regulated during development,

Table 1. Differential gene expression during development and following central and peripheral nerve injury in the rat lumbar DRG

Probe set	Gene	Fold difference from adult non-injured DRG										Pattern
		development					SNT			DR		
		E15	E18	E20	P0	3d	7d	21d	3d	7d	21d	
Proteoglycans												
S61868_g_at	Ryudocan=heparan sulfate proteoglycan core protein	A	-1.8	-1.5	-1.4	NC	NC	NC	NC	NC	NC	↓/-/ G
U33553_at	Neuroglycan C precursor	1.4	2.3	1.7	1.8	1.4	1.4	A	A	NC	NC	↑/↑/- A
X59859_i_at	Decorin	-42.7	A	-4.3	-4.8	NC	1.5	1.5	NC	NC	1.5	↓/↑/↑ E
X84039_at	Lumican	-3.2	NC	-1.6	-2.7	NC	NC	NC	NC	NC	NC	↓/↑/- G
Cytoskeletal proteins												
J02780_at	Tropomyosin (TM-4)	NC	NC	1.4	1.8	NC	NC	NC	NC	NC	NC	↑/-/ B
M75148_at	Kinesin light chain C	-1.9	NC	1.7	1.5	NC	NC	NC	NC	NC	NC	↑/-/ B
X66845_at	Cytoplasmic dynein 74 kD intermediate chain	NC	2.2	1.6	1.4	-1.9	-2.1	-1.4	-1.4	NC	NC	↑/↓/↑ H
Extracellular matrix proteins												
D83349_at	Short type PB-cadherin	NC	2.2	1.6	1.4	NC	NC	NC	NC	NC	NC	↑/-/ B
M21354_s_at	Collagen type III alpha-1	-1.9	NC	1.7	1.5	NC	NC	-1.4	NC	NC	-1.4	↑/↓/↑ H
X94551_at	Laminin gamma 1	NC	NC	1.4	1.8	NC	NC	NC	NC	NC	NC	↑/-/ B
Growth factors/receptors												
A03913cds_s_at	Glia-derived neurite-promoting factor (GdNPF)	NC	NC	-1.4	-1.5	NC	NC	-1.6	NC	NC	NC	↓/↓/- J
D14839_at	FGF-9	A	A	-2.6	-2.7	-2.2	-1.8	A	NC	-1.4	-1.5	↓/↓/↓ I
M74223_at	VGF	NC	2.3	2.1	2.8	3.8	2.9	3.9	3.1	3.2	NC	↑/↑/↑ C
U90610_at	CXC chemokine receptor (CXCR4)	NC	A	-1.4	NC	NC	NC	-1.8	A	NC	NC	↓/↓/- J
U97142_at	RET ligand 1 (RET1) = GDNF receptor alpha	-2	A	-2.7	-2.5	3.3	3.7	3.3	1.7	2.1	NC	↓/↑/↑ E
Neurotransmission												
AB016160_at	GABAB receptor 1c	NC	2.3	1.7	1.7	NC	NC	NC	-1.4	NC	NC	↑/↓/↓ K
S45812_s_at	Monoamine oxidase A	-1.8	-1.6	-1.4	-1.7	2	2.3	2.3	NC	NC	NC	↓/↑/- F
S50879_at	Acetylcholinesterase T subunit	A	A	NC	NC	-1.4	-1.6	-1.7	NC	NC	NC	-↓/↓/- L
U01227_s_at	5HT3 receptor subunit	-3.1	-3.3	-2.3	-2	-1.6	-1.6	-1.5	NC	NC	NC	↓/↓/- J
X53944_at	Dopamine D3 receptor	NC	NC	NC	NC	NC	NC	NC	NC	NC	-1.8	-↓/↓ O

Exocytosis/vesicles/synapses

AB003991_at	SNAP-25A	-2.9	-2	-2.1	A	NC	-1.4	-1.4	-1.6	NC	NC	I
AF054826_at	VAMP5	A	M	-1.7	-1.7	NC	A	NC	NC	NC	NC	G
D90211_s_at	96 Kd lysosomal membrane glycoprotein (LGP 96)	-5.1	-2.7	-1.9	-1.9	NC	NC	NC	NC	NC	NC	G
E13644cds_s_at	Neurodap-1	A	NC	NC	NC	-1.4	-1.4	NC	-1.8	-1.6	NC	H
L05435_at	Synaptic vesicle protein (SV2)	2.1	4.1	2.6	3.9	NC	2	1.8	A	M	NC	A
M24104_g_at	Vesicle associated membrane protein (VAMP-1 = synaptobrevin2)	A	A	-2.4	-1.6	NC	-1.5	-1.6	-1.5	-2.1	NC	I
M93669_at	Secretogranin II	A	A	NC	NC	-1.4	-2.4	-1.4	NC	NC	NC	L
U02983_at	Secretogranin III (SgIII)	NC	-2	-2.5	-2.3	NC	NC	NC	NC	NC	1.4	K
U14398_g_at	Synaptotagmin IV	NC	NC	NC	1.4	2.6	2.1	2.3	NC	1.5	NC	C
X06832cds#2_s_at	Prechromogranin A	NC	NC	-2	NC	-3.3	A	-8.5	-1.7	-1.9	-1.8	I
X06889cds_at	Rab3	-3	-1.6	-1.2	-1.2	-1.6	-1.6	-1.4	NC	-1.4	NC	I
X89968_g_at	Alpha-soluble NSF attachment protein	-2.6	-1.6	-1.9	-1.8	NC	NC	NC	NC	NC	NC	G

Lipid metabolism

AF036761_at	Stearoyl-CoA desaturase 2	-2.4	NC	-1.5	-1.9	NC	NC	-1.4	-2.9	-2.2	-1.6	I
DI3921_s_at	Mitochondrial acetoacetyl-CoA thiolase	1.7	1.6	1.6	1.7	NC	A	A	NC	NC	NC	B
J05122	Peripheral benzodiazepine receptor	A	-1.6	NC	NC	1.5	2.3	2.6	1.6	NC	NC	E
S75730_at	Stearoyl-CoA desaturase 2 SCD2 homologue	-1.4	NC	NC	-1.4	NC	NC	NC	-1.9	-1.6	NC	D
S76779_s_at	Apolipoprotein E	-67.8	-2.3	-2.7	-2.6	NC	NC	NC	NC	NC	NC	G
S81497_i_at	Lysosomal acid lipase=intracellular hydrolase	-2.6	-1.3	-1.4	-1.6	-1.4	-1.5	NC	-1.4	NC	NC	I
U67995_s_at	Stearyl-CoA desaturase 2	-2.2	-1.4	-1.8	-2.6	NC	NC	NC	NC	NC	-1.7	D
U90725_s_at	Caveolae-associated protein	-2.5	NC	NC	-1.9	NC	NC	-1.9	NC	NC	-1.4	I
X04979_at	Apolipoprotein E	-15.7	-1.9	-2.4	-2	NC	NC	NC	NC	NC	NC	G
X13527cds_s_at	Acyl carrier protein domain of fatty acid synthetase	1.7	3	1.6	1.6	NC	NC	NC	-1.4	NC	NC	K

Amino acid metabolism

M80804_s_at	Protein which stimulates transport of cystine and dibasic and neutral amino acids	-1.5	1.6	1.6	1.7	NC	-1.4	-1.5	-2.1	-1.4	NC	H
M91652complete_seq_at	Glutamine synthetase (glnA)	-2	A	-1.8	-2.3	1.5	NC	1.5	1.4	NC	1.7	E

Ion channels/transporters

AF055477_at	Pore-forming calcium channel alpha-1B	1.4	1.5	2.2	1.8	NC	NC	NC	NC	NC	NC	B
M28648_s_at	Na,K-ATPase alpha-2	A	A	-1.6	NC	-1.9	A	-1.5	-2.1	-1.4	NC	I
M74494_g_at	Sodium/potassium ATPase alpha-1	-6	-2.7	-1.8	-1.6	-2	-2	-2.1	-1.4	NC	NC	I
M86621_at	Dihydropyridine-sensitive L-type calcium channel alpha-2 subunit (CCHL2A)	1.8	2.2	NC	1.8	4.7	5.1	5	1.6	1.6	1.4	C
U79568_s_at	Voltage-dependent sodium channel PN1	2.6	M	2.8	3.2	NC	NC	A	NC	A	NC	B

X12589cds_s_at	Voltage-dependent potassium channel protein										I
Kinases	A	A	-43.6	-32.6	NC	-3.6	NC	-1.5	-2	-1.8	↓/↓/↓
D30040_at	NC	2	NC	1.4	NC	NC	NC	A	NC	NC	↑/-/ B
D78588_at	-1.8	NC	1.6	1.7	-1.6	NC	-1.5	NC	NC	NC	↑/↓/ L
J04063_at	A	-2.4	-2.1	-2.6	-1.8	-1.5	-1.8	-1.4	-1.8	NC	↓/↓/ I
M15523_s_at	NC	NC	NC	NC	-1.5	NC	NC	-1.8	NC	NC	-↓/↓ H
M18331_at	-1.5	NC	NC	NC	-1.6	-1.4	-1.6	NC	NC	NC	↓/↓/ J
M61177_s_at	-7.1	-1.6	-1.6	-1.8	NC	NC	NC	NC	NC	NC	↓/-/ G
U22297_at	NC	NC	NC	NC	NC	NC	-1.4	NC	NC	-1.6	-↓/↓ H
U36444cds#1_g_at	1.4	1.9	2	1.8	NC	NC	NC	NC	NC	NC	↑/-/ B
X59737mRNA_at	-8.4	-5.6	-3.4	-2.6	NC	-1.7	-1.8	NC	NC	NC	↓/↓/ J
Phosphatases											
AF095927_g_at	2	2	1.6	NC	NC	NC	NC	NC	NC	NC	↑/-/ B
L19933_s_at	1.8	2.4	1.5	1.6	NC	NC	NC	NC	NC	NC	↑/-/ B
M83298_at	1.6	M	1.5	1.5	NC	NC	NC	NC	NC	NC	↑/-/ B
S79213_at	1.4	1.6	1.7	2.1	NC	NC	NC	NC	NC	NC	↑/-/ B
U42627_at	2.1	1.6	2.2	2.2	NC	1.4	M	A	1.5	A	↑/↑/ C
Diverse enzymes											
AB008807_at	1.9	NC	1.5	1.5	NC	NC	NC	NC	NC	NC	↑/-/ B
AB009999_g_at	A	A	-2.7	-2.2	1.5	NC	NC	NC	NC	NC	↓/↑/ F
AF093773_s_at	-1.8	-1.7	-1.4	-1.5	NC	-1.5	-1.4	NC	NC	NC	↓/↓/ J
D10699_g_at	-2.2	-1.5	-1.4	-1.5	NC	NC	NC	NC	NC	NC	↓/-/ G
D28560_at	1.6	A	NC	-1.6	NC	NC	-1.4	NC	NC	NC	↓/↓/ J
L11319_g_at	2	NC	1.8	1.5	NC	NC	NC	NC	NC	-1.6	↑/-/↓ K
L27124_s_at	1.8	2.8	1.6	1.6	NC	NC	NC	NC	NC	NC	↑/-/ B
S77494_s_at	-2.1	6.2	6.8	4.1	NC	A	NC	NC	1.5	A	↑/-/↑ N
U50842_at	1.6	1.5	NC	NC	NC	NC	NC	-1.4	-1.4	NC	↑/-/↓ K
U52663mRNA#3_s_at	-2.5	-5.5	-2	-2.6	NC	NC	NC	NC	NC	NC	↓/-/ G
U54632_g_at	2.5	2.1	1.7	1.7	NC	NC	NC	NC	NC	NC	↑/-/ B
U60882_at	3.6	1.8	1.8	1.7	NC	NC	NC	NC	NC	NC	↑/-/ B
X06984cds_s_at	-3.4	-2.7	-2	-2	NC	NC	NC	NC	NC	NC	↓/-/ G
X07365_s_at	NC	1.5	-1.6	NC	NC	NC	NC	1.6	1.4	NC	↓/-/↑ K
X07944exon#1-12_s_at	1.8	1.7	NC	1.4	NC	NC	NC	NC	NC	NC	↑/-/ B

Transcription factors

AB012230_g_at	NF1-B1	1.9	1.7	1.6	NC	NC	NC	NC	A	NC	NC	↑/-	B
AB012231_s_at	NF1-B2	1.7	1.9	1.7	1.6	NC	NC	NC	NC	NC	NC	↑/-	B
AB016536_s_at	AIF-C1	1.5	1.7	1.7	1.6	1.4	1.4	NC	A	NC	A	↑/↑	A
L28801_at	Transcription factor IIIC alpha-subunit	NC	NC	-2.1	-1.4	-2	NC	-1.5	-2.9	-1.5	NC	↓/↓	I
U41164_at	Cys2/His2 zinc finger protein (rKr1)	-1.9	-2.1	-1.7	-2.2	NC	NC	NC	NC	NC	NC	↓/-	G

Immunological proteins

AF074609mRNA_f_at	MHC class I antigen (RT1.EC3)	-6	-3.4	-3	-2.1	NC	NC	NC	NC	NC	NC	↓/-	G
L40364_f_at	MHC class I RT.O type - 149 processed pseudogene	A	-12.8	-7.6	-4.8	NC	NC	NC	NC	NC	-1.4	↓/↓	D
M11071_f_at	MHC class I cell surface antigen	NC	-2.4	-1.6	-1.6	NC	NC	NC	NC	NC	NC	↓/-	G
M60103_at	Leukocyte common antigen related protein	2.1	1.6	1.7	1.4	NC	NC	NC	NC	NC	NC	↑/-	B
M92340_at	Interleukin 6 signal transducer	-4.3	A	-2.9	-1.9	-1.5	NC	-1.5	NC	-2	NC	↓/↓	I
U49062_at	Heat sle antigen CD24	7.4	3.7	3.6	3.1	NC	NC	NC	NC	NC	NC	↑/-	B
U75392_s_at	B-cell receptor associated protein 37 (BAP-37)	2.3	NC	1.7	1.6	NC	NC	NC	NC	NC	NC	↑/-	B
X61381cds_s_at	Interferon induced mRNA	-5.5	-3.4	-3.1	-2.9	1.5	1.5	1.4	NC	NC	NC	↓/↑	F

Diverse genes

AF071225_at	Cyclophilin B	1.9	1.4	NC	NC	NC	NC	NC	NC	NC	NC	↑/-	B
AF083269_g_at	p41-Arc	-4.1	-2.9	-1.4	NC	1.8	2.1	1.8	NC	2	NC	↓/↑	E
AJ001929_s_at	CBP-50 protein	1.5	1.8	1.6	NC	NC	NC	NC	NC	NC	NC	↑/-	B
AJ007291_g_at	CAPI gene	NC	NC	-1.6	-1.5	NC	NC	-1.6	NC	NC	NC	↓/↓	J
D14048_g_at	SP120	3.1	1.4	2	1.6	NC	NC	NC	NC	NC	NC	↑/-	B
D17445_at	14-3-3 protein eta-subtype	-3.5	-2.3	-1.7	-1.7	NC	-1.4	NC	NC	NC	NC	↓/↓	J
D30739_s_at	14-3-3 protein mRNA for mitochondrial import stimulation factor (MSF) L	2	1.6	1.7	1.6	NC	NC	NC	NC	NC	NC	↑/-	B
D37951UTR#1_at	MIBP1 (c-myc intron binding protein 1)	1.7	1.5	1.6	1.7	NC	NC	NC	NC	NC	NC	↑/-	B
L01793_g_at	Glycogenin	A	A	-2.3	-2.7	-2.1	-1.5	-1.6	-1.6	NC	NC	↓/↓	I
M19936_at	Sulfated glycoprotein 1 (SGP-1)	-3.1	-2.8	-2	-1.9	NC	NC	NC	1.4	1.5	NC	↓/-	K
M81088_at	EF-1-alpha	2.3	NC	NC	1.4	NC	NC	1.4	NC	NC	NC	↑/↑	A
S72594_s_at	TIMP-2=tissue inhibitor of metalloproteinase type 2	-13	-3.2	-1.9	-1.7	NC	NC	NC	NC	NC	NC	↓/-	G
S83025_s_at	TSH receptor suppressor element-binding protein-1=Y-box protein	3.2	2.6	2.7	2.5	NC	NC	NC	NC	NC	NC	↑/-	B
S83320_g_at	r-HuD=HuD	2.3	1.9	1.5	NC	NC	NC	NC	NC	NC	NC	↑/-	B
U03390_at	Protein kinase C receptor	4.1	3.1	2.1	NC	NC	1.6	NC	1.4	NC	NC	↑/↑	C
U03416_at	Neuronal olfactomedin-related ER localized protein (D2Sut1e)	1.8	2.6	2.6	2.5	NC	NC	NC	NC	NC	NC	↑/-	B
U08290_at	Neuronatin alpha	9.8	10.4	7	5.9	NC	NC	1.8	NC	NC	1.5	↑/↑	C

U12568_at	ADP-ribosylation factor-like protein 3 (rard3)	NC	A	1.5	NC	NC	NC	1.4	NC	1.5	1.7	↑/↑	C
U23769_at	CLP36 (clp36)	NC	NC	NC	NC	2.6	2.3	1.9	NC	NC	NC	-/-	M
U39875_at	EF-hand Ca2+-binding protein p22	-5.2	-1.5	-1.4	-1.9	NC	NC	NC	-1.4	NC	NC	↓/↓	D
U75928UTR#1_s_at	SPARC	-3.1	-2.6	-1.5	-1.7	NC	NC	NC	NC	NC	NC	↓/↓	G
U88958_at	Neuritin	-2.2	NC	1.4	1.5	-2	-1.9	-1.8	NC	NC	NC	↑/↓	L
U96130_at	Glycogenin	A	-7.1	-3	-3.9	-1.7	-1.7	-1.4	NC	NC	NC	↓/↓	J
V01543mRNA_at	Brain specific peptide	1.7	1.9	1.9	1.9	1.4	1.9	1.9	A	NC	NC	↑/↓	A
X06916_at	Protein p9Ka homologous to calcium-binding protein	M	A	M	-5.6	NC	NC	NC	NC	1.4	1.4	↓/↑	K
X07648cds_at	Amyloidogenic glycoprotein (rAG)	NC	1.7	1.4	1.6	NC	NC	NC	NC	NC	NC	↑/↓	B
X14265_at	CaMIII gene for calmodulin III	-1.4	NC	NC	NC	NC	NC	NC	NC	NC	-1.4	↓/↓	D
X17053cds_s_at	Immediate-early serum-responsive JE gene	-1.4	A	A	NC	2	1.6	1.5	1.6	1.4	1.4	↓/↑	E
X76489cds_g_at	CD9 cell surface glycoprotein	-11.1	-5.5	-4.8	-5.1	NC	-1.5	NC	NC	NC	-1.6	↓/↓	I
X82021cds_at	Heat shock related protein	NC	NC	NC	NC	-1.4	NC	-1.5	-1.6	-1.4	NC	-/↓	H
X82396_at	Cathepsin B	-6.1	-4.3	-3.2	-2.8	NC	NC	NC	NC	NC	NC	↓/↓	G
Y15068_at	Hsp70/Hsp90 organizing protein	NC	NC	-1.4	-1.7	-1.4	NC	-1.5	-1.5	NC	NC	↓/↓	I

Table 1. Differential gene expression during development and following central and peripheral nerve injury in the rat lumbar DRG

List of genes, detected to be regulated during development of the nervous system or after axonal injury by affymetrix gene chip analysis. Genes are listed as functional groups. Numbers show fold differences from adult non-injured (naïve) DRG. Every single gene was further assigned a capital letter (A-O) according to its expression pattern. SNT: sciatic nerve transection; DR: dorsal rhizotomy; E: embryonic day; P: postnatal day. (A): absent call by Affymetrix; (M): marginal call by Affymetrix; (P): present call by Affymetrix; (NC): no change (fold difference <1.4).

Table 2. Genes encoding ribosomal proteins

Probe set	Gene	Fold difference from adult DRG			
		E15	E18	E20	P0
X62166cds_s_at	Ribosomal protein L3	2.4	1.9	1.4	1.4
M17419_at	Ribosomal protein L5	2.6	1.9	NC	1.5
X15013cds_at	Ribosomal protein L7a	2.5	2.8	1.5	1.6
X62145cds_g_at	Ribosomal protein L8	2.4	1.6	NC	NC
X51706cds_at	Ribosomal protein L9	2.1	NC	NC	NC
X93352_at	Ribosomal protein L10a	2.9	2.3	1.8	1.7
X62146cds_at	Ribosomal protein L11	2.8	2.4	1.6	1.6
X53504cds_at	Ribosomal protein L12	2.6	2	1.4	1.5
X78327_at	Ribosomal protein L13	2.9	2.4	1.4	1.9
X58389cds_s_at	Ribosomal protein L17 ¹⁾	3	1.5	1.7	1.6
M20156_at	Ribosomal protein L18 ¹⁾	2.7	2.2	1.4	1.6
X14181cds_s_at	Ribosomal protein L18a	3.3	2.8	1.6	2
M27905_at	Ribosomal protein L21	1.9	1.4	NC	NC
X58200mRNA_at	Ribosomal protein L23	2.9	2	1.5	1.6
X65228cds_s_at	Ribosomal protein L23a ¹⁾	4.2	2.7	2.1	2.2
X14671cds_s_at	Ribosomal protein L26	2.1	1.4	1.4	1.4
X52733cds_s_at	Ribosomal protein L27a ¹⁾	2.6	2.1	1.6	1.6
X52619_at	Ribosomal protein L28	2.5	1.8	1.5	1.6
X68283_at	Ribosomal protein L29	2.8	2.4	1.9	1.8
X06483cds_at	Ribosomal protein L32	2.9	2	1.8	1.7
M34331_at	60S ribosomal subunit protein L35 ¹⁾	3.8	4	1.7	2.1
X66369_at	Ribosomal protein L37	3	1.7	1.9	1.7
X15096cds_s_at	Acidic ribosomal phosphoprotein P0	2	2.2	1.4	1.5
X55153mRNA_s_at	Ribosomal protein P2	2.2	2	NC	NC
X57432cds_s_at	Ribosomal protein S2 ¹⁾	2.9	2.8	1.6	1.8
X51536cds_at	Ribosomal protein S3	2.2	1.6	NC	NC
X14210cds_at	Ribosomal protein S4	2.2	1.6	1.4	1.4
X58465mRNA_g_at	Ribosomal protein S5	3	2.2	1.6	1.7
M29358_at	Ribosomal protein S6	2.6	1.9	NC	1.5
X53377cds_s_at	Ribosomal protein S7	4.5	3.1	2	2.2
X06423_at	Ribosomal protein S8	2.9	1.9	1.8	1.7
X66370_at	Ribosomal protein S9	2.8	2.1	1.7	1.6
X13549_s_at	Ribosomal protein S10	1.8	NC	NC	NC
K03250_at	Ribosomal protein S11	2.7	2	1.4	1.4
X53378cds_s_at	Ribosomal protein S13	2.8	2.2	1.6	1.6
X17665cds_s_at	Ribosomal protein S16	2.2	NC	NC	NC
X57529cds_s_at	Ribosomal protein S18	2.9	2.1	1.7	1.8
X51707cds_s_at	Ribosomal protein S19	3.2	2.5	1.8	1.5
M89646_g_at	Ribosomal protein S24	2.6	1.7	1.6	1.5
X62482mRNA_s_at	Ribosomal protein S25	3	1.8	1.6	1.7
X59051cds_s_at	Ribosomal protein S29	2.1	2.7	1.4	1.5
D25224_g_at	40kDa ribosomal protein	2.2	1.9	1.5	1.5

¹⁾ Genes changing at one time-point after peripheral or central nerve injury: X58389cds_s_at (21d SNT +1.6); M20156_at (7d SNT +1.4); X65228cds_s_at (21d SNT +1.4); X52733cds_s_at (7d SNT -1.4); M34331_at (7d DR +1.4); X57432cds_s_at (21d DR -1.6)

Table 2

Expression profiles of genes encoding ribosomal components throughout development in the lumbar DRG. ¹⁾ indicates genes that are regulated at one single time-point following central or peripheral nerve injury. All the remaining genes are not affected by either type of injury. NC: no change (fold difference <1.4).

shows a tendency of increasing mRNA levels reaching approximately P0 expression levels 21 days post-injury (Figure 1B). Glypican-1 appears up-regulated after SNT over the whole time-course investigated, revealing peak mRNA levels 7 days post-SNT (7d 1.9 fold, 21d 1.5 fold, Figure 1C). α -fodrin mRNA stays unchanged after SNT over the whole period examined (Figure 1D). Osteopontin and α 7-integrin share a common response in mRNA expression to SNT, as well for the time-course of induced changes as for absolute intensity levels. Both genes are quickly and massively induced, mRNA expression peaks at day 3 post-SNT (3d vs. uninjured, osteopontin 1.8 fold, α 7-integrin 1.9 fold) and levels stay slightly above uninjured 21 days post-injury (Figure 1E and 1F).

Using isotopic *in situ* hybridization we have investigated the localization of gene expression and verified changes seen in the gene chip analysis (Figure 1 and 2). GAP-43 is expressed by sensory DRG neurons in the non-injured animal. Its expression is strongly induced 3 days post-SNT and remains mainly neuronal (Figure 2). For α -internexin, mRNA is localized to neurons and no obvious regulation 3 days after SNT is found, probably due to the low abundance of mRNA in the DRG, a limiting factor for visualization by isotopic *in situ* hybridization (Figure 2). As previously shown (Bloechlinger *et al.*, 2004), glypican-1 mRNA is predominantly and clearly induced in primary sensory neurons 3 days following SNT compared to non-injured (Figure 2). α -fodrin mRNA is localized almost exclusively in neurons and is highly abundant in the non-injured DRG as well as 3 days post-SNT where no change in expression is detected (Figure 2). High levels of osteopontin mRNA are already present in the non-injured condition, but the intensity of mRNA signal is additionally induced 3 days after SNT. Like the other genes, osteopontin is mainly expressed by neurons (Figure 2). Induction of α 7-integrin mRNA after SNT is clearly confirmed by *in situ* hybridization. Very little signal is detected in the non-injured DRG, due to the short exposure time in order to show strong mRNA induction, whereas high levels of signal are found 3 days following

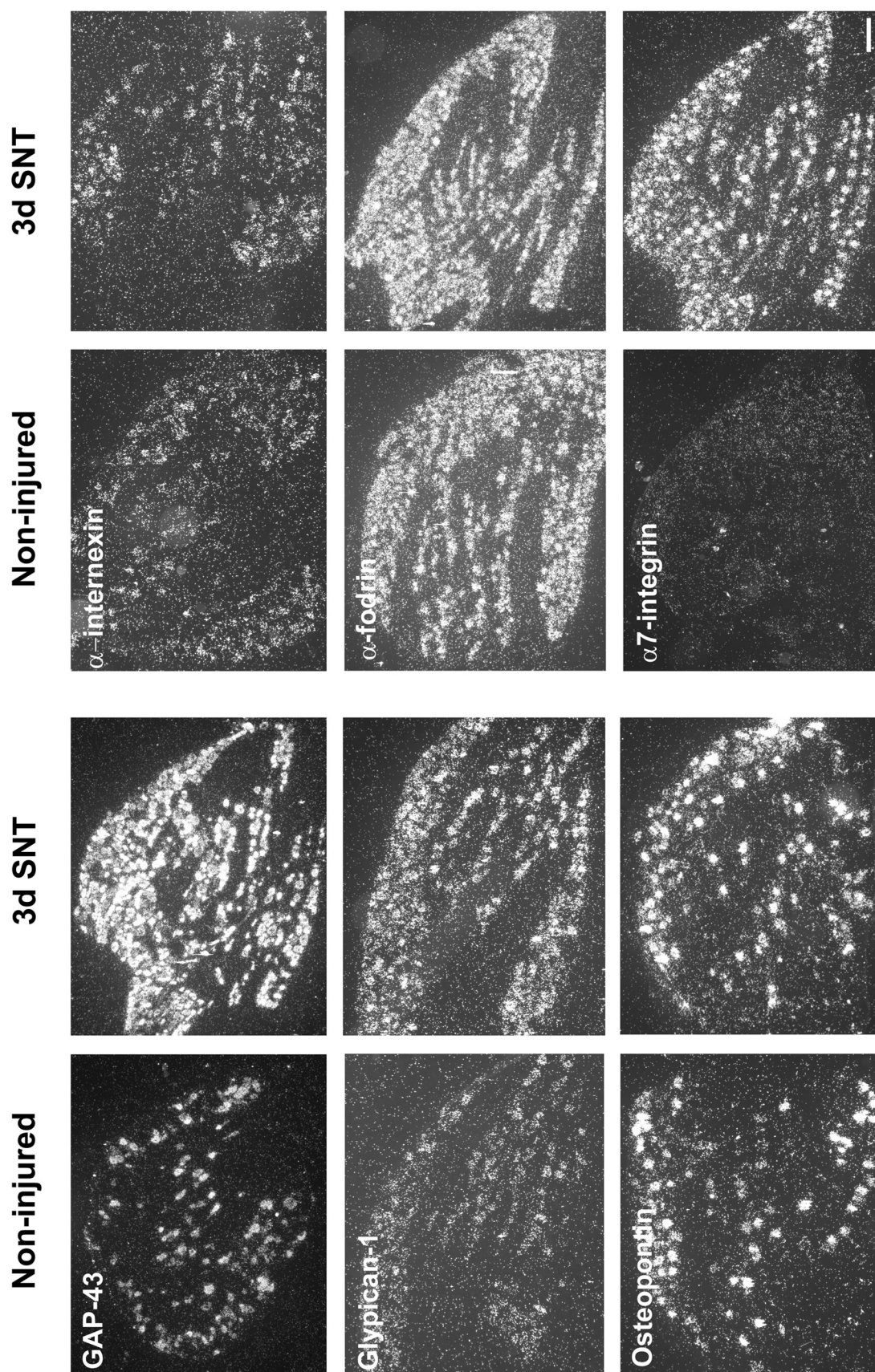


Figure 2

Photomicrographs of L4 DRG sections processed to detect mRNAs for six genes by *in situ* hybridization comparing levels of mRNA in the naïve and 3 day following a sciatic nerve transection (SNT). All genes examined are predominantly expressed in DRG-neurons and no expression was found in non-neuronal cells. Scale bar = 200 μ m.

SNT (Figure 2). In addition we find more than 50 genes whose expression is either up- or down-regulated 1.4 fold or more by SNT in the lumbar DRG of adult rats (Table 1).

Dorsal rhizotomy (DR) is not an adequate signal to induce GAP-43 expression whereas it regulates the expression of other genes.

A dorsal rhizotomy (DR) cuts all of the central axons of a single DRG. It is believed that injury to the central branch of a sensory ganglion neuron is generally not a strong enough signal to induce substantial changes in gene expression. GAP-43 expression is known not to be affected by DR (Chong *et al.*, 1994). Expression levels of α -internexin are not changed by DR and stay beyond the levels found for SNT at every time-point tested. We find that in contrast to the examples of GAP-43 and α -internexin (Figure 1A and B). DR can profoundly induce changes in gene expression in the adult lumbar DRG. Glypican-1 has been previously described to be up-regulated in the lumbar DRG after spinal cord injury as well as three days after DR (Bloechlinger *et al.*, 2004). We show here that glypican-1 mRNA levels peak 7 days post-DR (1.4 fold) and remain elevated for at least 21 days after DR (1.4 fold, Figure 1C). α -fodrin mRNA is not regulated by DR at any time-point investigated (Figure 1D). Osteopontin mRNA expression after DR mimics the expression profile seen after SNT, although changes are slightly less profound. mRNA levels are strongly up-regulated 3 days post-DR (1.6 fold), declining over time towards the non-injured condition (Figure 1E). Similar to osteopontin, changes in α 7-integrin mRNA after DR resemble the induction after SNT, although changes in α 7-integrin expression are very modest with a peak in intensity at 3 days post-DR (fold changes < 1.4, Figure 1F). Apart from Glypican-1 and Osteopontin, the expression of 50 genes is found to be regulated by injury to the central processes of DRG neurons by chip analysis (Table 1).

Slot-blot analysis compares gene expression in two different paradigms in which axons of DRG neurons are able to grow: the early postnatal state and peripheral axotomy (SNT).

Slot-blot analysis confirms the findings of the Affymetrix gene chips and *in situ* hybridization for GAP-43. GAP-43 mRNA is abundant in the naïve DRG, however its expression is much higher in states of axonal outgrowth, demonstrated for the case of early postnatal developing DRG neurons (postnatal day 0 (P0)) and reactive up-regulation after injury to the peripheral branch of DRG neurons at different time-points (3 days and 14 days post-SNT; Figure 3A). Furthermore, we confirm higher levels of α -internexin mRNA in P0 lumbar DRGs than in naïve adult (Figure 3B). As seen by *in situ* hybridization (Figure 2), no obvious induction of α -internexin mRNA is found either 3 days or 14 days following SNT. Glypican-1 mRNA expression is very much comparable to that of GAP-43 in terms of high expression in neurons whose axons are extending (Figure 3C, 1C and 2). α -fodrin mRNA is very abundant in DRGs in every state examined by slot-blotting confirming the results of the chip analysis and *in situ*-hybridization (Figure 3D). At P0, mRNA of osteopontin could not be detected, whereas it is strongly expressed in the naïve DRG (Figure 3E). SNT induces osteopontin mRNA expression profoundly, showing a short lasting peak in expression 3 days post-SNT, followed by mRNA levels that are close to non-injured levels 14 days after injury (Figure 3E). α 7-integrin mRNA expression is found lower at P0 compared to adult, and strongly induced following peripheral axotomy at both time-points examined (Figure 3F).

Gene expression in the motor-cortex is developmentally regulated, but a thoracic spinal cord injury does not influence mRNA levels of the genes investigated.

GAP-43 and glypican-1 share a common expression pattern in the motor cortical area of the adult rat brain. Both genes are highly expressed at P0 (Figure 3A and C), a stage in CNS development when neuronal differentiation and axonal plasticity is still very high (Bennett *et al.*, 1996; Koltzenburg, 1999; Marti *et al.*, 1987). The mRNA of both genes is

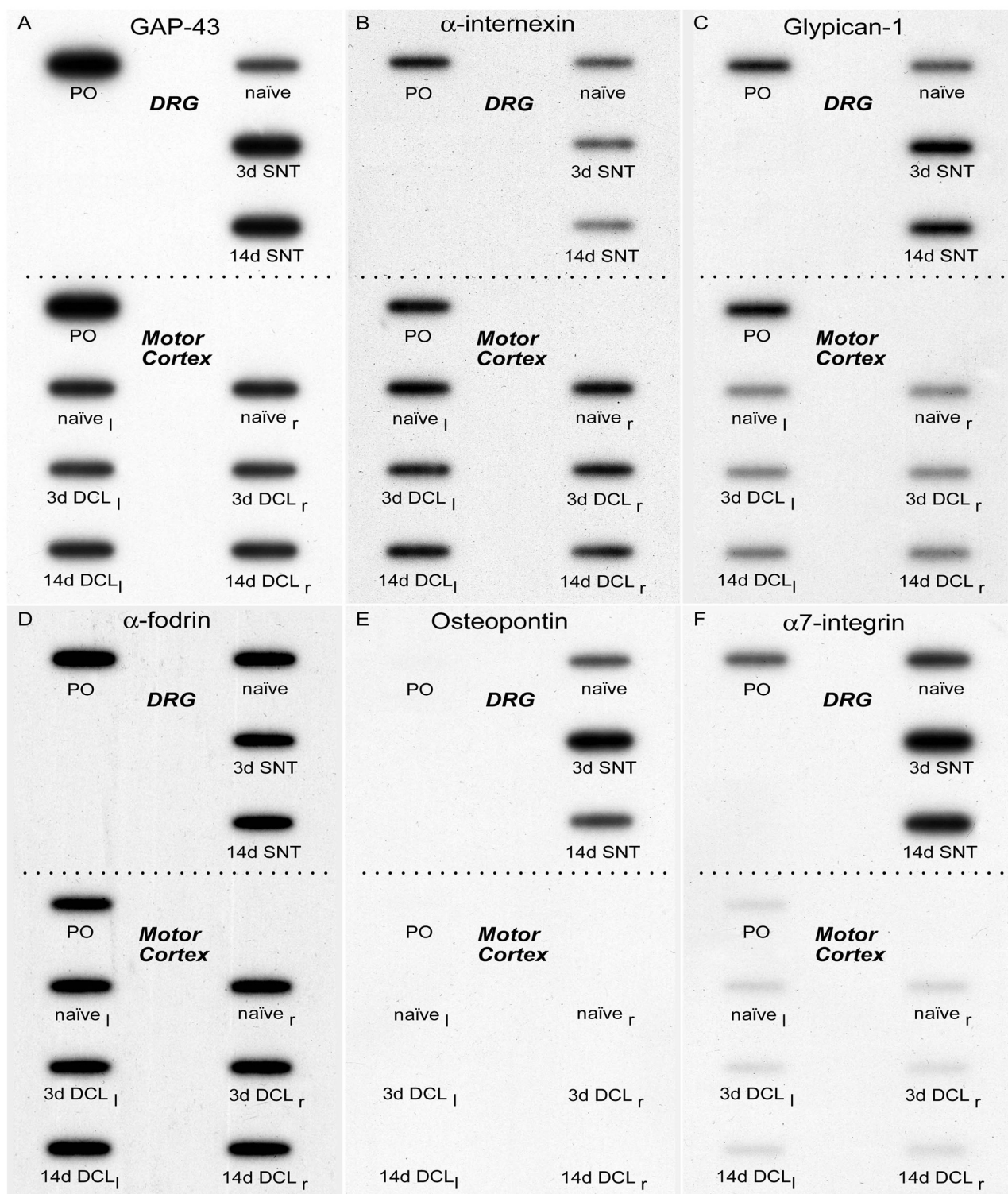


Figure 3

Slot blots showing mRNA expression of the indicated genes in DRG and Motor Cortex. mRNA expression in the non-injured adult DRG (naïve) is compared to its expression at postnatal day 0 and to mRNA levels 3 and 14 days following sciatic nerve transection (SNT). mRNA expression in the Motor Cortex is shown for postnatal day 0, for the naïve left and right Motor Cortex (naïve_l, naïve_r) and 3 as well as 14 days following a lesion of the dorsal funiculus of the spinal cord (DCL_l, DCL_r).

clearly detected in the adult motor-cortex revealing constitutive gene expression when CNS development is finished (Figure 3A and C). Cutting the axons of the major part of neurons contributing to the corticospinal tract and weakening ascending cortical input of dorsal column fibers via dorsal column nuclei and the thalamus by a dorsal column lesion (DCL) in the spinal cord does not visibly affect the expression of GAP-43 nor glypican-1 in the motor-cortical area (Figure 3A and C). α -internexin, with a similar expression pattern in the DRG during development as GAP-43 is, in contrast to GAP-43, constitutively expressed at high levels in the motor-cortex of neonatal and naïve adult rats (Figure 3B). There is no change in expression following DCL. Maintaining the very stable expression in the DRG during development and after injury, α -fodrin mRNA is strongly expressed at similar levels in the developing and mature motor-cortex, and its expression is not influenced by a lesion to the dorsal funiculus of the spinal cord (Figure 3D). Osteopontin mRNA is not detected in the P0 and adult motor-cortex (Figure 3E). In contrast to axonal injuries to DRG neurons, DCL does not induce mRNA expression in the area of projecting corticospinal neurons whose axons are injured (Figure 3E). Very low constitutive levels of α 7-integrin mRNA are found in the developing and mature motor-cortical areas and levels do not appear influenced by DCL at any time-point examined (Figure 3F). In summary, there is differential mRNA expression between P0 and adult for two genes examined, GAP-43 and glypican-1, whereas a spinal cord injury does not effect the expression of all examined genes in the motor-cortex.

Differentially regulated genes during development and after injury can be grouped according to their expression pattern.

Growth associated protein 43 (GAP-43) is characterized by its strong expression in DRG neurons during development and after peripheral nerve injury as well as by the lack of induction following injury to the central branch of DRG neurons. Using gene chip analysis we find five genes additional to GAP-43, namely neuroglycan C, synaptic vesicle protein (SV2),

EF-1-alpha, brain specific peptide and AIF-C1 which share the same features regarding their expression (Table 1 (A)).

We have further identified 7 genes whose mRNA is regulated as outlined for glypican-1, meaning high expression during development and enhanced levels following injury either to the peripheral or the central axons of DRG neurons: VGF, synaptotagmin IV, CCHL2A, dual specificity protein tyrosine phosphatase, protein kinase C receptor, neuronatin alpha and ADP-ribosylation factor-like protein 3; Table 1 (C)).

High developmental expression without changes in expression following injury as for α -fodrin is the expression pattern of thirty-two additional genes (Table 1 (B)).

Furthermore, six genes mimic the expression pattern of osteopontin, revealing decreased expression levels during development and induced mRNA levels following injury to the sciatic nerve as well as the corresponding dorsal root: decorin, RET ligand 1 = GDNF receptor alpha, glutamine synthetase glnA, p41-Arc and the immediate-early serum-responsive JE gene (Table 1 (E)).

Three genes show the same expression profile (low expression during development, induction only after peripheral but not following central axotomy) as α 7-integrin: monoamine oxidase A, CDP-diacylglycerol synthase and interferon induced mRNA (Table 1 (F)).

Five genes are found to have expression levels below the ones found in the adult non-injured DRG during development and after DR; they include stearoyl-CoA desaturase 2 and a homologue, EF-hand Ca^{2+} -binding protein p22, calmodulin III and MHC class I RT1.O type – 149 processed pseudogene (Table 1 (D)).

Nine genes show lowered mRNA levels during development and following SNT, but remain not influenced by DR (Table 1 (J)), seventeen are additionally down-regulated by DR (Table 1 (I)). Injury-induced down-regulation with normal or increased mRNA levels during development has been found for seven genes (Table 1 (H)). We find down-regulated mRNA expression during development without influence of injury in seventeen genes (Table 1 (G)).

The remaining 16 genes do not share the expression pattern of any of the groups described so far (Table 1 (K), (L), (M), (N) and (O)). Pattern K includes genes which are not regulated by SNT but show inverse regulation throughout development and after DR. Group L defines genes which are down-regulated by SNT whereas they show normal or increased mRNA levels during development. We never find genes that are inversely regulated following peripheral versus central injury and we never find mRNA up-regulation after central injury without regulation of the same gene during development.

Many genes coding for ribosomal proteins are highly expressed during nervous system development but their expression is not affected by peripheral or axonal injury.

Surprisingly, 42 genes encoding ribosomal components, are expressed at high levels during development compared to the adult DRG (Table 2). The mRNA levels of only six of them are affected in the adult at exclusively one time-point examined, by either central or peripheral axonal injury (Table 2). The mRNA levels of most of these ribosomal genes are highest around E15, with a constant decline towards P0 when most of the genes reveal still higher mRNA levels than in the adult state.

Discussion

In our study we profile more closely, based on data from microarray analysis in the rat lumbar DRG, the expression of five genes during development and after injury to the peripheral and the central nervous system and compare them to the expression of GAP-43. We selected a number of genes that may be important for growth and regeneration to compare with GAP-43, a well-known growth-associated gene, in order to test the hypotheses that growth-associated genes are regulated in primary sensory neurons after peripheral axotomy in

order to mount a growing phenotype seen during the development of the nervous system. The chosen genes differ in their cellular function, all of them have been shown to play roles in development, differentiation and growth. α -internexin, a 66kD type IV intermediate filament, is the earliest expressed type IV neurofilament during development, and as a structural protein involved in neuronal development and aging, with implications in axonal regeneration (Ching *et al.*, 1999; Chiu *et al.*, 1989; Levavasseur *et al.*, 1999; McGraw *et al.*, 2002). Glypican-1, a glycosyl phosphatidyl inositol linked proteoglycan carrying heparan sulphate side chains, is found in the nucleus of neurons, but has also been shown to act as a co-receptor at the cell membrane for several ligands influencing neuronal growth (Hu, 2001; Liang *et al.*, 1997). α -fodrin, a submembranous cytoskeletal protein, is involved in cell stability, neurite outgrowth and growth cone adhesion as well as thought to be associated with synaptic activity (Bockers *et al.*, 2001; Nakano *et al.*, 2001; Shea *et al.*, 1995; Sobue & Kanda, 1989; Ursitti *et al.*, 2001). Osteopontin, an RGD(Arg-Gly-Asp)-containing glycoprotein, involved in cell adhesion and neurite outgrowth has been described in myelinating Schwann cells of the sciatic nerve (Hikita *et al.*, 2003; Jander *et al.*, 2002; Selvaraju *et al.*, 2004). The α 7-integrin subunit of the laminin-1/-2 receptive molecule α 7/ β 1-integrin has been recently shown to be involved in the conditioning-lesion effect in DRG neurons *in vitro* and in α 7-integrin deficient mice have reduced facial nerve regeneration (Ekstrom *et al.*, 2003; Werner *et al.*, 2000).

In summary, developmentally up-regulated genes (GAP-43, glypican-1) are induced after SNT in the adult, although the changes differ profoundly in strength and dynamics. Glypican-1 and α -fodrin, both expressed at relatively constant levels in the embryonic and adult DRG, are differentially regulated by SNT. Glypican-1 is up-regulated over a long period of time, whereas α -fodrin mRNA shows no significant regulation. The two genes with the strongest expression in the adult compared to developmental stages, osteopontin and α 7-integrin, are identically up-regulated in the DRG after SNT, with mRNA levels peaking 3 days post-injury. DR is a strong inducer of changes in gene expression in the adult lumbar

DRG. Whereas GAP-43 and α -fodrin do not show any change in expression following DR, the expression of two examined genes does change after DR. Assuming cut off ≥ 1.4 fold change for significant changes in intensity, osteopontin (1.6 fold) is transiently up-regulated around day 3 post-DR, mimicking changes seen after SNT. Glypican-1 is the only gene that is found to be chronically up-regulated over 21 days (7d 1.4 fold, 21d 1.4 fold). $\alpha 7$ -integrin does not change following DR. All examined genes are predominantly expressed in DRG-neurons of the adult non-injured rat as well as following sciatic nerve transection.

The study of mRNA expression in the developing and adult motor-cortex reveals that only two out of the six examined genes, GAP-43 and glypican-1, are regulated. They both appear at high levels shortly after birth (P0) and are expressed at considerably lower levels in the adult cortex. Osteopontin is the only gene whose mRNA could not be detected in the motor-cortex. A spinal cord injury, cutting the axons running in the dorsal funiculus, including axons from the motor-cortex (dCST) and ascending fibers of the dorsal column system, is not a strong enough signal to evoke changes in the mRNA expression of the examined genes. This may be because the axonal injury site of CST fibers is at greater distance from the cell body and neural networks in the cortex may stabilize gene expression more successfully than in the periphery. Another explanation for the stable gene expression in the motor-cortical area following DCL may be that the pyramidal cells whose axons constitute the CST make up only a very minor proportion of all the cells in the motor-cortex. Therefore changes only in those injured pyramidal cells may not be detected with the technique we used.

Examining gene expression in the lumbar DRG during development and following injury to the peripheral or central branches of DRG axons show strong regulation of mRNA levels for more than 120 genes, whose expression patterns can be grouped comparing regulation during development and after injury, without taking further into account the dynamics of changes. We find for each closely examined gene, except for α -internexin that was attributed an absent (A) call in the naïve adult DRG, between 3 and 32 genes which show

the same expression pattern. In addition we define other expression patterns as shown in table 1, but interestingly, even though we find very different expression patterns, mRNA levels for a given gene have never been found to be inversely regulated following central and peripheral injury respectively. These data suggest that there is a common process underlying the transcriptional response to injury of the central and peripheral branches of DRG neurons, which can be tuned by the presence or lack of environmental factors acting on the injured axon at the site of injury or along the axon, or by the lack of target-derived signals. These mechanisms could therefore account for the differential gene expression seen in our injury paradigms and during development.

Many genes encoding for ribosomal proteins appear to be expressed at high levels during the embryonic period. It is quite remarkable the transcription of almost none of these genes is affected by either central or peripheral injury, an influence where one could assume that the translational machinery of a cell would have to be strengthened. We cannot exclude however that these changes occur on a translational level. For the genes not examined by *in situ*-hybridization it remains unclear whether non-neuronal cells in the DRG may account for some of the changes detected by microarray analysis.

From our study, it is clear that injury to the peripheral and central branch of DRG axons does not cause the recapitulation of a developmental transcriptional program for every gene that may be involved in growth- and regeneration-related functions in the nervous system. Therefore we suggest a more detailed classification of expression-profiles than that of growing versus not-growing phenotypes of DRG-neurons. According to our findings, we propose a further subdivision into a “developmental-growing phenotype” and an “injury-induced growing phenotype”. GAP-43, for example would fit both criteria, therefore defining the “growing phenotype”. On the other hand, osteopontin does not seem to be needed for developmental growth, although it may play roles in the “injury-induced growing phenotype”. Taking into account the findings of osteopontin and glypican-1 expression, it makes sense to

add a third category of gene expression patterns, the “central-injury-induced phenotype”. Osteopontin therefore can be clearly characterized as an injury-related (peripheral and central) gene in the adult nervous system, $\alpha 7$ -integrin as part of the “injury-induced growing phenotype” with possible functions in development. Glypican-1 shows the most complex differential expression, with components of the overall “growing phenotype” as well as overall “injury-related”. We clearly identify GAP-43 as a characteristic gene representing a “growing phenotype”. It is important to understand the growth and injury-regulated expression of genes in the nervous system in order to better understand the conditions required for re-growth and functional recovery after injury.

References

- Aigner, L., Arber, S., Kapfhammer, J. P., Laux, T., Schneider, C., Botteri, F., Brenner, H. R., and Caroni, P. (1995) Overexpression of the neural growth-associated protein GAP-43 induces nerve sprouting in the adult nervous system of transgenic mice. *Cell* **83**, 269-78.
- Aigner, L., and Caroni, P. (1993) Depletion of 43-kD growth-associated protein in primary sensory neurons leads to diminished formation and spreading of growth cones. *J Cell Biol* **123**, 417-29.
- Bandtlow, C. E., and Zimmermann, D. R. (2000) Proteoglycans in the developing brain: new conceptual insights for old proteins. *Physiol Rev* **80**, 1267-90.
- Bennett, D. L., Averill, S., Clary, D. O., Priestley, J. V., and McMahon, S. B. (1996) Postnatal changes in the expression of the trkA high-affinity NGF receptor in primary sensory neurons. *Eur J Neurosci* **8**, 2204-8.
- Bloechlinger, S., Karchewski, L. A., and Woolf, C. J. (2004) Dynamic changes in glypican-1 expression in dorsal root ganglion neurons after peripheral and central axonal injury. *Eur J Neurosci* **19**, 1119-32.
- Bockers, T. M., Mameza, M. G., Kreutz, M. R., Bockmann, J., Weise, C., Buck, F., Richter, D., Gundelfinger, E. D., and Kreienkamp, H. J. (2001) Synaptic scaffolding proteins in rat brain. Ankyrin repeats of the multidomain Shank protein family interact with the cytoskeletal protein alpha-fodrin. *J Biol Chem* **276**, 40104-12.
- Bomze, H. M., Bulsara, K. R., Iskandar, B. J., Caroni, P., and Skene, J. H. (2001) Spinal axon regeneration evoked by replacing two growth cone proteins in adult neurons. *Nat Neurosci* **4**, 38-43.
- Bray, G. M., Rasminsky, M., and Aguayo, A. J. (1981) Interactions between axons and their sheath cells. *Annu Rev Neurosci* **4**, 127-62.

- Cai, D., Qiu, J., Cao, Z., McAtee, M., Bregman, B. S., and Filbin, M. T. (2001) Neuronal cyclic AMP controls the developmental loss in ability of axons to regenerate. *J Neurosci* **21**, 4731-9.
- Caroni, P. (2001) New EMBO members' review: actin cytoskeleton regulation through modulation of PI(4,5)P(2) rafts. *Embo J* **20**, 4332-6.
- Chen, M. S., Huber, A. B., van der Haar, M. E., Frank, M., Schnell, L., Spillmann, A. A., Christ, F., and M.E., S. (2000) Nogo-A is a myelin-associated neurite outgrowth inhibitor and an antigen for monoclonal antibody IN-1. *Nature* **403**, 434-439.
- Ching, G. Y., Chien, C. L., Flores, R., and Liem, R. K. (1999) Overexpression of alpha-internexin causes abnormal neurofilamentous accumulations and motor coordination deficits in transgenic mice. *J Neurosci* **19**, 2974-86.
- Ching, G. Y., and Liem, R. K. (1991) Structure of the gene for the neuronal intermediate filament protein alpha-internexin and functional analysis of its promoter. *J Biol Chem* **266**, 19459-68.
- Chiu, F. C., Barnes, E. A., Das, K., Haley, J., Socolow, P., Macaluso, F. P., and Fant, J. (1989) Characterization of a novel 66 kd subunit of mammalian neurofilaments. *Neuron* **2**, 1435-45.
- Chong, M. S., Reynolds, M. L., Irwin, N., Coggeshall, R. E., Emson, P. C., Benowitz, L. I., and Woolf, C. J. (1994) GAP-43 expression in primary sensory neurons following central axotomy. *J Neurosci* **14**, 4375-4384.
- Chong, M. S., Woolf, C. J., Turmaine, M., Emson, P. C., and Anderson, P. N. (1996) Intrinsic versus extrinsic factors in determining the regeneration of the central processes of rat dorsal root ganglion neurons: the influence of a peripheral graft. *J Comp Neurol* **370**, 97-104.

- Coggeshall, R. E., Pover, C. M., and Fitzgerald, M. (1994) Dorsal root ganglion cell death and surviving cell numbers in relation to the development of sensory innervation in the rat hindlimb. *Brain Res Dev Brain Res* **82**, 193-212.
- Costigan, M., Befort, K., Karchewski, L., Griffin, R. S., D'Urso, D., Allchorne, A., Sitariski, J., Mannion, J. W., Pratt, R. E., and Woolf, C. J. (2002) Replicate high-density rat genome oligonucleotide microarrays reveal hundreds of regulated genes in the dorsal root ganglion after peripheral nerve injury. *BMC Neurosci* **3**, 16.
- Denhardt, D. T., and Guo, X. (1993) Osteopontin: a protein with diverse functions. *Faseb J* **7**, 1475-82.
- Denhardt, D. T., Noda, M., O'Regan, A. W., Pavlin, D., and Berman, J. S. (2001) Osteopontin as a means to cope with environmental insults: regulation of inflammation, tissue remodeling, and cell survival. *J Clin Invest* **107**, 1055-61.
- Donovan, S. L., Mamounas, L. A., Andrews, A. M., Blue, M. E., and McCasland, J. S. (2002) GAP-43 is critical for normal development of the serotonergic innervation in forebrain. *J Neurosci* **22**, 3543-52.
- Ekstrom, P. A., Mayer, U., Panjwani, A., Pountney, D., Pizzey, J., and Tonge, D. A. (2003) Involvement of $\alpha 7 \beta 1$ integrin in the conditioning-lesion effect on sensory axon regeneration. *Mol Cell Neurosci* **22**, 383-95.
- Fliegner, K. H., Ching, G. Y., and Liem, R. K. (1990) The predicted amino acid sequence of alpha-internexin is that of a novel neuronal intermediate filament protein. *Embo J* **9**, 749-55.
- Fransson, L. A. (2003) Glypicans. *Int J Biochem Cell Biol* **35**, 125-9.
- Frey, D., Laux, T., Xu, L., Schneider, C., and Caroni, P. (2000) Shared and unique roles of CAP23 and GAP43 in actin regulation, neurite outgrowth, and anatomical plasticity. *J Cell Biol* **149**, 1443-54.

- GrandPré, T., Nakamura, F., Vartanian, T., and Strittmatter, S. M. (2000) Identification of the Nogo inhibitor of axon regeneration as a reticulon protein. *Nature* **403**, 439-444.
- Hammarberg, H., Wallquist, W., Piehl, F., Risling, M., and Cullheim, S. (2000) Regulation of laminin-associated integrin subunit mRNAs in rat spinal motoneurons during postnatal development and after axonal injury. *J Comp Neurol* **428**, 294-304.
- Hartwig, J. H. (1995) Actin-binding proteins. 1: Spectrin super family. *Protein Profile* **2**, 703-800.
- Hikita, S. T., Cann, G. M., Wingerd, K. L., Mullick, L. H., Wayne, W. C., Webb, S. W., and Clegg, D. O. (2003) Integrin alpha4beta1 (VLA-4) expression and activity in retinal and peripheral neurons. *Mol Cell Neurosci* **23**, 427-39.
- Hu, H. (2001) Cell-surface heparan sulfate is involved in the repulsive guidance activities of Slit2 protein. *Nat Neurosci* **4**, 695-701.
- Jander, S., Bussini, S., Neuen-Jacob, E., Bosse, F., Menge, T., Muller, H. W., and Stoll, G. (2002) Osteopontin: a novel axon-regulated Schwann cell gene. *J Neurosci Res* **67**, 156-66.
- Kapfhammer, J. P., and Schwab, M. E. (1994) Inverse patterns of myelination and GAP-43 expression in the adult CNS: neurite growth inhibitors as regulators of neuronal plasticity? *J Comp Neurol* **340**, 194-206.
- Kaplan, M. P., Chin, S. S., Fliegner, K. H., and Liem, R. K. (1990) Alpha-internexin, a novel neuronal intermediate filament protein, precedes the low molecular weight neurofilament protein (NF-L) in the developing rat brain. *J Neurosci* **10**, 2735-48.
- Karimi-Abdolrezaee, S., Verge, V. M., and Schreyer, D. J. (2002) Developmental down-regulation of GAP-43 expression and timing of target contact in rat corticospinal neurons. *Exp Neurol* **176**, 390-401.

- Kitao, Y., Robertson, B., Kudo, M., and Grant, G. (1996) Neurogenesis of subpopulations of rat lumbar dorsal root ganglion neurons including neurons projecting to the dorsal column nuclei. *J Comp Neurol* **371**, 249-57.
- Koltzenburg, M. (1999) The changing sensitivity in the life of the nociceptor. *Pain Suppl* **6**, S93-102.
- Lawson, S. N., Caddy, K. W., and Biscoe, T. J. (1974) Development of rat dorsal root ganglion neurones. Studies of cell birthdays and changes in mean cell diameter. *Cell Tissue Res* **153**, 399-413.
- Levavasseur, F., Zhu, Q., and Julien, J. P. (1999) No requirement of alpha-internexin for nervous system development and for radial growth of axons. *Brain Res Mol Brain Res* **69**, 104-12.
- Liang, Y., Haring, M., Roughley, P. J., Margolis, R. K., and Margolis, R. U. (1997) Glypican and biglycan in the nuclei of neurons and glioma cells: presence of functional nuclear localization signals and dynamic changes in glypican during the cell cycle. *J Cell Biol* **139**, 851-64.
- Marti, E., Gibson, S. J., Polak, J. M., Facer, P., Springall, D. R., Van Aswegen, G., Aitchison, M., and Koltzenburg, M. (1987) Ontogeny of peptide- and amine-containing neurones in motor, sensory, and autonomic regions of rat and human spinal cord, dorsal root ganglia, and rat skin. *J Comp Neurol* **266**, 332-59.
- McGraw, T. S., Mickle, J. P., Shaw, G., and Streit, W. J. (2002) Axonally transported peripheral signals regulate alpha-internexin expression in regenerating motoneurons. *J Neurosci* **22**, 4955-63.
- McKerracher, L., David, S., Jackson, D. L., Kottis, V., Dunn, R. J., and Braun, P. E. (1994) Identification of myelin-associated glycoprotein as a major myelin-derived inhibitor of neurite growth. *Neuron* **13**, 805-11.

- Nakano, M., Nogami, S., Sato, S., Terano, A., and Shirataki, H. (2001) Interaction of syntaxin with alpha-fodrin, a major component of the submembranous cytoskeleton. *Biochem Biophys Res Commun* **288**, 468-75.
- Neumann, S., and Woolf, C. J. (1999) Regeneration of dorsal column fibers into and beyond the lesion site following adult spinal cord injury. *Neuron* **23**, 83-91.
- Pachter, J. S., and Liem, R. K. (1985) alpha-Internexin, a 66-kD intermediate filament-binding protein from mammalian central nervous tissues. *J Cell Biol* **101**, 1316-22.
- Rhodes, K. E., and Fawcett, J. W. (2004) Chondroitin sulphate proteoglycans: preventing plasticity or protecting the CNS? *J Anat* **204**, 33-48.
- Richardson, P. M., and Issa, V. M. (1984) Peripheral injury enhances central regeneration of primary sensory neurones. *Nature* **309**, 791-3.
- Schmitt, A. B., Breuer, S., Liman, J., Buss, A., Schlangen, C., Pech, K., Hol, E. M., Brook, G. A., Noth, J., and Schwaiger, F. W. (2003) Identification of regeneration-associated genes after central and peripheral nerve injury in the adult rat. *BMC Neurosci* **4**, 8.
- Schreyer, D. J., and Skene, J. H. (1991) Fate of GAP-43 in ascending spinal axons of DRG neurons after peripheral nerve injury: delayed accumulation and correlation with regenerative potential. *J Neurosci* **11**, 3738-51.
- Schreyer, D. J., and Skene, J. H. (1993) Injury-associated induction of GAP-43 expression displays axon branch specificity in rat dorsal root ganglion neurons. *J Neurobiol* **24**, 959-70.
- Schwab, M. E. (2004) Nogo and axon regeneration. *Curr Opin Neurobiol* **14**, 118-24.
- Schwab, M. E., and Bartholdi, D. (1996) Degeneration and regeneration of axons in the lesioned spinal cord. *Physiol Rev* **76**, 319-370.
- Selvaraju, R., Bernasconi, L., Losberger, C., Graber, P., Kadi, L., Avellana-Adalid, V., Picard-Riera, N., Van Evercooren, A. B., Cirillo, R., Kosco-Vilbois, M., *et al.* (2004)

- Osteopontin is upregulated during in vivo demyelination and remyelination and enhances myelin formation in vitro. *Mol Cell Neurosci* **25**, 707-21.
- Shea, T. B., Cressman, C. M., Spencer, M. J., Beermann, M. L., and Nixon, R. A. (1995) Enhancement of neurite outgrowth following calpain inhibition is mediated by protein kinase C. *J Neurochem* **65**, 517-27.
- Skene, J. H. (1989) Axonal growth-associated proteins. *Annu Rev Neurosci* **12**, 127-156.
- Sobue, K., and Kanda, K. (1989) Alpha-actinins, calspectin (brain spectrin or fodrin), and actin participate in adhesion and movement of growth cones. *Neuron* **3**, 311-9.
- Ursitti, J. A., Martin, L., Resneck, W. G., Chaney, T., Zielke, C., Alger, B. E., and Bloch, R. J. (2001) Spectrins in developing rat hippocampal cells. *Brain Res Dev Brain Res* **129**, 81-93.
- Wang, K. C., Koprivica, V., Kim, J. A., Sivasankaran, R., Guo, Y., Neve, R. L., and He, Z. (2002) Oligodendrocyte-myelin glycoprotein is a Nogo receptor ligand that inhibits neurite outgrowth. *Nature* **417**, 941-4.
- Wang, X., Loudon, C., Yue, T. L., Ellison, J. A., Barone, F. C., Solleveld, H. A., and Feuerstein, G. Z. (1998) Delayed expression of osteopontin after focal stroke in the rat. *J Neurosci* **18**, 2075-83.
- Werner, A., Willem, M., Jones, L. L., Kreutzberg, G. W., Mayer, U., and Raivich, G. (2000) Impaired axonal regeneration in alpha7 integrin-deficient mice. *J Neurosci* **20**, 1822-30.
- Yao, C. C., Ziober, B. L., Sutherland, A. E., Mendrick, D. L., and Kramer, R. H. (1996) Laminins promote the locomotion of skeletal myoblasts via the alpha 7 integrin receptor. *J Cell Sci* **109** (Pt 13), 3139-50.

Chapter 5

Dynamic changes in glypican-1 expression in dorsal root ganglion neurons after peripheral and central axonal injury

Stefan Bloechlinger, Laurie A. Karchewski and Clifford J. Woolf

Dynamic changes in glypican-1 expression in dorsal root ganglion neurons after peripheral and central axonal injury

Stefan Bloechlinger,* Laurie A. Karchewski*[†] and Clifford J. Woolf

Neural Plasticity Research Group, Department of Anaesthesia and Critical Care, Massachusetts General Hospital and Harvard Medical School, MGH-East, 149 13th Street, Rm 4309, Charlestown, MA 02129, USA

Keywords: adult, dorsal column, DRG, growth, heparan sulphate proteoglycan, nerve injury, rat, regeneration, robo, sensory neuron, slit, spinal cord

Abstract

Glypican-1, a glycosyl phosphatidyl inositol (GPI)-anchored heparan sulphate proteoglycan expressed in the developing and mature cells of the central nervous system, acts as a coreceptor for diverse ligands, including slit axonal guidance proteins, fibroblast growth factors and laminin. We have examined its expression in primary sensory dorsal root ganglion (DRG) neurons and spinal cord after axonal injury. In noninjured rats, glypican-1 mRNA and protein are constitutively expressed at low levels in lumbar DRGs. Sciatic nerve transection results in a two-fold increase in mRNA and protein expression. High glypican-1 expression persists until the injured axons reinnervate their peripheral targets, as in the case of a crushed nerve. Injury to the central axons of DRG neurons by either a dorsal column injury or a dorsal root transection also up-regulates glypican-1, a feature that differs from most DRG axonal injury-induced genes, whose regulation changes only after peripheral and not central axonal injury. After axonal injury, the cellular localization of glypican-1 changes from a nuclear pattern restricted to neurons in noninjured DRGs, to the cytoplasm and membrane of injured neurons, as well as neighbouring non-neuronal cells. Sciatic nerve transection also leads to an accumulation of glypican-1 in the proximal nerve segment of injured axons. Glypican-1 is coexpressed with robo 2 and its up-regulation after axonal injury may contribute to an altered sensitivity to axonal growth or guidance cues.

Introduction

Glypican-1, a protein bearing sulphated glycosaminoglycan side chains, is a member of the glycosyl phosphatidyl inositol (GPI)-anchored family of heparan sulphate proteoglycans that includes glypican 1–6 (reviewed in Bandtlow & Zimmermann, 2000). Known to interact with positively charged molecules to promote axonal growth, the glypicans are synthesized by a variety of tissue types in the body and glypican-1 is widely expressed in both the developing and adult nervous system and in cultured Schwann cells (Carey *et al.*, 1993; Halfter, 1993; Karthikeyan *et al.*, 1994; Litwack *et al.*, 1994; Litwack *et al.*, 1998; Moon *et al.*, 2002; Hagino *et al.*, 2003a). The spatio-temporal pattern of glypican-1 expression in the ventricular zone during early neural development strongly correlates with neurogenesis (Litwack *et al.*, 1998), although it is also expressed in postmitotic differentiated neurons during later embryonic development, and in regions of the mature brain, spinal cord and dorsal root ganglia (DRG) (Halfter, 1993; Karthikeyan *et al.*, 1994; Litwack *et al.*, 1994; Hagino *et al.*, 2003a; Hagino *et al.*, 2003b).

Membrane-attached glypican-1 acts as a coreceptor for a number of diverse ligands, including the slit family of axonal guidance proteins, members of the fibroblast growth factor (FGF) family, and the extracellular matrix molecule laminin (Bonneh-Barkay *et al.*, 1997; Steinfeld *et al.*, 1996; Herndon *et al.*, 1999; Liang *et al.*, 1999; Ronca *et al.*, 2001). *In vitro*, the affinity of slit 2 protein for its transmembrane receptor robo 1 is significantly increased by glypican-1 (Hu, 2001) and glypican-1 may also increase binding of FGF to the FGF receptor (Steinfeld *et al.*, 1996; Zhang *et al.*, 2001). The developmental expression of glypican-1 and its interactions with slit, FGF and laminin together imply a possible role for this proteoglycan in neuronal proliferation, differentiation, neurite outgrowth and cell survival. Less is known, however, regarding the role of glypican-1 in the adult nervous system.

Peripheral nerve injury in the adult evokes the recapitulation of many developmental events mediated by the re-expression of developmentally regulated genes including those involved in neurite outgrowth and guidance (Woolf *et al.*, 1990; De Leon *et al.*, 1991; Smith & Skene, 1997), and which may contribute to successful regeneration. The cell bodies of primary sensory neurons located in the DRG begin to express regeneration-associated genes such as growth-associated protein 43 (GAP-43) and cytoskeleton-associated protein 23 (CAP-23) after peripheral axonal injury and regenerate successfully (Frey *et al.*, 2000; Skene *et al.*, 1986; Woolf *et al.*, 1990; Strittmatter *et al.*, 1995). In contrast, injuries to the central axon of primary sensory neurons appear to have a limited effect on DRG neuron transcription

Correspondence: Dr Laurie A. Karchewski, at [†]current address below.
E-mail: lkarch@igbmc.u-strasbg.fr

[†]Current address: Institut de Génétique et de Biologie Moléculaire et Cellulaire, CNRS/INSERM/ULP, UMR7104, Parc d'Innovation, 1 rue Laurent Fries BP 10142, 67404 Illkirch Cedex, C.U.Strasbourg, France

*S.B. and L.A.K. contributed equally to this study.

Received 1 October 2003, revised 12 January 2004, accepted 14 January 2004

(Kenney & Kocsis, 1997; Schwaiger *et al.*, 2000), without up-regulation of GAP-43, and only limited regeneration in the dorsal root and no regeneration in the spinal cord (Lieberman, 1971; Schnell & Schwab, 1990; Chong *et al.*, 1994; Schwab & Bartholdi, 1996). We have now investigated whether changes in glypican-1 mRNA and protein expression occur in DRG neurons after injury to their peripheral or central axons.

Materials and methods

Animal surgery and tissue collection

All procedures were performed in accordance with the Massachusetts General Hospital Animal Research regulations. Adult male Sprague-Dawley rats (200–250 g) were anaesthetized with fluothane (induction 4%, maintenance 2.5%). Sciatic nerve transection (SNT) was performed on the left side at the mid-thigh level. The exposed nerve was ligated with 3/0 silk and transected distal to the ligation. To produce a nerve crush injury, the exposed sciatic nerve was crushed for 30 s, until completely translucent, using a smooth-bladed haemostat (Devor *et al.*, 1979). Dorsal rhizotomy (DR) was performed by exposing the lumbar dorsal roots on the left side via a hemi-laminectomy of the L3 vertebra and, after opening the dura, transecting the left L4 and L5 dorsal roots. Dorsal column lesion (DCL) was performed at the mid-thoracic level, after a laminectomy of T7, by transecting under direct microscopic vision the dorsal column on both sides using ophthalmic microscissors; it was later checked histologically for depth and width. For one group of rats, an SNT was performed 7 days prior to the DCL (pSNT + DCL). For all surgical procedures the wound was closed in two layers and the animals allowed to recover. After indicated survival times the animals were either terminally anaesthetized by exposure to CO₂ and exsanguinated for fresh tissue collection or perfused for histochemistry. For fresh tissue, the L4 and L5 DRGs were rapidly removed, frozen on dry ice in tubes or embedded in OCT compound (Tissue Tek, Fisher, PA, USA) and stored at –80 °C. For fixed tissue, animals were transcardially perfused with saline (250 mL) followed by Zamboni's fixative (500 mL). The L4 and L5 DRGs with associated dorsal roots, sciatic nerve and spinal cord were dissected and postfixed for 2 h or overnight, immersed in 30% sucrose, then embedded in OCT compound and frozen on dry ice. Fixed tissue sections were cut at 12–20 µm and fresh tissue sections were cut at 6 µm, mounted on Superfrost and Probe-On slides (Fisher, PA, USA), respectively, and stored at –20 °C until use. Tissue from naïve and experimental groups were cut and processed together on the same slide in order to ensure identical treatment.

Isotopic *in situ* hybridization

Isotopic *in situ* hybridization was carried out as described previously (Karchewski *et al.*, 1999). Forty-eight base-pair oligonucleotide probes were designed to have 50% G-C content and be complementary to and selective for glypican-1 (Accession NM_030828), c-jun (Accession X17163), slit 1 (Accession AF133738), slit 2 (Accession AF141386), slit 3 (Accession NM_031321), robo 1 (Accession AF041083) and robo 2 (Accession AF182037). Probes were 3'-end labelled with ³⁵S-dATP or ³³P-dATP (NEN, MA, USA) using a terminal transferase reaction and purified through spin columns (Qiagen, CA, USA). The specific activity used ranged from 2.0 to 5.0 × 10⁶ cpm/ng oligonucleotide. Slides were brought to room temperature and covered with a hybridization solution (50% formamide, 1 × Denhardt's solution, 1% sarcosyl, 10% dextran sulphate, 0.02 M phosphate buffer, 4 × SSC, 200 nM DTT and 500 mg/mL heated salmon sperm DNA) containing 10⁷ cpm/mL of labelled probe and incubated in a humidified chamber at 43 °C for 14–18 h, then washed four times for 15 min in 1 × SSC at 55 °C. In the final rinse, slides were

brought to room temperature, washed in dH₂O, dehydrated in ethanol and air-dried. Autoradiograms were generated by dipping slides in NTB2 nuclear track emulsion (1 : 1 with dH₂O; Kodak) and storing in the dark at 4 °C for times determined by test slides. Test slides for each probe were developed at periodic intervals in order to optimize exposure times for an ideal signal-to-noise ratio on the autoradiograms. After conventional developing and fixation, unstained tissue was viewed under darkfield conditions using a fibre-optic darkfield stage adapter (MVI, MA, USA), while stained tissue (0.5% Toluidine Blue, pH 4–4.5) was examined under brightfield conditions. Photographs were taken using a Spot camera (Diagnostic Instruments Inc., MVI, MA, USA).

For each experimental group (i.e. injury time point), 6–7 DRG sections from at least five animals were analysed. Control experiments were conducted to confirm the specificity of oligonucleotide probes with hybridization of adjacent sections of 1-week-axotomized L5 ganglia with labelled probe, labelled probe with a 1000-fold excess of cold probe, or labelled probe with a 1000-fold excess of another, dissimilar cold probe of the same length and similar G-C content.

Cell profiles were considered positively labelled if they contained more than five times background levels of silver grains (radiographic signal), as determined by manual grain counts over defined areas of neuropil devoid of positively labelled cell bodies.

RNAse protection assay (RPA)

Experiments were performed in triplicate using three independent sets of RNA prepared from pooled L4 and L5 DRGs from the side ipsilateral to the SNT and from the left side of centrally injured (DCL) animals and naïve controls. For combined lesions, ipsilateral and contralateral DRG were examined separately. Total RNA was extracted from homogenized DRG samples using acid phenol extraction (TRIzol, Gibco-BRL, CA, USA) and concentration determined by A₂₆₀ measurement. The template for a glypican-1 riboprobe was generated by PCR from rat DRG cDNA using primers 5'-GGTCA-ATCCCCATGGCTCTG-3' and 5'-GAAATCCCATTCAGCAGCG-3' and cloned into pCRII vector (TA cloning Kit, Invitrogen, CA, USA). Plasmids were linearized and antisense probes synthesized using RNA polymerase and labelled with ³²P-UTP (NEN, MA, USA). RPA was performed on total RNA extracts using the RPA III Kit (Ambion, TX, USA) (Samad *et al.*, 2001). Briefly, 2 µg of total RNA was hybridized with labelled probe overnight at 42 °C, followed by RNaseA/RNaseT1 digestion for 45 min at 37 °C. The samples were loaded and separated on a 5% denaturing acrylamide gel and visualized on X-ray film. For each RNA sample a β-actin probe was used as a loading control. Developed X-ray films were scanned and optical densities measured using Adobe Photoshop software. The values for the glypican-1 band were corrected for corresponding values of β-actin and expressed relative to the naïve control.

Immunohistochemistry

Slides were allowed to reach room temperature, washed in PBS, blocked for 1 h at RT in a PBS solution containing 5% bovine serum albumin and 0.1% Triton X-100, and incubated overnight at 4 °C with the primary antibody in blocking solution. Rabbit anti-glypican-1 343–1 (1 : 200; a gift from Dr A. Lander, UC Irvine), mouse anti-NeuN (1 : 500; Chemicon, CA, USA) and mouse anti-GFAP (1 : 300; Chemicon) antibodies were used. After washing the slides in PBS, secondary antibodies, Cy3-conjugated anti-rabbit (1 : 400; Jackson ImmunoResearch, ME, USA) and FITC-conjugated anti-mouse antibody (1 : 300; Jackson ImmunoResearch) in PBS containing 5% bovine serum albumin were left on the slides for 1 h at room temperature. Slides were washed in PBS and coverslipped using

Vectashield (Vector Laboratories, CA, USA). Sections were viewed with a fluorescent microscope (Nikon) and photographed using a Spot digital camera. Selected sections were viewed using a Biorad MRC confocal microscope. In total, ≈ 70 sections from 15 animals were analysed.

For activating transcription factor 3 (ATF3) staining, slides adjacent to those used for *in situ* hybridization were placed in Zamboni's fixative for 30 min followed by washes in PBS. Tissue was blocked for 30 min at room temperature in a PBS solution containing 10% horse serum and 0.1% Triton X-100. Primary antibody, rabbit anti-ATF3 (1:300; Santa Cruz, CA, USA) in blocking solution was left on tissue overnight at 4 °C, washed, and the secondary antibody, biotinylated anti-rabbit IgG (1:200; Jackson ImmunoResearch) in PBS with 10% horse serum, was left on for 30 min at room temperature. Slides were further processed using the ABC Kit (Vector Laboratories) with visualization by DAB staining and results viewed under brightfield conditions and photographed using a Spot camera. For all immunostaining, negative control sections were processed in the same manner, but with blocking solution replacing the primary antibodies.

Western blotting

Experiments were performed in triplicate using three different animals at each time point. The pooled L4 and L5 DRG from injured and naïve rats were homogenized in 8 μ g/mL RIPA buffer, and total protein was measured by Bradford assay. For each lane, 20 μ g of total cell lysate was separated on 4–15% SDS gradient polyacrylamide ReadyGels (Bio-Rad, CA, USA) and transferred to nitrocellulose membranes (Immobilon-P, Millipore, MA, USA). Membranes were first blocked using 5% nonfat milk in PBST and then incubated with rabbit anti-glypican-1 343-1 (1:2000; a gift from Dr A. Lander, UC Irvine) for 48 h at 4 °C. Following washing in PBST, membranes were incubated in horseradish peroxidase (HRP)-conjugated donkey anti-rabbit IgG (1:2000, Amersham, IL, USA) for 1 h at room temperature and washed; proteins were detected with the enhanced chemiluminescence system (NEN). For loading control, membranes were stripped and reprobed with rabbit anti-p42 MAP kinase (ERK42) 1:3000, Cell Signalling Technology, MA, USA (Moore *et al.*, 2002). Developed X-ray films were scanned and optical densities measured using Adobe Photoshop software. The values for glypican-1 were corrected relative to the corresponding value for the loading control and expressed relative to the naïve.

Statistical evaluation

The two-sample *t*-test assuming unequal variances was used to test for significant differences. All data are represented as mean \pm SEM.

Results

Glypican-1 mRNA was present in sensory neurons of the DRG of adult rats and was up-regulated after peripheral and central nerve injury

Peripheral injury

In noninjured animals, glypican-1 mRNA detected by RPA was constitutively expressed at relatively low levels in lumbar L4 and L5 DRGs (Fig. 1A). Sciatic nerve transection (SNT), which cuts the peripheral axons of $\approx 60\%$ of L4 and L5 DRG neurons (Himes & Tessler, 1989), increased glypican-1 mRNA levels substantially in DRGs ipsilateral to the injury (Fig. 1A). A significant increase was present as early as 1 day (2.03 ± 0.23 times control) and then plateaued for 3, 7 and 14 days. A significantly elevated level was maintained,

although somewhat reduced, at the longest time examined, 28 days (1.77 ± 0.16). Examination of the cellular localization of glypican-1 mRNA by *in situ* hybridization revealed that both constitutively expressed and nerve injury-induced glypican-1 mRNA were present in small- and large-diameter DRG neurons known to carry each mode of sensory input, including proprioceptive, mechanoreceptive and nociceptive information (Fig. 1B, a–d and g). No change in glypican-1 mRNA expression was detectable in the DRG contralateral to the SNT. The immediate-early gene activating transcription factor 3 (ATF3) is expressed in neurons with peripheral axonal injury (Tsujino *et al.*, 2000) and is therefore used as a marker for this type of injury. ATF3 immunoreactivity was strongly induced in the nuclei of a large number of DRG cells 3 days after SNT (Fig. 1B, e, f and h).

Central injury

Transecting the dorsal columns (dorsal column lesion; DCL) injures the central axons only of those DRG neurons that send axons directly to the brainstem, mainly large muscle afferents and cutaneous proprioceptive A β sensory fibers (Neumann & Woolf, 1999). A DCL differs from a peripheral nerve injury in that it elicits substantially fewer changes in gene expression and a smaller injury-induced cell body response, and there is no spontaneous regeneration of the injured fibers (Dusart & Schwab, 1994; Neumann & Woolf, 1999). Surprisingly, we found that this lesion increases glypican-1 mRNA in L4 and L5 DRG neurons. The time-course of the change in glypican-1 mRNA, detected by RPA (Fig. 2A), showed an initial increase at 1 day after injury (2.06 ± 0.36), that remained until ≈ 14 days, when expression declined toward preinjury levels (14-day value, 1.46 ± 0.08 times control; 28-day, 1.07 ± 0.05). Similar to that found after SNT, *in situ* hybridization revealed that up-regulation of glypican-1 mRNA expression occurred in large and small DRG neurons after DCL (Fig. 2B, a–c and g). This type of central injury did not induce expression of ATF3 in DRG neurons (Fig. 2B, e and f).

A dorsal rhizotomy (DR) injures the central axons of all neurons (large and small) in its corresponding DRG. Similar to DCL, DR creates a smaller cell-body response and minimal axonal regrowth than SNT (Lieberman, 1971; Chong *et al.*, 1994). Three days after L4 and L5 DR, a substantial increase in glypican-1 mRNA occurred in the DRGs, effectively identical to that produced by an SNT at this time-point and more than after a DCL (Fig. 2B, d). In contrast to SNT, this injury produced only a minor increase in ATF3 staining in the DRG (Fig. 2B, h).

SNT 7 days before DCL caused an additive increase in glypican-1 mRNA

At the time of the highest measured induction of glypican-1 mRNA after SNT (7 days; 2.15 ± 0.22), a DCL further increased glypican-1 mRNA expression (Fig. 3A). RPA shows that 3 days following DCL a strong (3.45 ± 0.29 -fold) change was present in the DRG whose axons had undergone an SNT 10 days previously (Fig. 3B). The contralateral DRG showed glypican-1 mRNA levels similar to those found 3 days after DCL (2.27 ± 0.32 ; data not shown). Compared to either injury alone, the combined peripheral and central axonal lesions lead to a greater increase in glypican-1 expression in DRG neurons, which remained elevated at 7 (Fig. 3A) and 28 days after DCL (mean change 2.72-fold, $n = 2$; Fig. 3B).

Glypican-1 mRNA expression is down-regulated in injured sensory neurons if their axons are allowed to regenerate

A sciatic nerve crush injury differs from an SNT with ligation in that with the crush injury the extracellular matrix stays in continuity, allowing regeneration and eventual reinnervation of targets, whereas

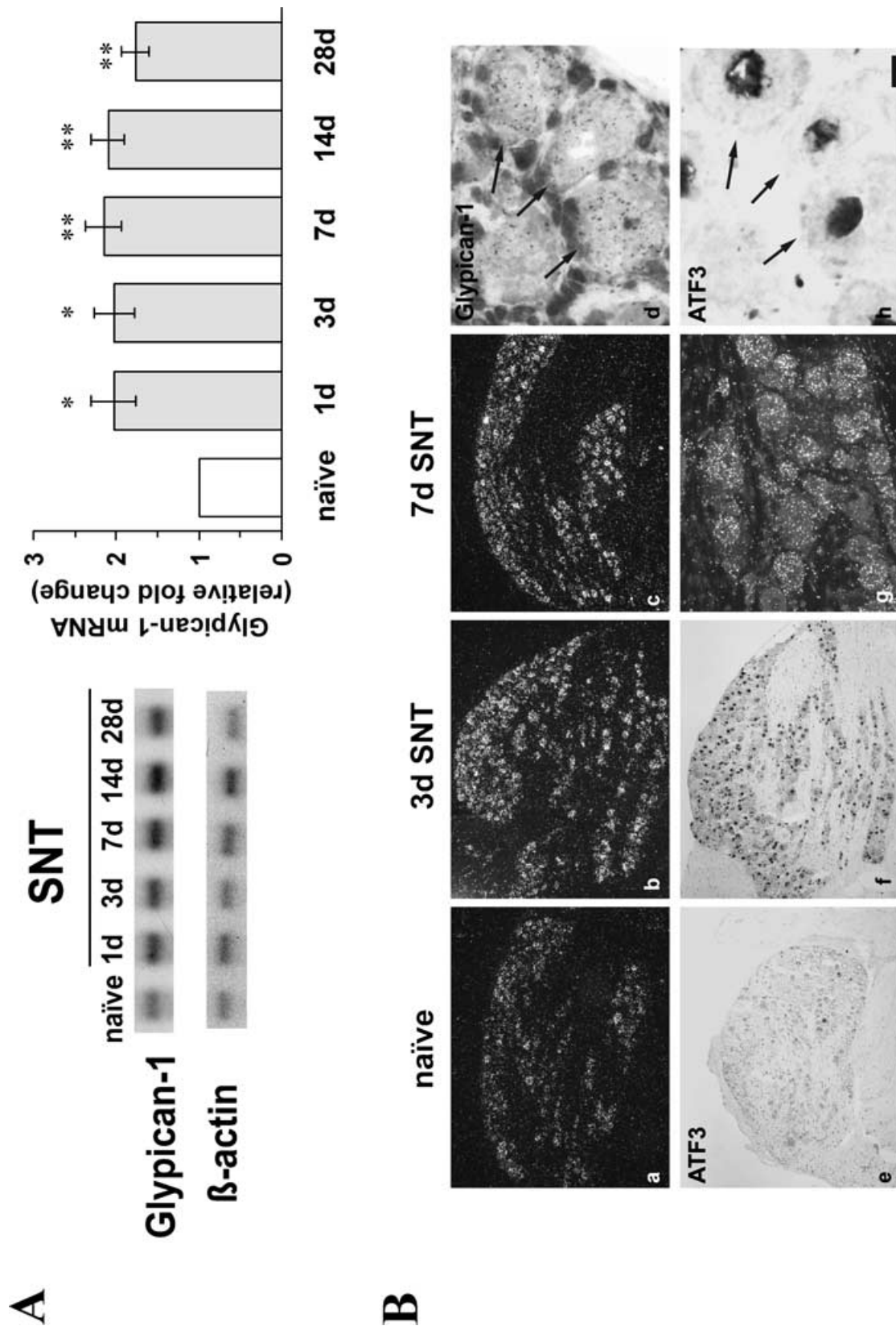


Fig. 1. Glypican-1 mRNA up-regulation in primary sensory neurons after peripheral axotomy. (A) Representative autoradiogram of an RNase protection assay (RPA) experiment on naïve and injured L4 and L5 pooled DRG samples showing glypican-1 and control β -actin mRNA at the time points indicated. The bar graph shows the change in glypican-1 mRNA quantified from three independent RPA experiments and normalized to naïve at the time points indicated ($P < 0.05$, $^{**}P < 0.01$). SNT, sciatic nerve transection. (B) Representative photomicrographs of L4 DRG sections processed for glypican-1 mRNA by *in situ* hybridization (a–d and g) or ATF3 by immunohistochemistry (e, f and h) in adjacent tissue sections. Many injured (ATF3-labelled) neurons were glypican-1 mRNA-positive 3 days following a sciatic nerve transection (arrows, d and h). (g) Both large- and small-diameter neurons expressed glypican-1 mRNA at 7 days after injury. Scale bar, 200 μ m (a–c, e, f), 60 μ m (g), 10 μ m (d, h).

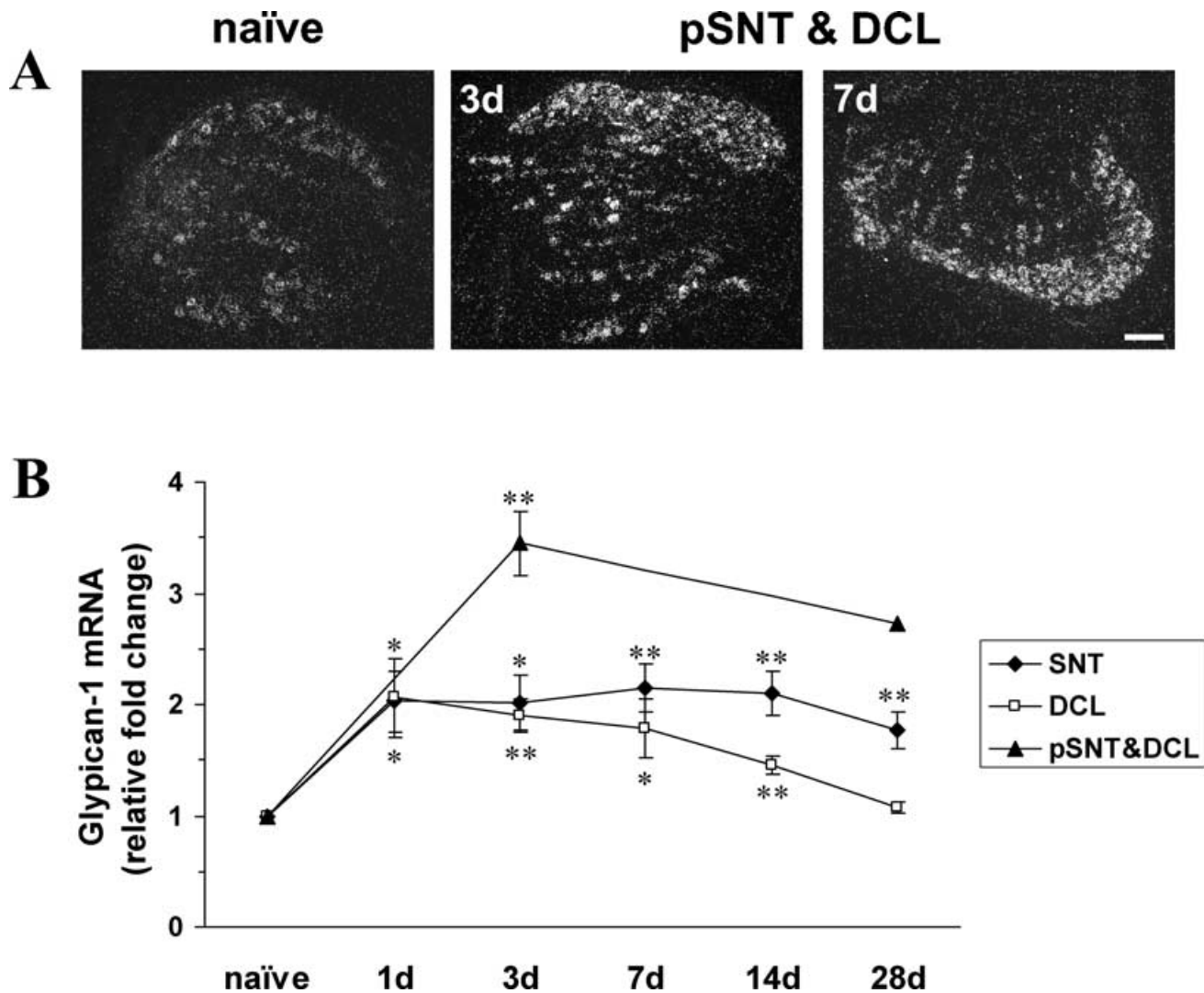


FIG. 3. Glypican-1 mRNA up-regulation in injured DRG following combined peripheral and central lesion. (A) Darkfield photomicrographs showing glypican-1 mRNA hybridization signal in sections of L4 DRGs from rats 3 and 7 days after a DCL which followed an SNT 7 days earlier (pSNT & DCL). At both time points after DCL, there was a strong increase in glypican-1 mRNA in the DRG ipsilateral to the SNT. (B) Change in glypican-1 mRNA quantified from three independent RPA experiments and normalized to naïve at the time points indicated. The combined lesions lead to a greater increase in glypican-1 expression in DRG neurons than either injury alone. The signal was highest at 3 days and remained elevated 28 days after DCL (* $P < 0.5$, ** $P < 0.01$).

in the SNT with ligation, regeneration does not take place and the injured sensory neurons remain separated from their original targets. Sciatic nerve crush elevated glypican-1 mRNA in L4 and L5 DRG at early timepoints in a manner equivalent to SNT (Figs 1B and 4). In contrast to SNT, however, glypican-1 mRNA levels declined to the baseline level by 28 days after the crush, a time by which most peripheral target reconnections have occurred (Devor & Govrin-Lippmann, 1979; Devor *et al.*, 1979). The temporal changes in glypican-1 mRNA after sciatic nerve crush are paralleled by the immediate-early transcription factor c-jun mRNA, a marker of axonal injury (Jenkins & Hunt, 1991; Jenkins *et al.*, 1993; Kenney & Kocsis, 1998), which also showed early induction and decrease to constitutive levels after reinnervation occurred (Fig. 4).

Changes in glypican-1 mRNA were paralleled by changes in protein expression

Western blot analysis of DRGs using the 343-1 antiglypican-1 antibody revealed two bands known to represent the protein (Litwack *et al.*, 1998). At ≈ 110 kDa is the core protein with heparan sulphate side

chains (Fig. 5A), previously described as intact glypican-1 proteoglycan. At ≈ 65 kDa is the core glypican protein without side chains (Litwack *et al.*, 1994; Liang *et al.*, 1997; Litwack *et al.*, 1998). Seven days after SNT, there was a significant increase in both the core (65 kDa) and the intact (110 kDa) glypican proteins (1.84 ± 0.20 and 2.48 ± 0.47 times control, respectively), representing increased translation and heparan sulphate substitution of the protein (Fig. 5). By 28 days, the increase in intact glypican protein with side chains remained significantly higher than naïve (2.18 ± 0.31 times), while levels of core protein returned towards the preinjured state (1.42 ± 0.20 times). In contrast, there was no significant increase in glypican-1 core protein after DCL, whereas the glycosylated form of glypican-1 was elevated 7 days postinjury (1.44 ± 0.14 times; Fig. 5). Because glypican-1 expression differed between peripheral and central injuries, the localization of the protein was examined.

Glypican-1 immunoreactivity was redistributed after nerve injury

Glypican-1 immunohistochemistry in DRGs from naïve animals shows prominent label in the nucleus of most neurons as indicated

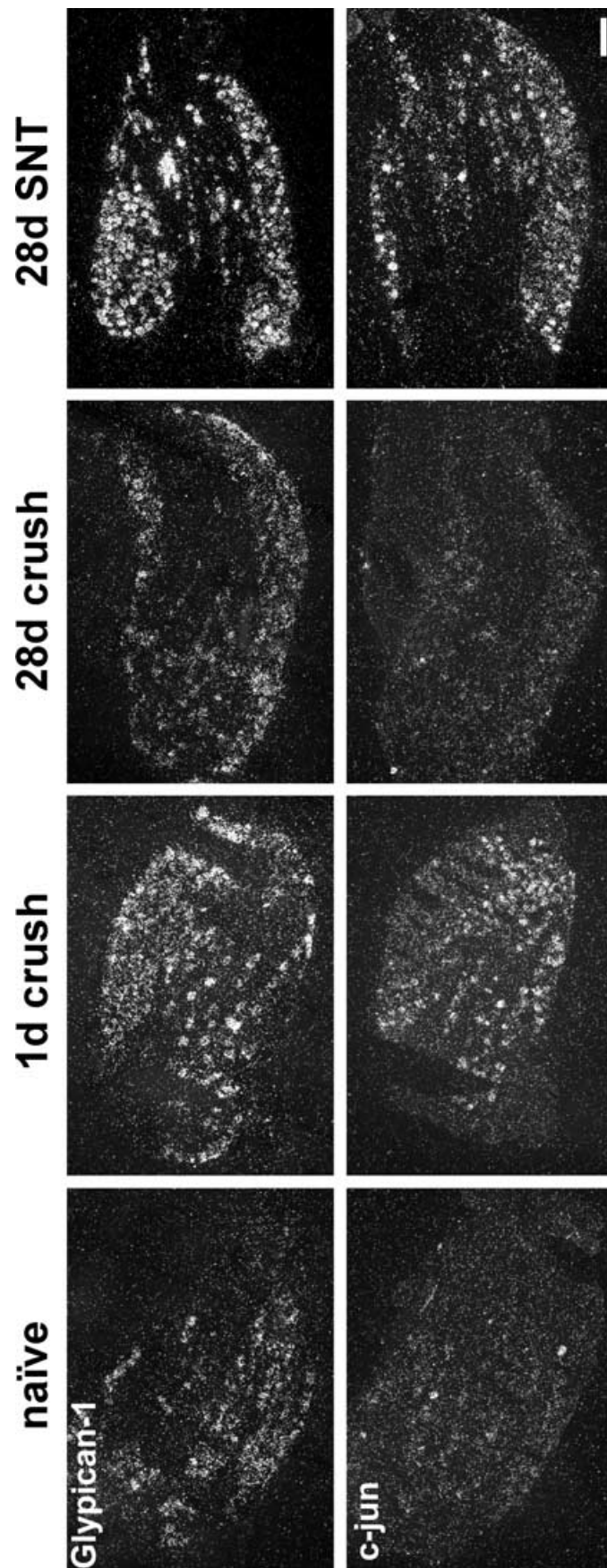


FIG. 4. Effect of sciatic nerve crush injury on glypican-1 mRNA expression in the DRG. Darkfield photomicrographs showing mRNA for glypican-1 and c-jun in adjacent sections of L4 DRGs from naïve, 1 day and 28 days after a sciatic nerve crush and 28 days after complete nerve transection with ligation (SNT). Expression of both markers was elevated 1 day after nerve crush but declined towards preinjury levels by 28 days postcrush. Expression remained high if regrowth was prevented (28 day SNT). Scale bar, 200 μ m.

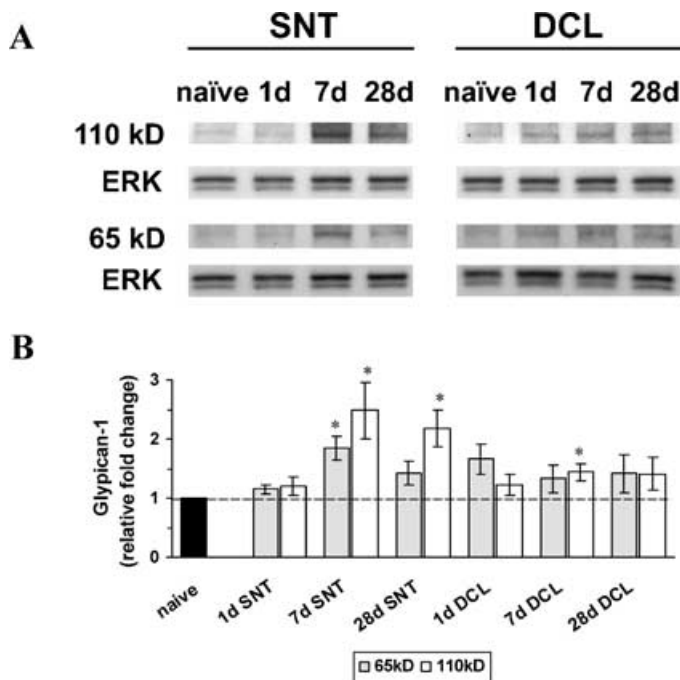


FIG. 5. Glypican protein in primary sensory neurons after peripheral and central axonal injury. (A) Western blot for glypican-1 and ERK42 loading control using naïve and injured L4 and L5 pooled DRG samples at the time points indicated. The 65-kDa band is the core glypican protein while the 110-kDa band is glypican protein with attached heparan sulphate side chains. SNT, sciatic nerve transection; DCL, dorsal column lesion. (B) Change in glypican-1 quantified from three independent Western blots and normalized to naïve levels at the time points indicated (* $P < 0.05$).

by colocalization with NeuN immunoreactivity, which strongly stains neuronal nuclei (Fig. 6A; also Liang *et al.*, 1997). There was no colocalization with GFAP-labelled non-neuronal cells (Fig. 6B). After nerve injury, however, the pattern of glypican-1 protein localization changed profoundly. Twenty-one days after SNT the nuclei of neurons showed much less staining and colocalization with NeuN disappeared (Fig. 6A). The cytoplasm of DRG neuron cell bodies and the satellite cells surrounding the DRGs became highly glypican-1 immunoreactive. A similar but slightly less robust change was also found following DCL.

An examination of these changes by a more detailed time course revealed little movement of glypican-1 from the nuclei at 1 day post-SNT or -DCL; however, stronger staining became apparent in non-neuronal cells surrounding the neurons (Fig. 7). By 3 days post-SNT, glypican-1 staining appeared in the neuronal cytoplasm while at the same time some remained in nuclei. The observed distribution 3 days after SNT looked similar to that seen after 21 days (Fig. 6) indicating a translocation to the cytoplasm and around the cell perimeter. A similar but less obvious change appeared three days after DCL when neuronal nuclei showed stronger glypican-1 immunoreactivity than in the outer regions of the cells. At 7 days post-SNT, the time when the greatest changes in core and intact glypican-1 proteins were detected by Western blot (Fig. 5B), the shift in protein localization appeared the most obvious with almost all staining existing in the cytoplasm and around the neurons, and little staining remaining in the nuclei. Seven days after DCL, glypican-1 immunostaining remained in some nuclei but also appeared around the cells (Fig. 7), a finding that fits well with the increase in intact protein and little change in the core protein found by Western blot at this stage (Fig. 5B).

Glypican-1 immunoreactivity was present in a large number of axons in the intact sciatic nerve, as well as in some Schwann cells and

non-neuronal cells (Fig. 7B). Twenty-one days following SNT, glypican-1 staining was stronger in axonal profiles of the sciatic nerve ≈ 3 mm proximal to the lesion site, whereas no change was apparent in this location 3 days after SNT (data not shown).

High expression of glypican-1 protein was detected in the intact spinal cord grey matter and was limited to neurons, as indicated by the lack of overlap with the astrocytic marker GFAP (Fig. 8A). Very little glypican-1 staining appeared in the dorsal columns running in the dorsal funiculus or in the lateral and ventral funiculus. No change of glypican-1 expression in the spinal cord was observed after SNT (data not shown). DCL, which disrupts the dorsal funiculus, resulted in the accumulation of glypican-1 staining at the lesion site 3 days after injury (Fig. 8A). Glypican-1 immunoreactivity showed up mainly in cells infiltrating the lesion site, most probably macrophages and other inflammatory cells known to appear at this stage (Dusart & Schwab, 1994; Carlson *et al.*, 1998; Frei *et al.*, 2000; Moon *et al.*, 2002; Boilard *et al.*, 2003). Twenty-one days after DCL, strong glypican-1 immunoreactivity was present at the lesion site. No double-labelling with GFAP at either 3 or 21 days following DCL indicated that there was no expression of glypican-1 in reactive astrocytes forming the glial scar (Fig. 8A). No obvious change in glypican-1 immunostaining was observed in the dorsal root nerve segment 3 days (data not shown) and 21 days (Fig. 8B) following DCL.

mRNA for members of the slit and robo family are differentially expressed in the adult DRG

The presence of potential interacting molecules with glypican-1 in the DRG was investigated by *in situ* hybridization. The slit proteins are a family of secreted guidance molecules that can direct neuronal migration and axon growth by interacting with their cellular roundabout receptors (robos) in the growing nervous system (Brose *et al.*, 1999; Wang *et al.*, 1999). These interactions are enhanced by glypican-1: slits, robos and glypican-1 form a complex which acts to augment the effects of these guidance molecules (Liang *et al.*, 1999; Hu, 2001; Ronca *et al.*, 2001). mRNA for slit 1 and robo 2 were present in the DRG at relatively abundant levels (Fig. 9A) while slit 3 was found to have low to moderate expression. Slit 2 and robo 1 mRNA were not detectable. Examination of serial sections of DRG tissue showed colocalization between mRNA for glypican-1 and robo 2 (Fig. 9B). No significant change in expression in the slit and robo mRNA was apparent after axotomy (data not shown).

Discussion

In this study we provide evidence that the expression of the proteoglycan glypican-1 is regulated in DRG neurons in a growth-dependent and injury-induced manner. A lesion to peripheral as well as central axons of these neurons was able to induce strong glypican-1 expression in the DRG. Depending on the type of injury, the observed changes lasted for >1 month in the case of peripheral injury but were of a shorter duration following central axotomy. The changing levels of glypican-1 were paralleled by a shift in localization from a predominantly nuclear to cytoplasmic and membrane-associated expression. We also show that the members of the robo and slit family of guidance molecules, known for their interactions with glypican-1 in the developing nervous system, are differentially expressed in adult DRG neurons.

Peripherally injured neurons regain a growth capacity in part through recapitulation of a developmental phenotype. Cutting a peripheral nerve changes the expression of hundreds of genes in the DRG including many that are expressed at high levels in development (Costigan *et al.*, 2002; Wang *et al.*, 2002; Xiao *et al.*, 2002), and many of these are believed to be involved in the regeneration of

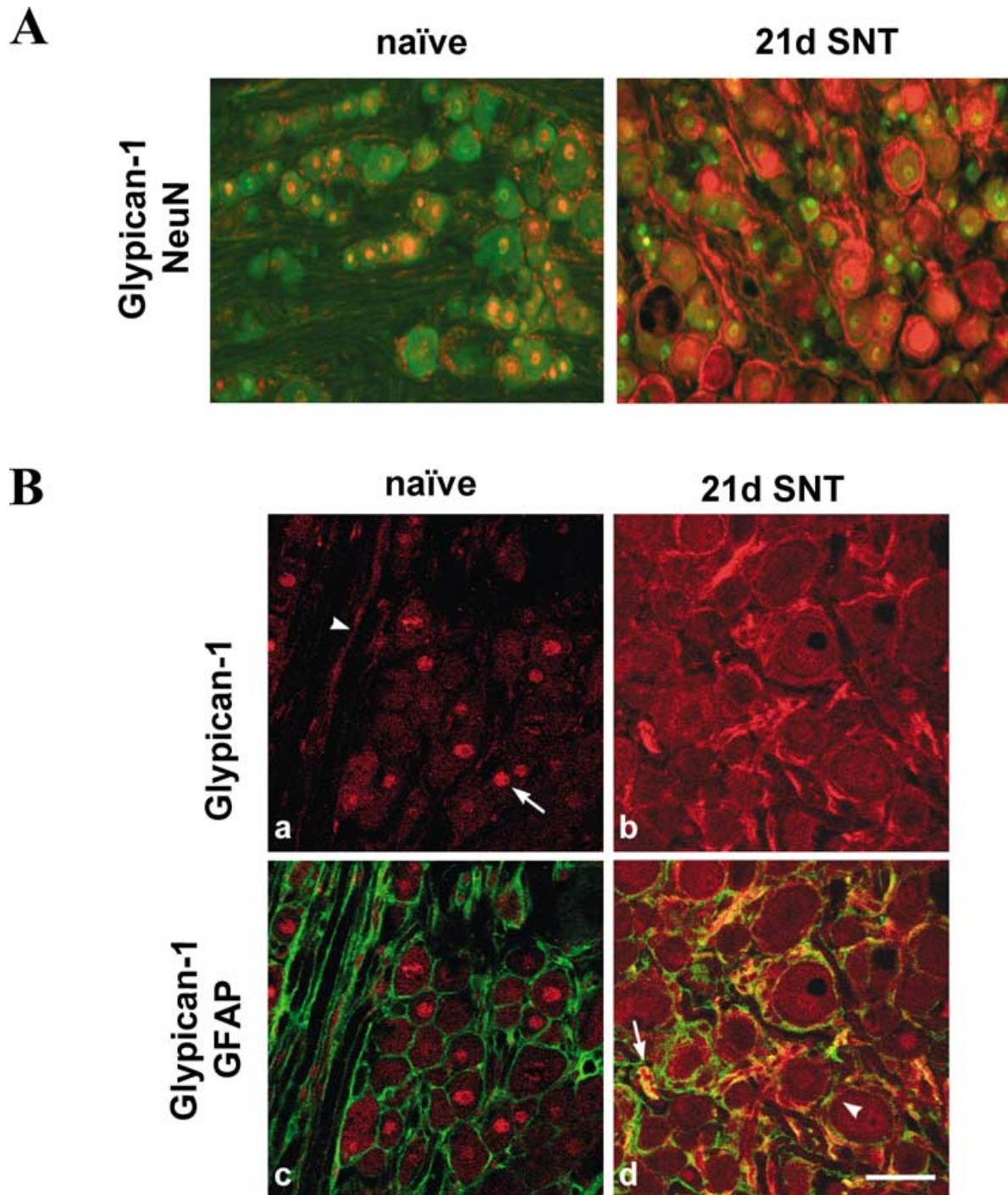


FIG. 6. Immunostaining for glypican-1 in lumbar DRG following nerve injury. (A) Adult L4 DRG sections from naïve animals and 21 days after SNT, double-stained for glypican-1 (red) and the neuronal marker NeuN (green). Glypican-1 and NeuN immunoreactivity were highly colocalized in the nuclei of naïve DRGs. This colocalization was less 21 days after SNT and glypican-1 immunoreactivity was more prominent in the cytoplasm of the NeuN positive neurons. (B) Confocal microscopy showing glypican-1 immunoreactivity (a) in nuclei of naïve DRG cells and (b) in the cytosol and plasma membrane of neurons as well as in satellite cells, 21 days after SNT. (c) Double labelling of glypican-1 and GFAP indicating no colocalization in naïve DRGs. (d) Twenty-one days following SNT there was colocalization in non-neuronal structures while cytoplasm and neuronal cell membrane only appeared glypican-1-positive. Arrows indicate examples of non-neuronal staining while arrowheads show the region of neuronal cell membrane. Scale bar, 60 μ m.

peripheral axons. We show here that glypican-1 expression is up-regulated in DRG neurons of adult rats after both peripheral and central injuries to their axons. The latter finding is remarkable because very few molecules have been shown to change expression in DRG neurons following central injury (Chong *et al.*, 1994; Kenney & Kocsis, 1997; Schwaiger *et al.*, 2000).

Although glypican-1 was up-regulated following injury to either the peripheral or the central branch of sensory neurons, the dynamics of this change in expression differed. The increase in glypican-1 mRNA expression after axonal injury began to return towards constitutive levels sooner following DCL (around 14 days) than after SNT (still up-regulated after 28 days) and the changes seen in glypican-1 protein

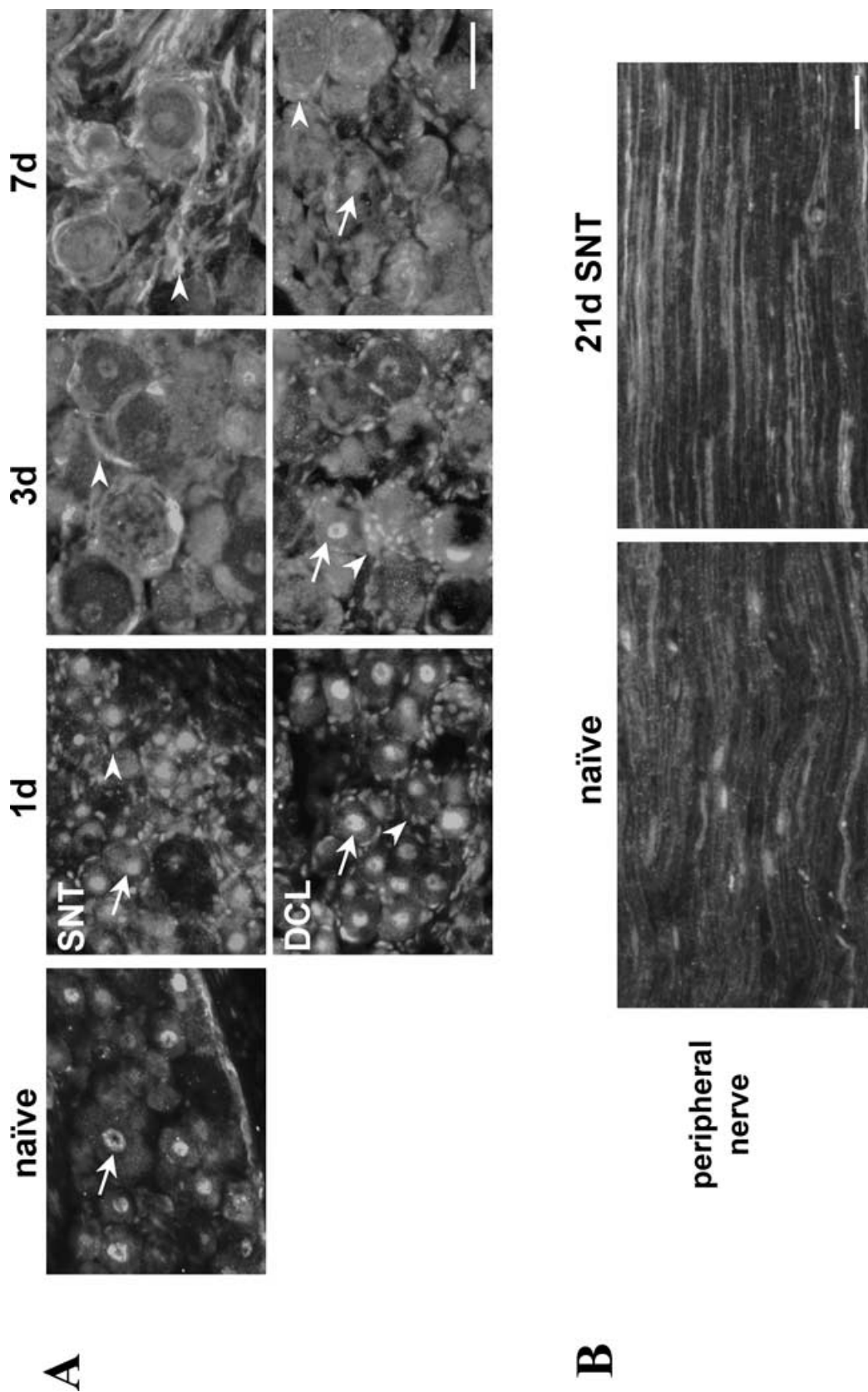


Fig. 7. Time course for glypican-1 immunoreactivity in the lumbar DRG and peripheral nerve following injury. (A) Adult L4 DRG sections from naïve animals and at 1, 3 and 7 days after SNT (upper) and DCL (lower) stained for glypican-1. In the naïve DRG glypican-1 was predominantly expressed in the nuclei (arrow) of sensory neurons whereas the cytoplasm showed only very light labelling. One day following SNT and DCL the nuclei remained highly glypican-1 immunoreactive (arrows) and some non-neuronal staining appeared (arrowheads). At 3 and 7 days post-SNT, non-neuronal glypican-1 expression became progressively stronger (arrowheads). At the same time the signal in neuronal nuclei declined to cytoplasmic levels. Three and seven days following DCL, glypican-1 staining of the nuclei became weaker although some nuclei remained glypican-1 positive (arrows). Non-neuronal staining after DCL was observed at all time-points examined (arrowheads). (B) Longitudinal sections of naïve and injured sciatic nerve stained for glypican-1. Twenty-one days after SNT, strong glypican-1 staining appeared in the nerve \approx 3 mm proximal to the lesion site. Scale bars, 60 μ m (A), 15 μ m (B).

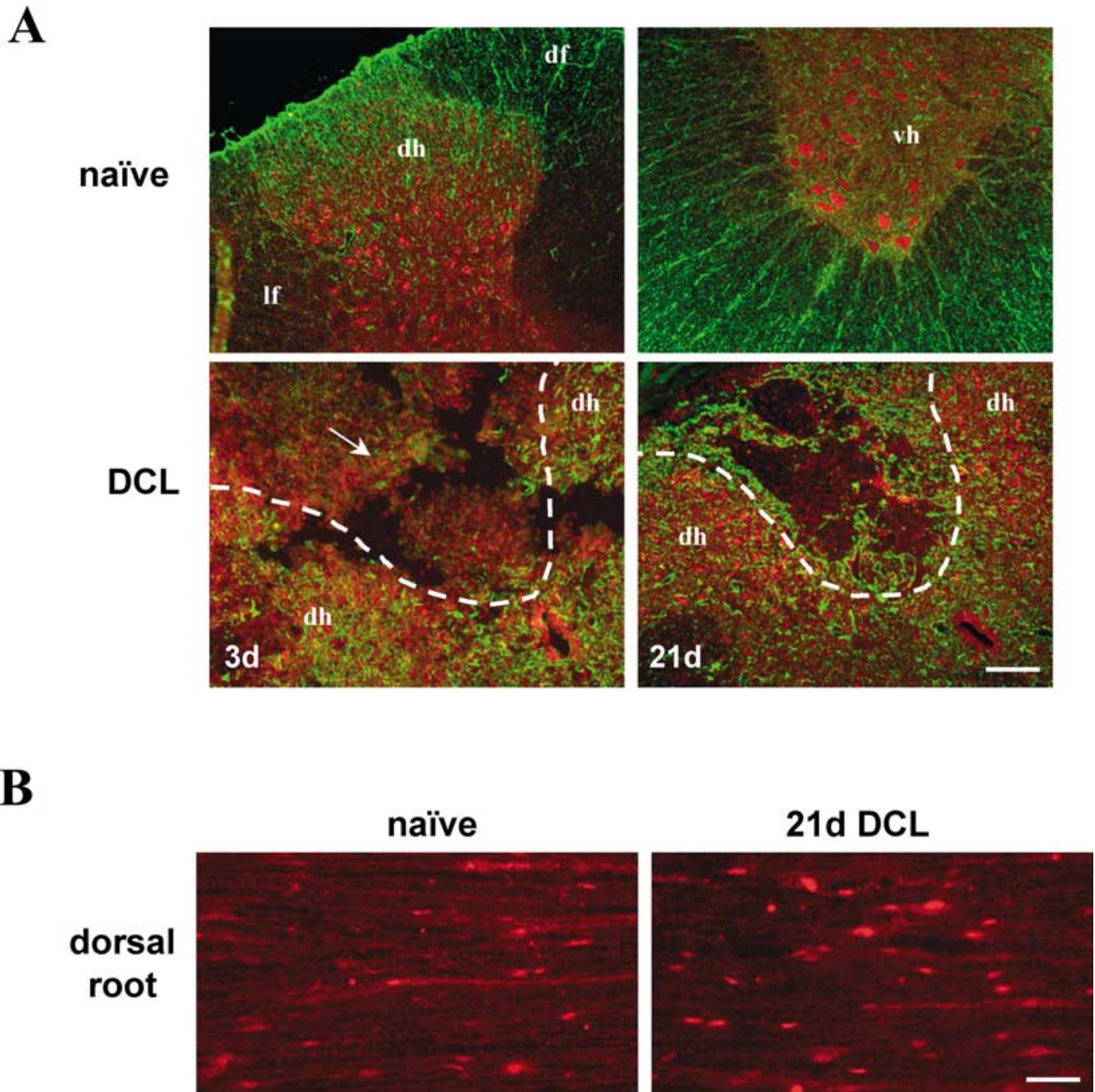


FIG. 8. Glypican-1 immunoreactivity in the lumbar spinal cord and dorsal root. (A) Cross-sectional areas of the lumbar spinal cord stained for glypican-1 (red) and GFAP (green). (Upper panels) Double staining showed no colocalization in the dorsal (dh) or ventral horn (vh) of the lumbar spinal cord in naïve rats. Glypican-1 immunoreactivity was found in neuronal cell bodies of the dorsal horn as well as at low levels in the dorsal and lateral funiculus (df and lf). In the ventral horn, glypican-1 expression was restricted to neurons, predominately motoneurons. (Lower panels) Cross-sections through the lumbar spinal cord at the site where the DCL was performed, 3 and 21 days post-DCL. The dotted line separates the grey matter of the spinal cord from the white matter site of the lesion. Three days following DCL, infiltrating cells showed high glypican-1 immunoreactivity at the site of lesion in the dorsal funiculus (arrow). Twenty-one days post-DCL, strong GFAP expression revealed the formation of the glial scar at the injury site. Glypican-1 was not expressed by reactive astrocytes but staining was found in neuronal profiles in the dorsal horn as well as in non-GFAP-positive cells infiltrating the lesion site. (B) Longitudinal sections of the L4 dorsal root stained for glypican-1. Strong glypican-1 immunoreactivity was found in axonal profiles as well as in non-neuronal cell bodies in naïve animals as well as 21 days following a DCL. Scale bars, 200 μ m (A), 15 μ m (B).

levels were apparent but not as prominent after DCL. It appears that axonal injury *per se* is sufficient to invoke an increase in glypican-1 mRNA and changes in the protein, yet the overall cell body response after central injury is weaker and shorter, possibly because, unlike peripheral axotomy, the peripheral branch of the sensory neuron remains in contact with target tissues, providing trophic support (Aldskogius *et al.*, 1985; Woolf *et al.*, 1990; Smith & Skene,

1997). In contrast to glypican-1, we have shown minimal ATF3 induction after central compared to peripheral injury.

Glypican-1 induction after both central and peripheral injury may reflect injured primary sensory neurons attempting to mount a regenerative program. In the CNS, inhibitory factors in the local environment limit regeneration (Li *et al.*, 1996; McKerracher *et al.*, 1994; Schwab & Bartholdi, 1996) and this, together with the absence of

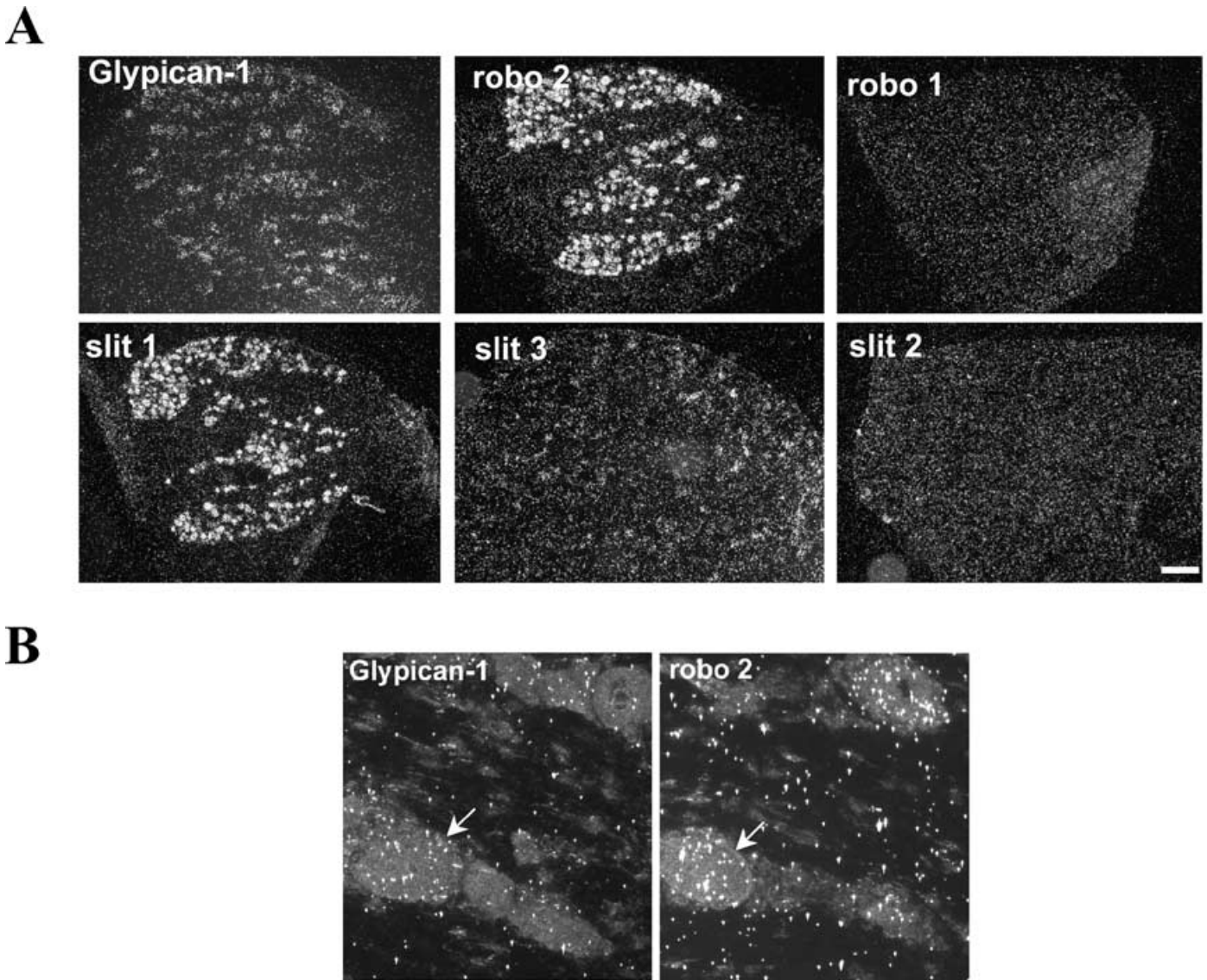


FIG. 9. Comparison of mRNA expression in uninjured DRG for glypican-1 and members of the slit-robo family. (A) Slit 1 and robo 2 mRNA had moderate to high levels of constitutive expression in uninjured L4 DRG, while expression of slit 3 mRNA was more modest. A hybridization signal for robo 1 and slit 2 was not detectable. (B) Photomicrographs show adjacent L4 DRG sections with examples of neurons that have positive levels of hybridization signal for both glypican-1 and robo 2 (arrows). Scale bars, 200 μ m (A), 30 μ m (B).

up-regulation of regeneration-associated genes such as GAP-43, may result in failure of regrowth of primary sensory central axons. A peripheral nerve transection can prime DRG neurons to overcome the normal obstacles to central axonal regeneration, possibly by increasing their intrinsic growth capacity through overexpression of injury- and growth-associated molecules (Richardson & Issa, 1984; Neumann & Woolf, 1999; Bomze *et al.*, 2001). The effect of both peripheral and central injuries on glypican-1 mRNA expression is additive and may contribute to the increased intrinsic growth capacity of centrally injured neurons after a peripheral nerve conditioning lesion.

Here we have shown the prominent nuclear localization of glypican-1 in noninjured primary sensory neurons where it may modulate transcription factors or structural proteins involved in DNA stabilization (Liang *et al.*, 1997). The presence of glypican-1 in the nucleus of central neurons has previously been described and attributed to the existence of a nuclear localization signal in the protein sequence (Liang *et al.*, 1997). The shift of glypican-1 protein from the nucleus

to the cytoplasm and membrane in DRG neurons after axonal injury hints at cell surface roles for glypican-1 after injury. This could include interaction with extracellular matrix molecules, cell adhesion molecules, growth factors and cytokines involved in axonal outgrowth, pathfinding and synapse formation (reviewed in Bernfield *et al.*, 1999; Bandtlow & Zimmermann, 2000; Fransson, 2003). The injury-induced distribution of glypican-1 not only to the cell body membrane but also along the injured peripheral axon after SNT is a potential factor for axonal regrowth, because a similar distribution is not found along the injured central branch after DCL.

Glypican-1 protein was up-regulated after SNT as early as 7 days postinjury and stayed expressed at high levels for >1 month. These changes include elevated levels of intact glypican-1 carrying heparan sulphate side chains over 1 month as well as increased expression of nonglycosylated glypican-1 core protein around day 7 postinjury. There was also a modest increase in glypican-1 protein after DCL, although this change was only significant for intact glypican-1 7 days after the lesion. Elevated glypican-1 protein levels were paralleled by a

redistribution of the protein, revealing more glypican-1 in the cytosol and along the cell membrane of DRG neurons after injury to the central and even more pronounced after injury to the peripheral axon. The increased amount of intact glypican-1 could therefore account for some of the cytosolic and membrane-associated portion of glypican-1 immunoreactivity, whereas glypican-1 core protein was more likely to be found in the nucleus. There is evidence that heparan sulphate proteoglycans can be liberated from GPI linkage for release from the cell surface, which probably accounts for the non-neuronal staining that we observe in the DRG (Carey *et al.*, 1993; Ishihara *et al.*, 1987). Glypican-1 is present in the sciatic nerve, in axons and some non-neuronal cells, both in naïve and, in greater concentrations, in the axotomized condition, suggesting glypican-1 trafficking and accumulation along the peripheral axons. In the dorsal root glypican-1 is also found in axons and non-neuronal cells. A DCL does not evoke a strong enough signal to lead to an obvious accumulation in dorsal root neurites, possibly because only a minor proportion of the axons running in the dorsal root are actually injured by a DCL. It is remarkable, though, that the DCL acts as a signal to induce mRNA expression in many neurons in a single DRG. The shift in glypican to cell membranes may alter the responsiveness of injured DRG neurons to growth-related factors such as FGF2 (Steinfeld *et al.*, 1996; Bonneh-Barkay *et al.*, 1997; Zhang *et al.*, 2001; Malave *et al.*, 2003) and the slit proteins (Hu, 2001; Liang *et al.*, 1999; Ronca *et al.*, 2001).

We have shown the presence of slit 1, robo 2 and glypican-1 in the adult DRG. These molecules could potentially form a functional complex that may regulate axonal growth in the adult nervous system when glypican-1 is presented at the cell surface. The role of slits and robos in the DRG neurons remains to be elucidated, yet it is possible that robos form a functional receptor complex at the plasma membrane that renders neurons responsive to the action of slits. This interaction may occur in the DRG itself as a paracrine signal among neurons as well as at the growth cone. Robos and slits have crucial functions in axonal pathfinding during the development of the central nervous system (Zou *et al.*, 2000; Bagri *et al.*, 2002). Slit–robo interactions have been shown to positively regulate axonal elongation and branching, to cause growth cone collapse, and to direct axonal growth, acting as chemorepulsive guidance cues, for example along the midline of the CNS, for which heparan sulphate has recently been shown to be necessary (Bagri *et al.*, 2002; Nguyen Ba-Charvet *et al.*, 1999; Wang *et al.*, 1999; Inatani *et al.*, 2003). In the injured spinal cord, robos may work as a guide, leading axons in specific directions and preventing random and uncontrolled axonal growth. The full influence of the slits and robos in adult DRG neurons may only manifest itself after axotomy, when glypican levels are increased at the cell membrane. These data suggest a role for glypican-1 in the response of primary sensory neurons to axonal injury.

Acknowledgements

This work was funded by the NIH HD38533 and NS38253 (C.J.W.). We thank Arthur Lander for the supply of glypican antibody, Katia Befort and Michaela Thallmair for critical discussion and reading, and Tarek Samad for technical assistance.

Abbreviations

ATF3, activating transcription factor 3; CAP-23, cytoskeleton-associated protein 23; DCL, dorsal column lesion; DR, dorsal rhizotomy; DRG, dorsal root ganglion; FGF, fibroblast growth factor; GAP-43, growth-associated protein 43; GPI, glycosyl phosphatidyl inositol; HRP, horseradish peroxidase; robos, roundabout receptors; RPA, RNase protection assay; SNT, sciatic nerve transection.

References

- Aldskogius, H., Arvidsson, J. & Grant, G. (1985) The reaction of primary sensory neurons to peripheral nerve injury with particular emphasis on transganglionic changes. *Brain Res.*, **357**, 27–46.
- Bagri, A., Marin, O., Plump, A.S., Mak, J., Pleasure, S.J., Rubenstein, J.L. & Tessier-Lavigne, M. (2002) Slit proteins prevent midline crossing and determine the dorsoventral position of major axonal pathways in the mammalian forebrain. *Neuron*, **33**, 233–248.
- Bandtlow, C.E. & Zimmermann, D.R. (2000) Proteoglycans in the developing brain: new conceptual insights for old proteins. *Physiol. Rev.*, **80**, 1267–1290.
- Bernfield, M., Gotte, M., Park, P.W., Reizes, O., Fitzgerald, M.L., Lincecum, J. & Zako, M. (1999) Functions of cell surface heparan sulfate proteoglycans. *Annu. Rev. Biochem.*, **68**, 729–777.
- Boillard, E., Bourgoin, S.G., Bernatchez, C., Poubelle, P.E. & Surette, M.E. (2003) Interaction of low molecular weight group IIA phospholipase A2 with apoptotic human T cells: role of heparan sulfate proteoglycans. *Faseb J.*, **17**, 1068–1080.
- Bomze, H.M., Bulsara, K.R., Iskandar, B.J., Caroni, P. & Skene, J.H. (2001) Spinal axon regeneration evoked by replacing two growth cone proteins in adult neurons. *Nat. Neurosci.*, **4**, 38–43.
- Bonneh-Barkay, D., Shlissel, M., Berman, B., Shaoul, E., Admon, A., Vlodavsky, I., Carey, D.J., Asundi, V.K., Reich-Slotky, R. & Ron, D. (1997) Identification of glypican as a dual modulator of the biological activity of fibroblast growth factors. *J. Biol. Chem.*, **272**, 12415–12421.
- Brose, K., Bland, K.S., Wang, K.H., Arnott, D., Henzel, W., Goodman, C.S., Tessier-Lavigne, M. & Kidd, T. (1999) Slit proteins bind Robo receptors and have an evolutionarily conserved role in repulsive axon guidance. *Cell*, **96**, 795–806.
- Carey, D.J., Stahl, R.C., Asundi, V.K. & Tucker, B. (1993) Processing and subcellular distribution of the Schwann cell lipid-anchored heparan sulfate proteoglycan and identification as glypican. *Exp. Cell Res.*, **208**, 10–18.
- Carlson, S.L., Parrish, M.E., Springer, J.E., Doty, K. & Dossett, L. (1998) Acute inflammatory response in spinal cord following impact injury. *Exp. Neurol.*, **151**, 77–88.
- Chong, M.S., Reynolds, M.L., Irwin, N., Coggeshall, R.E., Emson, P.C., Benowitz, L.I. & Woolf, C.J. (1994) GAP-43 expression in primary sensory neurons following central axotomy. *J. Neurosci.*, **14**, 4375–4384.
- Costigan, M., Befort, K., Karchewski, L., Griffin, R.S., D'Urso, D., Allchorne, A., Sitarski, J., Mannion, J.W., Pratt, R.E. & Woolf, C.J. (2002) Replicate high-density rat genome oligonucleotide microarrays reveal hundreds of regulated genes in the dorsal root ganglion after peripheral nerve injury. *BMC Neurosci.*, **3**, 16.
- De Leon, M., Welcher, A.A., Suter, U. & Shooter, E.M. (1991) Identification of transcriptionally regulated genes after sciatic nerve injury. *J. Neurosci. Res.*, **29**, 437–448.
- Devor, M. & Govrin-Lippmann, R. (1979) Maturation of axonal sprouts after nerve crush. *Exp. Neurol.*, **64**, 260–270.
- Devor, M., Schonfeld, D., Seltzer, Z. & Wall, P.D. (1979) Two modes of cutaneous reinnervation following peripheral nerve injury. *J. Comp. Neurol.*, **185**, 211–220.
- Dusart, I. & Schwab, M.E. (1994) Secondary cell death and the inflammatory reaction after dorsal hemisection of the rat spinal cord. *Eur. J. Neurosci.*, **6**, 712–724.
- Fransson, L.A. (2003) Glypicans. *Int. J. Biochem. Cell Biol.*, **35**, 125–129.
- Frei, E., Klusman, I., Schnell, L. & Schwab, M.E. (2000) Reactions of oligodendrocytes to spinal cord injury: cell survival and myelin repair. *Exp. Neurol.*, **163**, 373–380.
- Frey, D., Laux, T., Xu, L., Schneider, C. & Caroni, P. (2000) Shared and unique roles of CAP23 and GAP43 in actin regulation, neurite outgrowth, and anatomical plasticity. *J. Cell Biol.*, **149**, 1443–1454.
- Hagino, S., Iseki, K., Mori, T., Zhang, Y., Hikake, T., Yokoya, S., Takeuchi, M., Hasimoto, H., Kikuchi, S. & Wanaka, A. (2003a) Slit and glypican-1 mRNAs are coexpressed in the reactive astrocytes of the injured adult brain. *Glia*, **42**, 130–138.
- Hagino, S., Iseki, K., Mori, T., Zhang, Y., Sakai, N., Yokoya, S., Hikake, T., Kikuchi, S. & Wanaka, A. (2003b) Expression pattern of glypican-1 mRNA after brain injury in mice. *Neurosci. Lett.*, **349**, 29–32.
- Halfter, W. (1993) A heparan sulfate proteoglycan in developing avian axonal tracts. *J. Neurosci.*, **13**, 2863–2873.
- Herndon, M.E., Stipp, C.S. & Lander, A.D. (1999) Interactions of neural glycosaminoglycans and proteoglycans with protein ligands: assessment of selectivity, heterogeneity and the participation of core proteins in binding. *Glycobiology*, **9**, 143–155.

- Himes, B.T. & Tessler, A. (1989) Death of some dorsal root ganglion neurons and plasticity of others following sciatic nerve section in adult and neonatal rats. *J. Comp. Neurol.*, **284**, 215–230.
- Hu, H. (2001) Cell-surface heparan sulfate is involved in the repulsive guidance activities of Slit2 protein. *Nat. Neurosci.*, **4**, 695–701.
- Inatani, M., Irie, F., Plump, A.S., Tessier-Lavigne, M. & Yamaguchi, Y. (2003) Mammalian brain morphogenesis and midline axon guidance require heparan sulfate. *Science*, **302**, 1044–1046.
- Ishihara, M., Fedarko, N.S. & Conrad, H.E. (1987) Involvement of phosphatidylinositol and insulin in the coordinate regulation of proteoglycan sulfate metabolism and hepatocyte growth. *J. Biol. Chem.*, **262**, 4708–4716.
- Jenkins, R. & Hunt, S.P. (1991) Long-term increase in the levels of c-jun mRNA and jun protein-like immunoreactivity in motor and sensory neurons following axon damage. *Neurosci. Lett.*, **129**, 107–110.
- Jenkins, R., McMahon, S.B., Bond, A.B. & Hunt, S.P. (1993) Expression of c-Jun as a response to dorsal root and peripheral nerve section in damaged and adjacent intact primary sensory neurons in the rat. *Eur. J. Neurosci.*, **5**, 751–759.
- Karchewski, L.A., Kim, F.A., Johnston, J., McKnight, R.M. & Verge, V.M. (1999) Anatomical evidence supporting the potential for modulation by multiple neurotrophins in the majority of adult lumbar sensory neurons. *J. Comp. Neurol.*, **413**, 327–341.
- Karthikeyan, L., Flad, M., Engel, M., Meyer-Puttlitz, B., Margolis, R.U. & Margolis, R.K. (1994) Immunocytochemical and in situ hybridization studies of the heparan sulfate proteoglycan, glypican, in nervous tissue. *J. Cell Sci.*, **107**, 3213–3222.
- Kenney, A.M. & Kocsis, J.D. (1997) Temporal variability of jun family transcription factor levels in peripherally or centrally transected adult rat dorsal root ganglia. *Brain Res. Mol. Brain Res.*, **52**, 53–61.
- Kenney, A.M. & Kocsis, J.D. (1998) Peripheral axotomy induces long-term c-Jun amino-terminal kinase-1 activation and activator protein-1 binding activity by c-Jun and junD in adult rat dorsal root ganglia. *In vivo. J. Neurosci.*, **18**, 1318–1328.
- Li, M., Shibata, A., Li, C., Braun, P.E., McKerracher, L., Roder, J., Kater, S.B. & David, S. (1996) Myelin-associated glycoprotein inhibits neurite/axon growth and causes growth cone collapse. *J. Neurosci. Res.*, **46**, 404–414.
- Liang, Y., Annan, R.S., Carr, S.A., Popp, S., Mevissen, M., Margolis, R.K. & Margolis, R.U. (1999) Mammalian homologues of the *Drosophila* slit protein are ligands of the heparan sulfate proteoglycan glypican-1 in brain. *J. Biol. Chem.*, **274**, 17885–17892.
- Liang, Y., Haring, M., Roughley, P.J., Margolis, R.K. & Margolis, R.U. (1997) Glypican and biglycan in the nuclei of neurons and glioma cells: presence of functional nuclear localization signals and dynamic changes in glypican during the cell cycle. *J. Cell Biol.*, **139**, 851–864.
- Lieberman, A.R. (1971) The axon reaction: a review of the principal features of perikaryal responses to axon injury. *Int. Rev. Neurobiol.*, **14**, 49–124.
- Litwack, E.D., Ivins, J.K., Kumbasar, A., Paine-Saunders, S., Stipp, C.S. & Lander, A.D. (1998) Expression of the heparan sulfate proteoglycan glypican-1 in the developing rodent. *Dev. Dyn.*, **211**, 72–87.
- Litwack, E.D., Stipp, C.S., Kumbasar, A. & Lander, A.D. (1994) Neuronal expression of glypican, a cell-surface glycosylphosphatidylinositol-anchored heparan sulfate proteoglycan, in the adult rat nervous system. *J. Neurosci.*, **14**, 3713–3724.
- Malave, C., Villegas, G.M., Hernandez, M., Martinez, J.C., Castillo, C., Suarez de Mata, Z. & Villegas, R. (2003) Role of glypican-1 in the trophic activity on PC12 cells induced by cultured sciatic nerve conditioned medium: identification of a glypican-1-neuregulin complex. *Brain Res.*, **983**, 74–83.
- McKerracher, L., David, S., Jackson, D.L., Kottis, V., Dunn, R.J. & Braun, P.E. (1994) Identification of myelin-associated glycoprotein as a major myelin-derived inhibitor of neurite growth. *Neuron*, **13**, 805–811.
- Moon, L.D., Asher, R.A., Rhodes, K.E. & Fawcett, J.W. (2002) Relationship between sprouting axons, proteoglycans and glial cells following unilateral nigrostriatal axotomy in the adult rat. *Neuroscience*, **109**, 101–117.
- Moore, K.A., Kohno, T., Karchewski, L.A., Scholz, J., Baba, H. & Woolf, C.J. (2002) Partial peripheral nerve injury promotes a selective loss of GABAergic inhibition in the superficial dorsal horn of the spinal cord. *J. Neurosci.*, **22**, 6724–6731.
- Neumann, S. & Woolf, C.J. (1999) Regeneration of dorsal column fibers into and beyond the lesion site following adult spinal cord injury. *Neuron*, **23**, 83–91.
- Nguyen Ba-Charvet, K.T., Brose, K., Marillat, V., Kidd, T., Goodman, C.S., Tessier-Lavigne, M., Sotelo, C. & Chedotal, A. (1999) Slit2-Mediated chemorepulsion and collapse of developing forebrain axons. *Neuron*, **22**, 463–473.
- Richardson, P.M. & Issa, V.M. (1984) Peripheral injury enhances central regeneration of primary sensory neurones. *Nature*, **309**, 791–793.
- Ronca, F., Andersen, J.S., Paech, V. & Margolis, R.U. (2001) Characterization of Slit protein interactions with glypican-1. *J. Biol. Chem.*, **276**, 29141–29147.
- Samad, T.A., Moore, K.A., Sapirstein, A., Billet, S., Allchorne, A., Poole, S., Bonventre, J.V. & Woolf, C.J. (2001) Interleukin-1 β -mediated induction of Cox-2 in the CNS contributes to inflammatory pain hypersensitivity. *Nature*, **410**, 471–475.
- Schnell, L. & Schwab, M.E. (1990) Axonal regeneration in the rat spinal cord produced by an antibody against myelin-associated neurite growth inhibitors. *Nature*, **343**, 269–272.
- Schwab, M.E. & Bartholdi, D. (1996) Degeneration and regeneration of axons in the lesioned spinal cord. *Physiol. Rev.*, **76**, 319–370.
- Schwaiger, F.W., Hager, G., Schmitt, A.B., Horvat, A., Streif, R., Spitzer, C., Gamal, S., Breuer, S., Brook, G.A., Nacimiento, W. & Kreutzberg, G.W. (2000) Peripheral but not central axotomy induces changes in Janus kinases (JAK) and signal transducers and activators of transcription (STAT). *Eur. J. Neurosci.*, **12**, 1165–1176.
- Skene, J.H., Jacobson, R.D., Snipes, G.J., McGuire, C.B., Norden, J.J. & Freeman, J.A. (1986) A protein induced during nerve growth (GAP-43) is a major component of growth-cone membranes. *Science*, **233**, 783–786.
- Smith, D.S. & Skene, J.H. (1997) A transcription-dependent switch controls competence of adult neurons for distinct modes of axon growth. *J. Neurosci.*, **17**, 646–658.
- Steinfeld, R., Van Den Berghe, H. & David, G. (1996) Stimulation of fibroblast growth factor receptor-1 occupancy and signaling by cell surface-associated syndecans and glypican. *J. Cell Biol.*, **133**, 405–416.
- Strittmatter, S.M., Fankhauser, C., Huang, P.L., Mashimo, H. & Fishman, M.C. (1995) Neuronal pathfinding is abnormal in mice lacking the neuronal growth cone protein GAP-43. *Cell*, **80**, 445–452.
- Tsujino, H., Kondo, E., Fukuoka, T., Dai, Y., Tokunaga, A., Miki, K., Yonenobu, K., Ochi, T. & Noguchi, K. (2000) Activating transcription factor 3 (ATF3) induction by axotomy in sensory and motoneurons: a novel neuronal marker of nerve injury. *Mol. Cell Neurosci.*, **15**, 170–182.
- Wang, K.H., Brose, K., Arnott, D., Kidd, T., Goodman, C.S., Henzel, W. & Tessier-Lavigne, M. (1999) Biochemical purification of a mammalian slit protein as a positive regulator of sensory axon elongation and branching. *Cell*, **96**, 771–784.
- Wang, H., Sun, H., Della Penna, K., Benz, R.J., Xu, J., Gerhold, D.L., Holder, D.J. & Koblin, K.S. (2002) Chronic neuropathic pain is accompanied by global changes in gene expression and shares pathobiology with neurodegenerative diseases. *Neuroscience*, **114**, 529–546.
- Woolf, C.J., Reynolds, M.L., Molander, C., O'Brien, C., Lindsay, R.M. & Benowitz, L.I. (1990) The growth-associated protein GAP-43 appears in dorsal root ganglion cells and in the dorsal horn of the rat spinal cord following peripheral nerve injury. *Neuroscience*, **34**, 465–478.
- Xiao, H.S., Huang, Q.H., Zhang, F.X., Bao, L., Lu, Y.J., Guo, C., Yang, L., Huang, W.J., Fu, G., Xu, S.H., Cheng, X.P., Yan, Q., Zhu, Z.D., Zhang, X., Chen, Z., Han, Z.G. & Zhang, X. (2002) Identification of gene expression profile of dorsal root ganglion in the rat peripheral axotomy model of neuropathic pain. *Proc. Natl Acad. Sci. USA*, **99**, 8360–8365.
- Zhang, Z., Coomans, C. & David, G. (2001) Membrane heparan sulfate proteoglycan-supported FGF2-FGFR1 signaling: evidence in support of the 'cooperative end structures' model. *J. Biol. Chem.*, **276**, 41921–41929.
- Zou, Y., Stoeckli, E., Chen, H. & Tessier-Lavigne, M. (2000) Squeezing axons out of the gray matter: a role for slit and semaphorin proteins from midline and ventral spinal cord. *Cell*, **102**, 363–375.

Chapter 6

Axonal injury-dependent induction of the peripheral benzodiazepine receptor in small-diameter adult rat primary sensory neurons

Laurie A. Karchewski, Stefan Bloechlinger and Clifford J. Woolf

Axonal injury-dependent induction of the peripheral benzodiazepine receptor in small-diameter adult rat primary sensory neurons

Laurie A. Karchewski,^{1,2} Stefan Bloechlinger^{1,3} and Clifford J. Woolf¹

¹Neural Plasticity Research Group, Department of Anaesthesia and Critical Care, Massachusetts General Hospital and Harvard Medical School, MGH-East, 149 13th Street, Rm 4309, Charlestown, MA 02129, USA

²Institut de Génétique et de Biologie Moléculaire et Cellulaire, CNRS/INSERM/ULP, UMR7104, Parc d'Innovation, 1 rue Laurent Fries BP 10142, 67404 Illkirch Cedex, C.U. Strasbourg, France

³Brain Research Institute, University of Zürich, Department of Biology, Swiss Federal Institute of Technology, Winterthurerstrasse 190, CH-8057 Zürich, Switzerland

Keywords: axotomy, DBI, DRG, nerve injury, PBR, PK11195

Abstract

The peripheral benzodiazepine receptor (PBR), a benzodiazepine but not γ -aminobutyric acid-binding mitochondrial membrane protein, has roles in steroid production, energy metabolism, cell survival and growth. PBR expression in the nervous system has been reported in non-neuronal glial and immune cells. We now show expression of both PBR mRNA and protein, and the appearance of binding of a synthetic ligand, [³H]PK11195, in dorsal root ganglion (DRG) neurons following injury to the sciatic nerve. In naïve animals, PBR mRNA, protein expression and ligand binding are undetectable in the DRG. Three days after sciatic nerve transection, however, PBR mRNA begins to be expressed in injured neurons, and 4 weeks after the injury, expression and ligand binding are present in 35% of L4 DRG neurons. PBR ligand binding also appears after injury in the superficial dorsal horn of the spinal cord. The PBR expression in the DRG is restricted to small and medium-sized neurons and returns to naïve levels if the injured peripheral axons are allowed to regrow and reinnervate targets. No non-neuronal PBR expression is detected, unlike its putative endogenous ligand the diazepam binding inhibitor (DBI), which is expressed only in non-neuronal cells, including the satellite cells that surround DRG neurons. DBI expression does not change with sciatic nerve transection. PBR acting on small-calibre neurons could play a role in the adaptive survival and growth responses of these cells to injury of their axons.

Introduction

Primary sensory neurons, with cell bodies in the dorsal root ganglion (DRG) convey information along their axons from the periphery to the central nervous system. The diameter of the sensory neuron cell bodies and their axons, as well as their degree of myelination, corresponds to the modality of the information they convey. In general, large and medium diameter myelinated neurons carry proprioceptive and cutaneous mechanoreceptive information, respectively, whereas smaller myelinated and unmyelinated neurons transmit thermoreceptive and nociceptive information (Lawson, 2002).

When an adult peripheral nerve is injured, the injured sensory neurons show altered levels of mRNA and proteins for numerous molecules, in the switch from a differentiated transducing and neurotransmitting state, to one in which the need for survival and regrowth becomes predominant (Lieberman, 1971; Aldskogius *et al.*, 1985). Microarray analysis has recently revealed the extent and complexity of the injury-induced changes in gene-expression identifying

hundreds of up- and downregulated genes in the DRG after axotomy (Costigan *et al.*, 2002; Xiao *et al.*, 2002).

Among those genes of which the expression increases in the DRG after axonal injury, is the peripheral benzodiazepine receptor (PBR; Costigan *et al.*, 2002; Xiao *et al.*, 2002). Like the central γ -aminobutyric acid (GABA)_A receptor, PBR binds benzodiazepines, but unlike the GABA_A receptor it does not bind GABA and has a distribution and action quite distinct from the central benzodiazepine receptor, which is a chloride ion channel inserted in the plasma membrane (DeLorey & Olsen, 1992). First identified in peripheral, non-nervous tissues (Braestrup & Squires, 1977), PBR is a mitochondrial membrane protein with widespread expression throughout the body, particularly in steroidogenic tissues (Amsterdam & Suh, 1991; Papadopoulos, 1993) and in leukocytes (Cahard *et al.*, 1994). In the nervous system, PBR has been identified in the choroid plexus, the ependymal linings, astrocytes and microglia (Benavides *et al.*, 1983; Moynagh *et al.*, 1991; Itzhak *et al.*, 1993; Park *et al.*, 1996).

The diazepam binding inhibitor (DBI), a 10 kDa polypeptide found within brain and other regions of the body, along with porphyrins, have been proposed to be endogenous ligands for the peripheral benzodiazepine receptor (Guidotti *et al.*, 1983; Snyder *et al.*, 1987; Verma *et al.*, 1987). Several pharmacological ligands also bind to the receptor and

Correspondence: Dr Laurie A. Karchewski, ²Institut de Génétique et de Biologie Moléculaire et Cellulaire, as above.
E-mail: lkarch@igbmc.u-strasbg.fr

Received 29 March 2004, revised 19 May 2004, accepted 24 May 2004

elicit a wide range of effects (Braestrup & Squires, 1978; Le Fur *et al.*, 1983; Trapani *et al.*, 1999; Ferzaz *et al.*, 2002). PBR-activating ligands stimulate steroidogenesis (Besman *et al.*, 1989; McCauley *et al.*, 1995; Lacor *et al.*, 1999), have anti-inflammatory and antinociceptive effects (Bressan *et al.*, 2003; Torres *et al.*, 2000; Lazzarini *et al.*, 2001; DalBo *et al.*, 2004; Farges *et al.*, 2004), promote the survival and repair of injured motor neurons (Ferzaz *et al.*, 2002) and protect against apoptosis (Bono *et al.*, 1999; Strohmeier *et al.*, 2002). Increases in PBR levels and binding occurs in the nervous system in microglia in a number of neuropathological conditions including Alzheimer's disease (Diorio *et al.*, 1991), Huntington's disease (Messmer & Reynolds, 1998), multiple sclerosis (Vowinckel *et al.*, 1997) and amyotrophic lateral sclerosis (Sitte *et al.*, 2001) and, because of this, PBR has been used clinically as a microglial marker (Miettinen *et al.*, 1995; Leong *et al.*, 1996). PBR expression also increases in glia following nerve injury (Gehlert *et al.*, 1997; Lacor *et al.*, 1996), neurotoxic lesions (Kuhlmann & Guilarte, 2000) and ischemia (Stephenson *et al.*, 1995).

In this study, we now examine the extent, timing and cellular localization of the increased PBR expression and ligand binding in DRG following sciatic nerve transection and crush injury, along with the expression of its putative endogenous ligand, DBI.

Materials and methods

Animal surgery and tissue preparation

All procedures were performed in accordance with Massachusetts General Hospital Animal Research regulations. To produce sciatic nerve transection and crush injuries, adult male Sprague–Dawley rats (200–300 g; Charles River Laboratories, MA, USA) were anaesthetized with isoflurane (inhalation induction, 4%; maintenance, 2.5%), the left sciatic nerve was exposed at the mid-thigh level, ligated with 3/0 silk and sectioned immediately distal to the ligation (sciatic nerve transection lesion; SNT), or exposed and crushed with a fine, smooth-bladed haemostat forceps for 30 s (crush injury). Two other partial peripheral nerve injuries known to produce neuropathic pain-like hypersensitivity were also performed. The spared nerve injury model (SNI) involves ligation and section of two of the three terminal branches of the sciatic nerve, the tibial and common peroneal nerves, leaving the sural nerve intact, and was performed as previously described (Decosterd & Woolf, 2000). For the chronic constriction injury model (CCI), four 4–0 chromic gut sutures spaced ~1 mm apart were tied loosely around the sciatic nerve proximal to its trifurcation (Bennett & Xie, 1988). The wound was sutured in two layers and the animals were allowed to recover for 1–28 days.

For collection of fresh tissue, animals were terminally anaesthetized by exposure to CO₂ and exsanguinated. The L4 and L5 DRGs and lumbar spinal cord were rapidly removed, embedded in OCT compound (Tissue Tek, Fisher, PA, USA), frozen, and stored at –80 °C. Additional DRGs were taken from rat pups at postnatal days 0, 7 and 10 (P0, P7 and P10) after the animals had been decapitated. For fixed tissue, rats were anaesthetized, perfused transcardially with phosphate-buffered saline (PBS) followed by Zamboni's fixative. Dissected tissue was postfixed for 60 min, cryoprotected in 10% sucrose in 0.1 M phosphate buffer overnight at 4 °C before being fast frozen in cryomolds. Before cryostat sectioning, frozen blocks containing spinal cords or pairs of DRGs from animals injured at different time points and from naïve animals were blocked together with OCT compound to ensure processing of different experimental groups under identical conditions on the same slide. Serial sections of fresh and fixed frozen tissue were cut at 6 µm, thaw-mounted onto cold Probe-On slides (Fisher) and stored at –20 °C.

Isotopic in situ hybridization

In situ hybridization was carried out as described previously (Karchewski *et al.*, 1999) using 48-base pair oligonucleotide probes complementary to, and selective for, the following mRNAs: peripheral benzodiazepine receptor (PBR; Accession #J05122); neurofilament heavy chain (NFH; Accession #AF031879); and DBI (Accession #NM031853). Each oligonucleotide probe (80 ng) was labelled at the 3' end with α -[³⁵S]dATP or α -[³³P]dATP (NEN, MA, USA) in a terminal transferase reaction and purified through a spin column (Qiagen, CA, USA). Specific activities ranged from 2.0–5.2 × 10⁶ c.p.m./ng oligonucleotide.

Slides were hybridized at 43 °C for 14–18 h in a buffer containing 50% formamide, 4 × saline sodium citrate (SSC), 1 × Denhardt's solution (0.02% bovine serum albumin, 0.02% Ficoll and 0.02% polyvinylpyrrolidone), 1% sarcosyl (N-laurylsarcosine), 0.02 M phosphate buffer (pH 7.0), 10% dextran sulphate, 500 mg/mL heat-denatured salmon sperm, 200 mM dithiothreitol and 10⁷ c.p.m./mL of radiolabelled oligonucleotide probe. The slides were then washed four times for 15 min in 1 × SSC at 55 °C, brought to room temperature, dipped twice in distilled water, dehydrated in ascending alcohols and air-dried. The hybridization stringency conditions used required homologies >90% for retention of the transcripts following the washes (Dagerlind *et al.*, 1992). Slides were stored at 4 °C until processed by emulsion autoradiography.

The specificity of the hybridization signal for each probe was ascertained by hybridization of adjacent sections with labelled probe, labelled probe with a 1000-fold excess of cold probe, or labelled probe with a 1000-fold excess of another, dissimilar cold probe of the same length and similar G–C content.

In situ [³H]PK11195 binding

In situ PBR ligand binding was performed by incubating slides of unfixed tissue for 2 h at 4 °C in 50 mM saline Tris-HCl (pH 7.4) containing 2 nM [³H]PK11195 ([1-(2-chlorophenyl)-N-methyl-N-(1-methylpropyl)-3-isoquinoline carboxamide]; specific activity 85 Ci/mmol, NEN). To assess nonspecific binding, control slides were incubated in a similar solution containing unlabelled 10 µM PK11195 (Sigma, MO, USA). Following incubation, the slides were washed in cold buffer and air-dried before being processed by emulsion autoradiography.

Emulsion autoradiography

Under safelight conditions, slides were dipped in NTB-2 nuclear track emulsion (Kodak; 1 : 1 in distilled water) dried and stored in light-proof slide boxes with desiccant at 4 °C. The sections were exposed for 1–12 weeks (time determined by test slides) before being developed and fixed. For viewing under darkfield conditions using a fibre-optic darkfield stage adapter (MVI, MA, USA), slides were left unstained and coverslipped using glycerol. For viewing under the brightfield microscope, slides were counterstained with 0.5% Toluidine blue (pH 4–4.5), differentiated and coverslipped using Permount (Fisher). Photographs were taken using a Spot camera (MVI).

Quantification and analysis

Using single section profile counts, 4–6 sections chosen randomly from each L4 and L5 DRG were counted in 3–4 animals from naïve,

3 days, 1 week and 3 and 4 weeks post-SNT, and the proportion of labelled neuronal profiles for each time point calculated. To reduce bias and to prevent the counting of cell edges, a neuron was only counted if its nucleus was visible. Cells were considered positively labelled if they had more than five times background level of autoradiographic label (silver grains) when observed under brightfield conditions with a $20\times$ objective.

For mRNA and binding size frequency distributions of neuronal profiles, brightfield microscope images were captured using a Spot camera from five sections per L4 DRG from four animals at each time point (naïve and 4 weeks) following SNT. Using photomontages of each DRG, cell diameters were measured across the widest portion of every positively and negatively labelled cell containing a nucleus. Values reflect measurements adjusted according to scale. Diameters $<30\text{ }\mu\text{m}$, $30\text{--}45\text{ }\mu\text{m}$ and $>45\text{ }\mu\text{m}$ represent small, medium and large neurons. Prism 4 software (Graphpad, San Diego, CA, USA) was used for statistical analysis and graphing. One-way ANOVA followed by Dunnett's multiple comparison tests were used to test for significant differences. All data are presented as mean \pm SEM.

Immunohistology

Slides for PBR and NF200 immunohistology (cut from fresh tissue) were fixed in cold 70% ethanol for 10 min at $20\text{ }^{\circ}\text{C}$. Tissue sections were washed in PBS (0.1 M) and blocked for 1 h at room temperature in a PBS solution containing 5% bovine serum albumin and 0.1% Triton X-100. Slides for DBI and glial fibrillary acidic protein (GFAP) immunohistology (cut from fixed tissue) were washed in PBS (0.1 M) and treated with a blocking solution containing 10% horse serum and 0.1% Triton X-100 in PBS for 1 h at $4\text{ }^{\circ}\text{C}$. All slides were incubated overnight at $4\text{ }^{\circ}\text{C}$ with their primary antibodies diluted in blocking solution: rabbit anti-PBR (1:200; R & D Systems, MN, USA); mouse anti-neurofilament 200 (NF200, 1:800; Sigma); rabbit anti-DBI fragment (1:300; Peninsula Laboratories Inc, CA, USA); and mouse anti-GFAP (1:200, final concentration $5\text{ }\mu\text{g/mL}$; Chemicon, CA, USA). PBS washes were followed by incubation with Cy3-conjugated goat anti-rabbit IgG (1:400; Jackson ImmunoResearch, ME, USA) and FITC-conjugated donkey anti-mouse IgG (1:200; Jackson ImmunoResearch) in blocking solution without Triton X-100 for 1 h at room temperature.

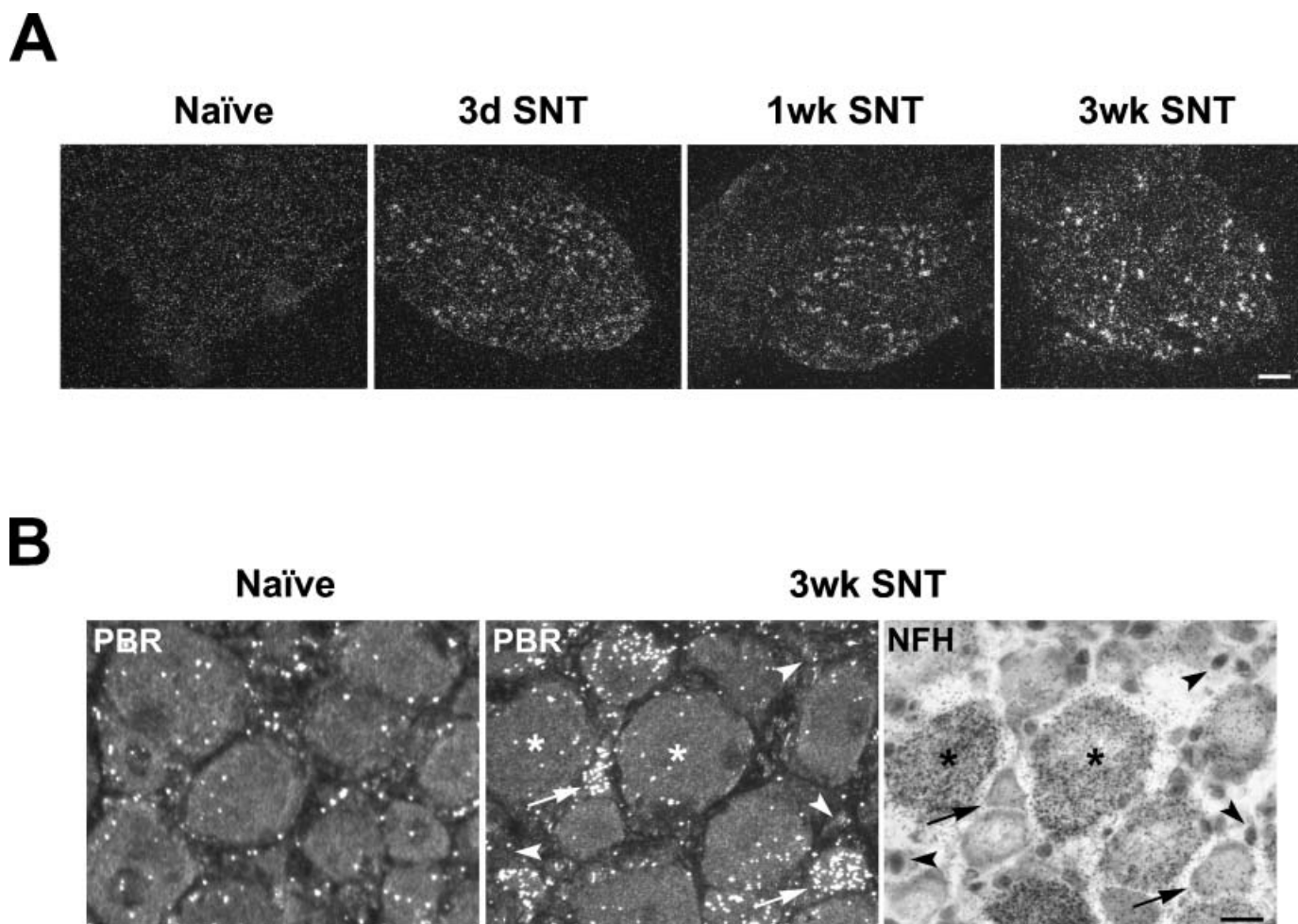


FIG. 1. PBR mRNA is induced in small and medium-sized primary sensory neurons after SNT. (A) Representative photomicrographs of L4 DRG sections processed for PBR mRNA by *in situ* hybridization from naïve animals and 3 days, 1 week and 3 weeks after sciatic nerve transection. Scale bar, $200\text{ }\mu\text{m}$. (B) Photomicrographs showing adjacent $6\text{ }\mu\text{m}$ DRG sections processed by *in situ* hybridization for PBR mRNA and neurofilament heavy chain (NFH; a marker of large-diameter neurons) mRNA expression 3 weeks post-SNT. Stars show examples of large-sized neurons, indicated by a positive NFH signal, that have no detectable signal for PBR mRNA. Arrows show small and medium-sized neurons, not labelled for NFH, with positive hybridization signal for PBR. Arrowheads point to unlabelled, non-neuronal cells. Scale bar, $50\text{ }\mu\text{m}$.

in the dark. Slides were washed in PBS and coverslipped with Vectashield (Vector Laboratories Inc., CA, USA). Sections were viewed with a fluorescent microscope (Nikon) and photographed using a Spot digital camera. Immunohistology controls showed no signal when primary antibody was replaced with blocking solution.

Results

Peripheral axotomy induces PBR mRNA expression in small and medium-sized primary sensory neurons

In a previous Affymetrix microarray screen of changes in gene expression in the DRG after peripheral nerve injury, we found 240 genes that were significantly up- or downregulated in the L4 and L5 DRG 3 days after a sciatic nerve transection (Costigan *et al.*, 2002). The peripheral benzodiazepine receptor (Accession #J05122) was increased 1.56-fold relative to naïve ($P = 0.0139$) at this time.

Isotopic *in situ* hybridization detecting PBR mRNA corresponding to the isoquinoline binding protein (IBP) component of the receptor was used to examine adult rat DRGs at different times following SNT. No constitutive PBR mRNA is detectable in the naïve, noninjured DRG (Figs 1A and 4A). Three days following a SNT, PBR mRNA expression is detected in a subset of sensory neurons in the DRG ipsilateral to the injury ($20.36 \pm 0.98\%$) and this becomes even more pronounced 1 and 3 weeks post-SNT

($30.93 \pm 2.03\%$ and $32.59 \pm 1.11\%$; Figs 1A and 4A). At the longest time examined after the injury, 4 weeks, the PBR hybridization signal remained highly elevated compared with naïve and contralateral DRGs (4 weeks: $33.47 \pm 0.92\%$). No detectable hybridization signal for PBR mRNA is observed in non-neuronal cells in DRGs from either naïve or nerve-injured animals (Fig. 1B). Size frequency histograms of DRG neuron cell diameters and of PBR mRNA-positive neurons, reveal that PBR mRNA expression is restricted to small and medium diameter neurons when measured at 4 weeks post-injury (Fig. 4D). Out of 269 neuronal profiles labelled for PBR mRNA at 4 weeks post-injury, 108 (40.15%) had diameters between 30 μm and 45 μm , 158 (58.74%) were less than 30 μm and none were larger than 45 μm (Fig. 4D). PBR mRNA is virtually undetectable in cells with large diameters at any time point after injury (Fig. 4D) and no coexpression is found with NFH mRNA, a marker of neurons with myelinated axons (Fig. 1B; Michael & Priestley, 1999).

Axotomy induces PBR protein expression in small and medium primary sensory neurons

Peripheral nerve transection produces changes in PBR protein expression similar to that of its mRNA. Immunostaining does not show any detectable PBR protein in naïve DRGs or those contralateral

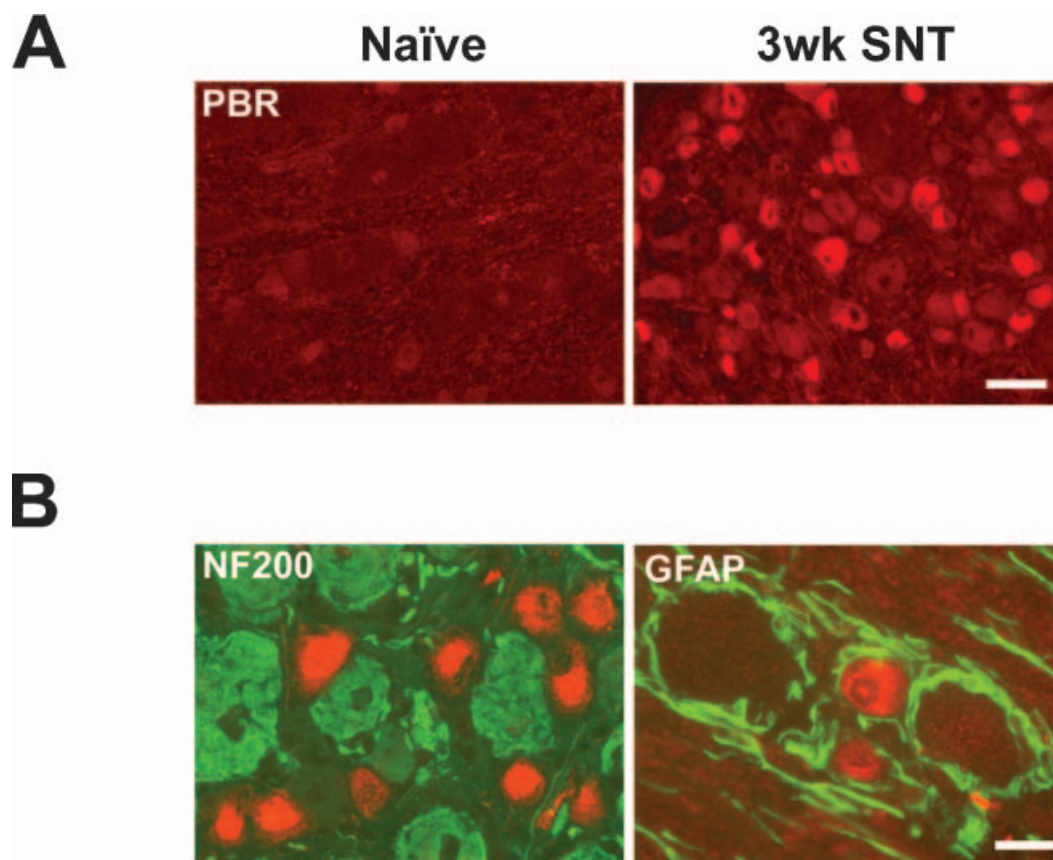


FIG. 2. PBR protein expression is induced in small and medium-sized primary sensory neurons after SNT. (A) Photomicrographs show PBR immunoreactivity in DRG from naïve animals and 3 weeks after SNT. Scale bar, 100 μm . (B) Double-labelling of PBR (red) with NF200 (green) to show large-sized neurons or with GFAP (green) to show non-neuronal cells in the DRG 3 weeks after SNT. PBR expression is limited to the small- to medium-sized neurons of the injured DRG. Scale bar, 50 μm .

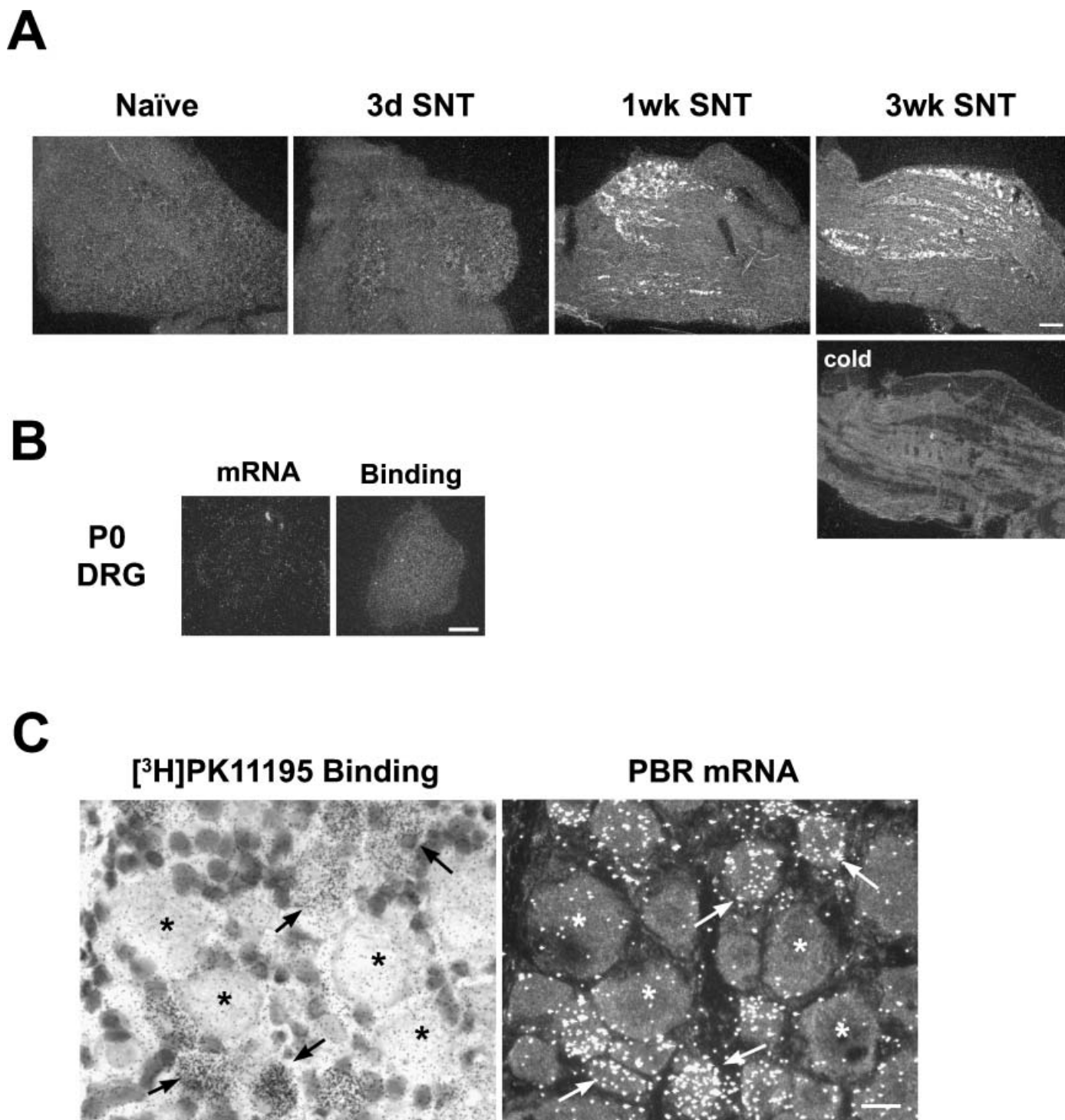


FIG. 3. [^3H]PK11195 binding appears in primary sensory neurons after SNT. (A) Representative darkfield photomicrographs of L4 DRG sections processed to detect PBR binding sites by *in situ* receptor binding using the high-affinity PBR ligand [^3H]PK11195 in naïve and 3 days, 1 week and 3 weeks after SNT. Specific PBR binding appears 1 week after SNT and shows an increase to 3 weeks. All specific binding is successfully competed using an excess of unlabelled specific ligand (cold). Scale bar, 200 μm . (B) No PBR mRNA or [^3H]PK11195 binding is detectable in the naïve, early postnatal DRG (P0). Scale bar, 10 μm . (C) Photomicrographs showing [^3H]PK11195 binding in a DRG 3 week post-SNT with an adjacent 6- μm -thick DRG section processed by *in situ* hybridization to detect mRNA for PBR. Arrows show examples of neurons in adjacent sections with positive signal of both [^3H]PK11195 binding and PBR mRNA, whereas stars show examples of neurons without positive levels of either binding or PBR mRNA. Scale bar, 50 μm .

to the injury (Fig. 2A). Levels of PBR immunostaining are present 3 weeks post-SNT. No overlap when double-labelled with NF200 (marker of A-fibre neurons) and GFAP (marker of non-neuronal cells

in the DRG) antibodies indicates that PBR immunoreactivity, similar to its mRNA expression, appears only in small and medium-sized neurons after SNT (Fig. 2B).

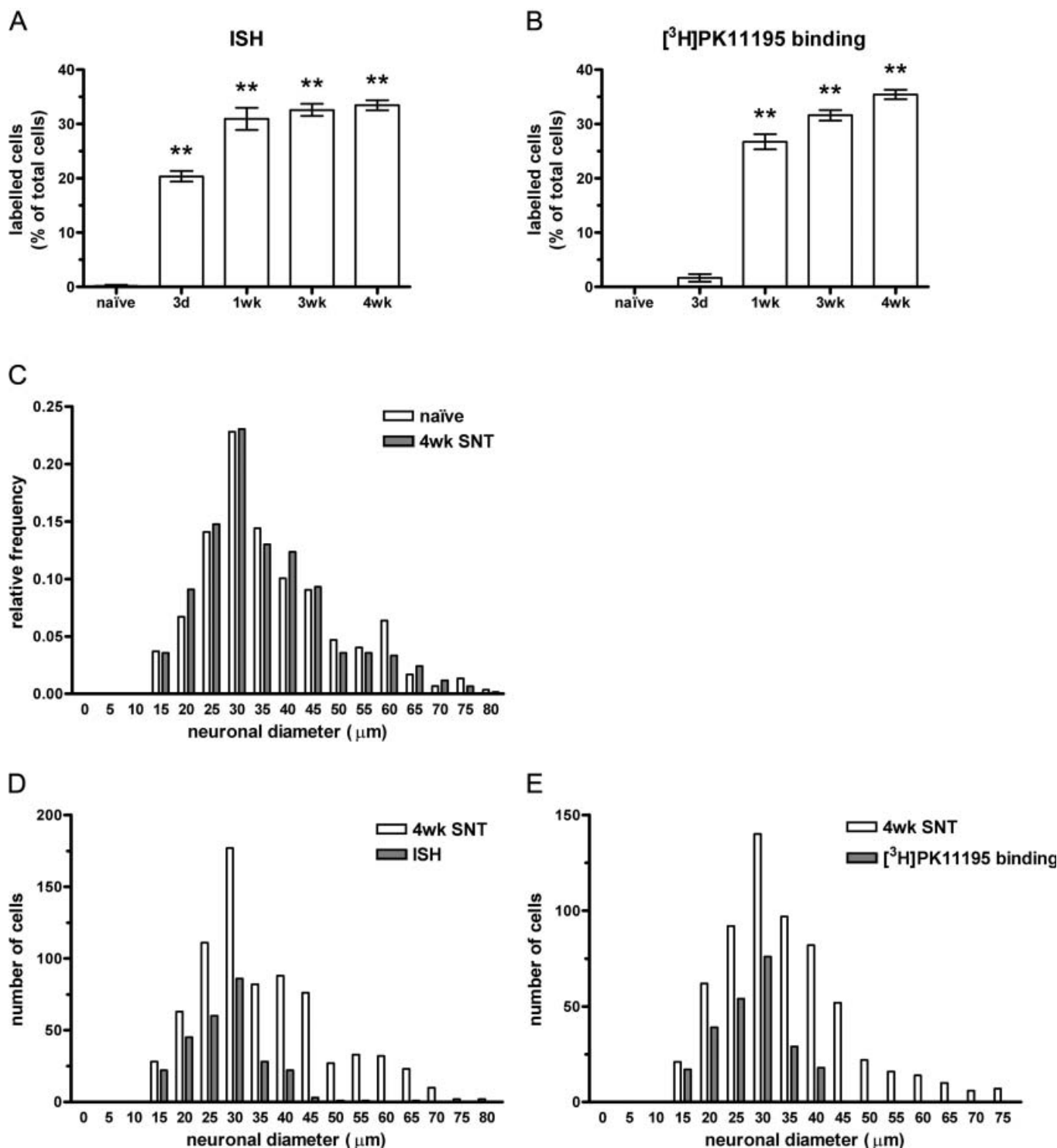


FIG. 4. Quantification of injured primary sensory neurons showing parallel changes in [^3H]PK11195 binding and PBR mRNA expression. (A) The percentage of L4 DRG neurons positively labelled for PBR mRNA after SNT ($n = 5\text{--}8$ DRG at each time point, 4–5 sections per DRG). $F_{4,33} = 136.7$, $P < 0.0001$ (one-way ANOVA); $**P < 0.01$ (Dunnett's multiple comparison test). (B) The percentage of DRG neurons positive for [^3H]PK11195 binding after SNT ($n = 5\text{--}7$ DRG at each time point, 4–5 sections per DRG). $F_{4,25} = 356.4$, $P < 0.0001$ (one-way ANOVA); $**P < 0.01$ (Dunnett's multiple comparison test). (C) Histogram showing the relative size distribution of L4 DRG neurons in naïve and 4 weeks following SNT. (D and E) Histograms showing the number and size distribution of PBR mRNA (D) and [^3H]PK11195 binding (E) positive cells in comparison with the whole DRG cell population 4 weeks following SNT.

PBR ligand binds to small and medium primary neurons in the DRG following sciatic nerve transection

To determine if the increases in PBR mRNA and protein after nerve injury are accompanied by changes in functional binding properties of

DRG neurons to a ligand for the peripheral benzodiazepine receptor, we examined PBR binding using [^3H]PK11195, a high affinity PBR ligand (Le Fur *et al.*, 1983). PBR mRNA and [^3H]PK11195 binding is not detectable in naïve DRG neurons when they are still in the

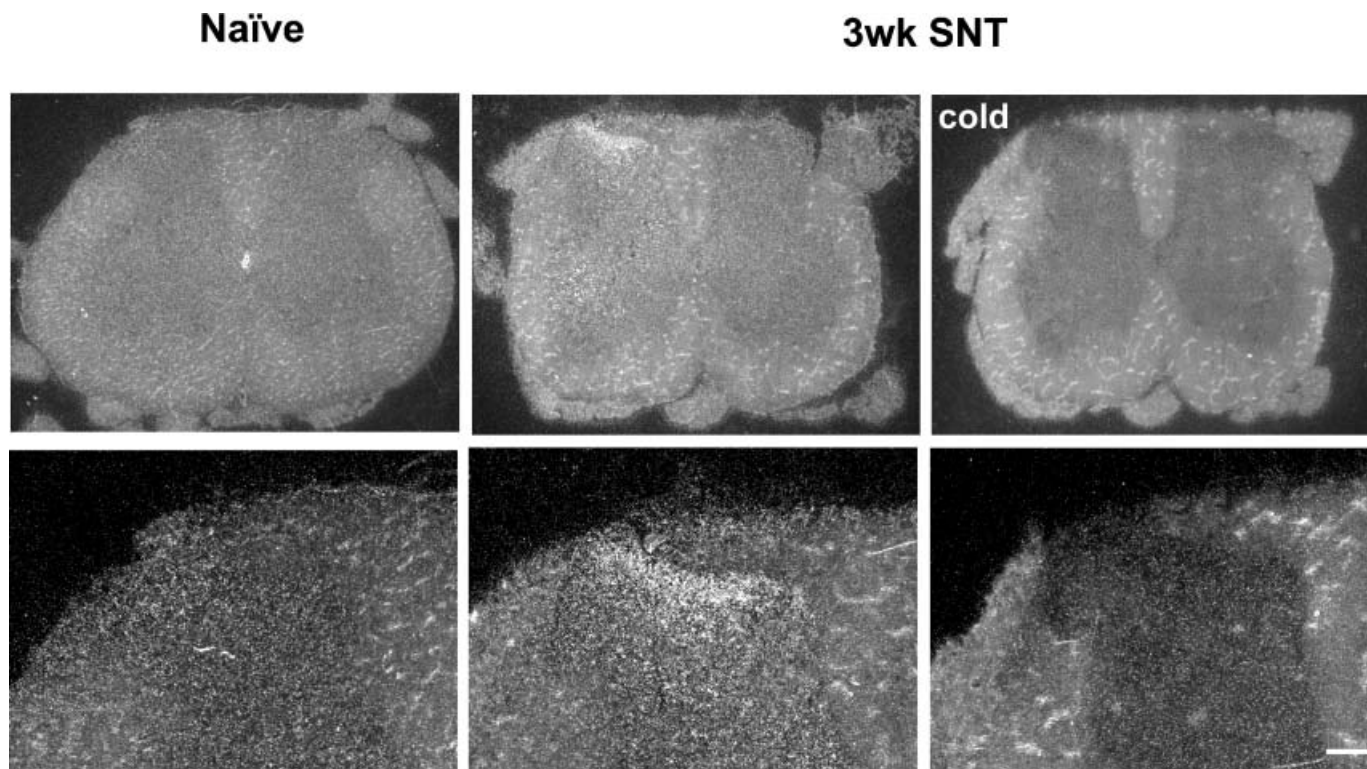


FIG. 5. Sciatic nerve transection induces [^3H]PK11195 binding in the lumbar spinal cord. Darkfield photomicrographs showing 6- μm -thick sections of adult rat lumbar spinal cord processed for *in situ* receptor binding using the high affinity PBR ligand [^3H]PK11195 to detect PBR binding sites in naïve animals and 3 weeks following SNT. Specific binding appears in laminae I and II of the dorsal horn (bottom panels). All specific binding is successfully competed using an excess of unlabelled specific ligand (cold). Scale bars, 300 μm (top panels); 130 μm (lower panels).

postnatal growing phase at P0 (Fig. 3B) or at P7 or P10 (data not shown), suggesting that PBR is not required in the DRG under normal circumstances or during periods of developmental growth. Virtually no [^3H]PK11195 binding occurs in naïve adult DRG sections and receptor binding is also not detectable 3 days post-injury (Figs 3A and 4B). At both 1 and 3 weeks after SNT, clear [^3H]PK11195 binding is present in $26.76 \pm 1.40\%$ and $31.62 \pm 0.96\%$ of all DRG neuronal profiles. At 4 weeks post-injury, the latest time point examined, $35.45 \pm 0.87\%$ of DRG neuron profiles were positive (Fig. 4B). The [^3H]PK11195 binding colocalizes with PBR mRNA in DRG neurons after injury (Fig. 3C). Changes in the proportion of neuronal profiles positive for [^3H]PK11195 binding 1 week and 3 weeks after SNT follows the timecourse of PBR mRNA induction following SNT (Fig. 1), with a slight delay (Fig. 4B).

Size-frequency histograms of cell diameters in the DRG show that [^3H]PK11195 binding is only found in small and medium diameter neurons 4 weeks post-injury (Fig. 4E). Out of 233 neuronal profiles, 97 (41.63%) had diameters between 30 μm and 45 μm and 136 (58.37%) had diameters <30 μm (Fig. 4E). Specificity of ligand binding is confirmed by the competition of [^3H]PK11195 with excess concentrations of unlabelled cold PK11195 (Fig. 3A).

Binding of [^3H]PK11195 increases in lumbar spinal cord following a sciatic nerve transection

No [^3H]PK11195 binding is detectable in naïve spinal cord, but is found following SNT (Fig. 5). Three days after SNT, binding appears

in the spinal cord (data not shown) and 3 weeks post-SNT a strong PBR binding signal is found in the dorsal horn. [^3H]PK11195 autoradiographic signal is most abundant in laminae I and II of the dorsal horn.

PBR mRNA and [^3H]PK11195 binding in the DRG show target-dependent expression in the adult

Similar to SNT, a sciatic nerve crush injury causes induction of PBR mRNA and binding with a slow onset and high levels of expression 2 weeks post-injury in the adult (Fig. 6). In contrast to SNT with ligation, crushed fibres are provided with an endoneurial tract along which to grow and are capable of successful regeneration. Four weeks after the nerve crush the levels of PBR mRNA and [^3H]PK11195 binding are reversed close to the levels before injury, unlike after a transected sciatic nerve where PBR expression and binding remain elevated (Fig. 6). At this time most crush-injured fibers will have regrown to innervate peripheral targets (Devor *et al.*, 1979).

The endogenous ligand for PBR, DBI, is present in the injured and noninjured DRG

Coexpression of PBR with its putative endogenous ligand, DBI, was explored by *in situ* hybridization. DBI mRNA is expressed in DRG but exclusively in non-neuronal cells, as indicated by hybridization signal appearing only in rings surrounding DRG neurons and no colocali-

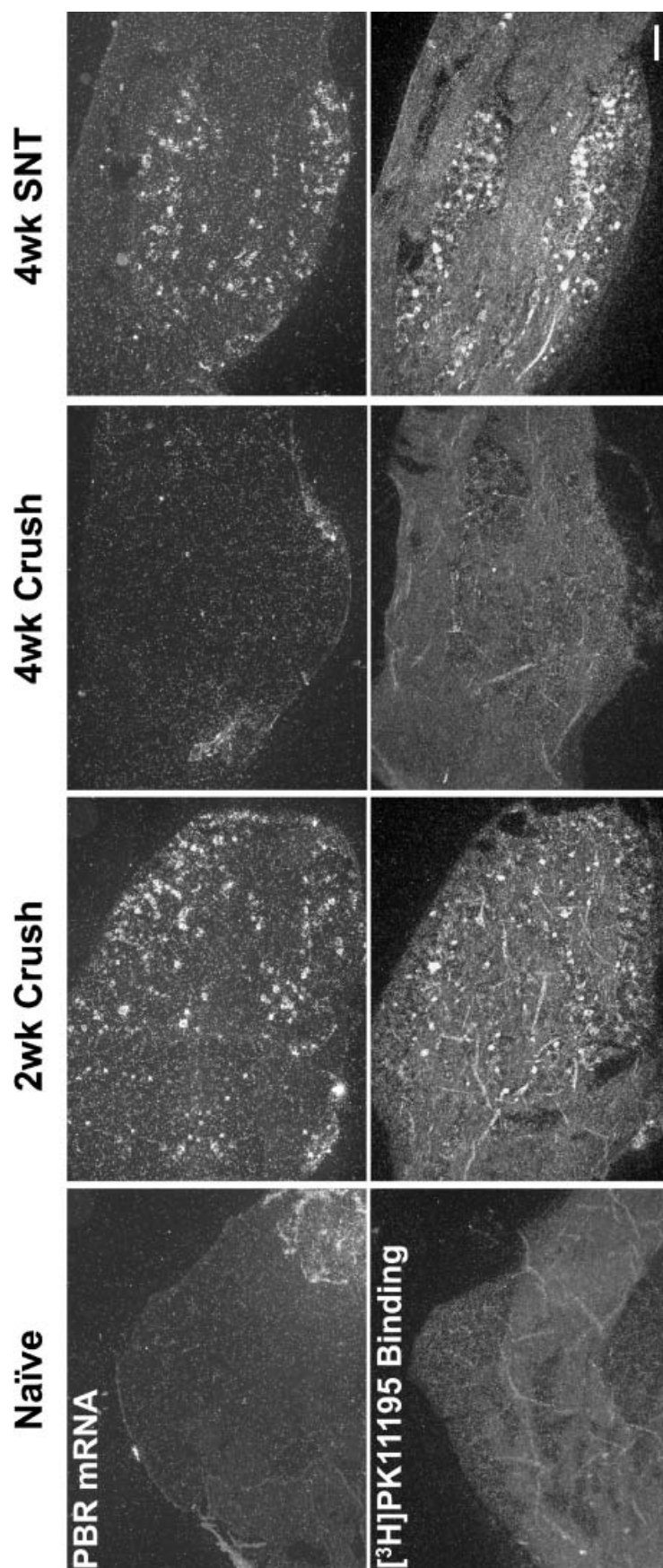


FIG. 6. Effect of sciatic nerve crush injury on PBR mRNA expression and $[^3\text{H}]$ PK11195 binding in the DRG. Darkfield photomicrographs showing PBR mRNA and $[^3\text{H}]$ PK11195 binding 2 and 4 weeks following sciatic nerve crush or 4 weeks after SNT with ligation in the adult. mRNA and binding are elevated 2 weeks after the nerve crush but return towards preinjury levels at 4 weeks, unlike 4 week post-SNT where regrowth is prevented. Scale bar, 200 μm .

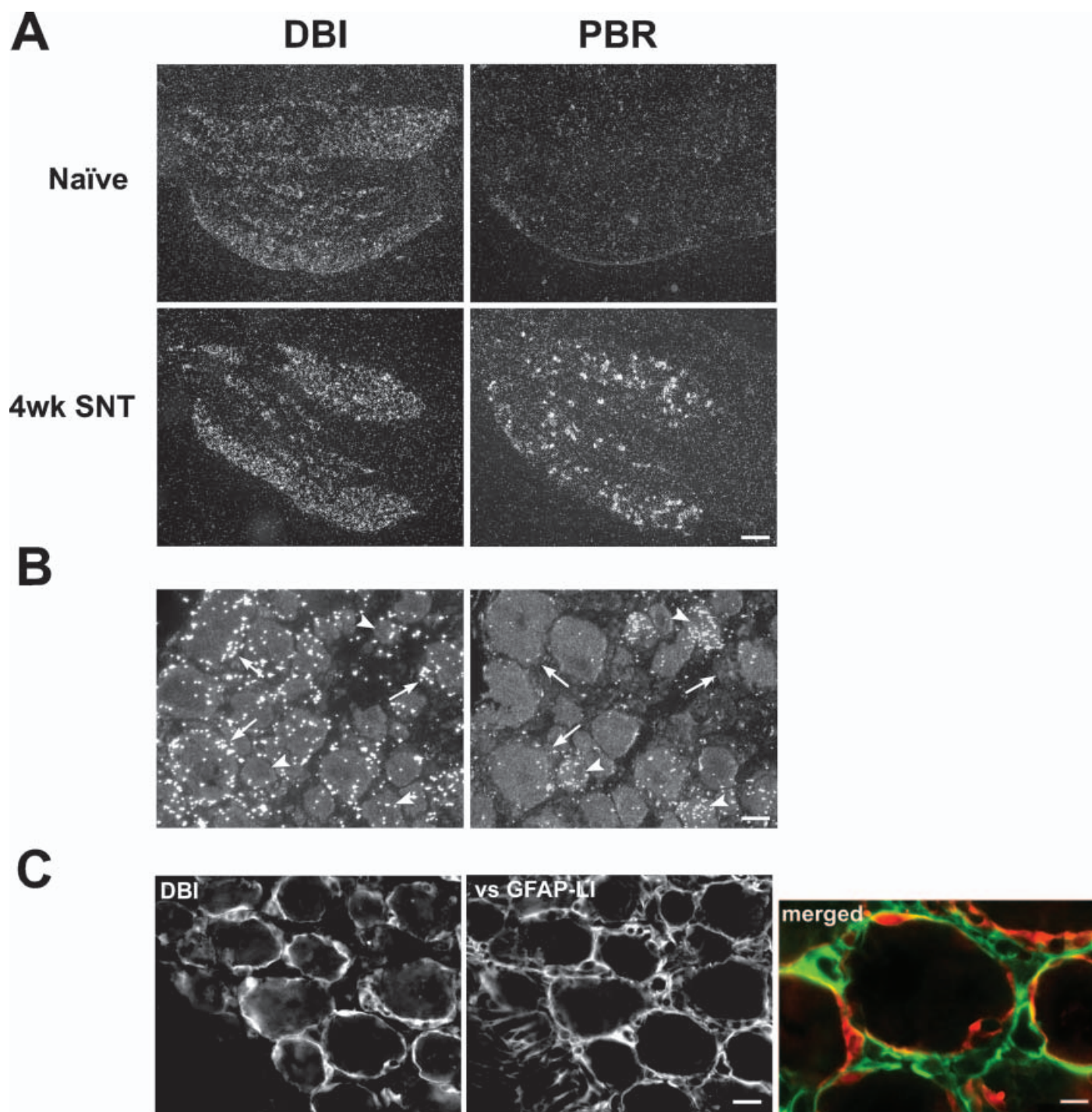


FIG. 7. Diazepam binding inhibitor (DBI) is present in non-neuronal cells of the DRG. (A) Darkfield photomicrographs showing 6-μm-thick adjacent DRG sections from naïve and 4 weeks post-SNT processed for *in situ* hybridization to detect mRNA for DBI and PBR. No changes in DBI levels are detectable. Scale bar, 200 μm. (B) Arrowheads show examples of injured DRG neurons positive for PBR mRNA and not DBI, while arrows point to non-neuronal cells surrounding neurons that show strong levels of DBI signal but remain PBR-negative. Scale bar, 50 μm. (C) Photomicrographs show DBI and GFAP immunoreactivity in the DRG 4 weeks after injury. Scale bar, 40 μm. Right, double-labelling shows that DBI (red) is found perineuronally and colocalizes with GFAP (green). Scale bar, 20 μm.

zation with PBR mRNA (Fig. 7A and B). Similarly, abundant DBI protein is not localized in DRG neurons but only appears non-neuronally and partly colocalizes with GFAP, a marker of non-neuronal cells in the DRG (Fig. 7C). No obvious changes in DBI levels or expression pattern are detected at any time point following transection of the sciatic nerve (Fig. 7A).

PBR mRNA and binding are upregulated in small and medium DRG neurons after partial injuries to the sciatic nerve

Examination of PBR expression 3 weeks after different injuries to the sciatic nerve shows induction of PBR mRNA expression and an increase in [³H]PK11195 binding (Fig. 8A). Each injury model produces a partial transection of the sciatic nerve. In the SNI, two of three distal

contributing branches of the sciatic are cut whereas in the CCI, only a proportion of the fibres are damaged through a combination of inflammation and strangulation of the sciatic nerve. For each partial injury, as with complete SNT, PBR mRNA and binding remains restricted to the small and medium-sized neurons of the DRG (Fig. 8B).

Discussion

Until recent studies by ourselves and others using microarrays reported upregulation of PBR mRNA in the DRG after nerve injury

(Costigan *et al.*, 2002; Xiao *et al.*, 2002), expression of PBR in the peripheral nervous system (PNS) had been described only in non-neuronal cells (Lacor *et al.*, 1996; Lacor *et al.*, 1999). Here we show that PBR mRNA expression appears in the DRG in sensory neurons after sciatic nerve transection, with a concomitant increase in PBR protein from essentially undetectable levels in naïve, noninjured animals to presence in a substantial proportion of small-caliber sensory neurons post-injury. To further investigate whether PBR detected by immunohistology is present in a conformation that can bind ligand, we have performed *in situ* receptor binding using the

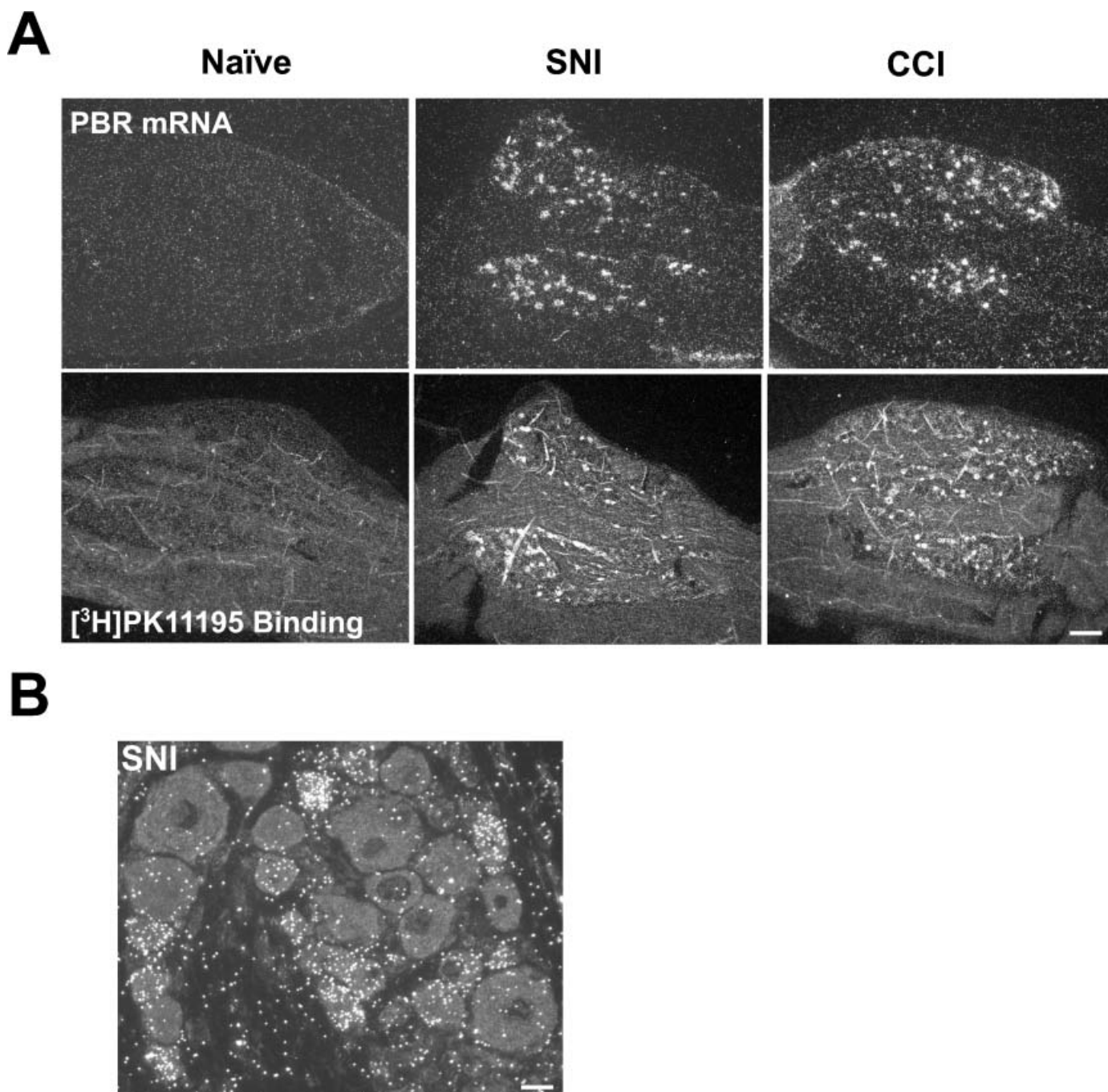


FIG. 8. Sciatic nerve injuries related to neuropathic pain induce PBR mRNA expression and ligand binding in the DRG. (A) Darkfield photomicrographs show DRG sections (L4/L5) processed for *in situ* hybridization to detect mRNA for PBR with adjacent sections showing *in situ* receptor binding for [³H]PK11195. Three weeks after SNI and CCI, PBR mRNA and binding are significantly increased in the DRG. Scale bar, 200 μ m. (B) Photomicrographs showing an example of DRG neurons 3 weeks after SNI processed for *in situ* hybridization to detect PBR mRNA. Expression of PBR mRNA appears only in small and medium-sized neurons. Scale bar, 60 μ m.

high-affinity PBR ligand [³H]PK11195. We detect strong binding 1 week following axotomy, in contrast to PBR mRNA which appears after 3 days, a delay likely to reflect the translational and post-translational dynamics of PBR in DRG neurons. Furthermore, PBR ligand binding appears in the superficial dorsal horn of the spinal cord following axotomy in those laminae where small-caliber afferents terminate. The induced PBR expression in the DRG returns towards preinjury levels if reinnervation is allowed to occur after a peripheral nerve crush injury, but not if axonal growth is prevented by a nerve ligation. No non-neuronal expression of PBR is detectable in the DRG at any time point following peripheral nerve injury and PBR expression does not overlap with that of its putative endogenous ligand DBI, which has an exclusively non-neuronal expression pattern that does not change following injury. These findings indicate the need for a major re-evaluation of the role of PBR in the PNS in general and particularly in injured small DRG neurons.

PBR is a mitochondrial membrane protein that is involved in the mitochondrial respiratory chain (Szabo *et al.*, 1993) as well as having a structural contribution to the mitochondrial permeability transition pore (MPTP; McEnery *et al.*, 1992; McEnery *et al.*, 1993). PBR activation initiates steroid biosynthesis (Besman *et al.*, 1989; Papadopoulos & Brown, 1995) by facilitating transport of cholesterol from the outer to the inner mitochondrial membrane making cholesterol available to cytochrome p450 for the biosynthesis of pregnenolone, the rate-limiting step in steroid production (Krueger & Papadopoulos, 1990; Krueger, 1995). Cholesterol is a major membrane lipid and is required both for axonal elongation (de Chaves *et al.*, 1997) and myelin formation (Magnaghi *et al.*, 2001; Hasse *et al.*, 2002). Neurosteroid hormones have protective effects and support repair (Jones, 1993; Schumacher *et al.*, 2000) by both providing metabolic energy to cells and inhibiting inflammatory mediators, and in Schwann cells they activate the myelin genes, P0 and PMP22 (Koenig *et al.*, 1995; Ghomari *et al.*, 2003; Farges *et al.*, 2004). Repair and recovery of lesioned peripheral nerves has been correlated to PBR activation by agonists and subsequent increases in local pregnenolone levels (Ferzaz *et al.*, 2002; Lacor *et al.*, 1999).

In the adult rat, injured DRG neurons survive for many weeks in the absence of trophic support from their targets (Lewis *et al.*, 1999). This appears to be the result of induction of intrinsic anti-apoptotic survival molecules such as the small heat shock protein Hsp27 (Benn *et al.*, 2002). PBR might be an intrinsic injury-induced neuronal survival molecule and PBR ligands could have a role in preventing sensory neuron loss in peripheral neuropathies. PBR ligands might also have an indirect beneficial effect on injured neurons through their actions on glia and immune cells (Zavala *et al.*, 1990; Waterfield *et al.*, 1999; Torres *et al.*, 2000). PBR ligand binding modulates the mitochondrial transmembrane potential (Chelli *et al.*, 2001; Tanimoto *et al.*, 1999) and protects cells from damage by reactive oxygen species (Carayon *et al.*, 1996). These two actions help prevent apoptotic death by inhibiting cytochrome-c release from mitochondria and subsequent caspase activation (Bono *et al.*, 1999; Stoeber *et al.*, 2001; Ferzaz *et al.*, 2002; Strohmeier *et al.*, 2002). The induction of PBR could have a role therefore in preventing small DRG neurons from dying after injury to their peripheral axons.

The exclusive neuronal localization of PBR expression and binding in the DRG after nerve injury suggests a specific role for this mitochondrial protein in injured small but not large sensory neurons. Recently PBR ligands have been shown to cause a steroid-dependent antinociception (Bressan *et al.*, 2003; DalBo *et al.*, 2004). This, together with our findings, suggests that PBR could be a target for pharmacological intervention in neuropathic pain. DBI is expressed in satellite cells in the DRG and, if released by these cells, might

represent a source of endogenous ligand for PBR induced in the injured small DRG neurons, a paracrine glial-neuronal signalling in the DRG. What action DBI has in noninjured DRG where no PBR is expressed is not clear. Nevertheless the discovery that PBR is induced in small-calibre DRG neurons, together with the different functions that PBR mediates on mitochondria, suggest that this protein takes part in the important adaptive survival and growth responses of these cells after injury of their peripheral axons.

Acknowledgements

This work was funded by the NIH NS038253 (C.J.W.). We thank Katia Befort, Michaela Thallmair and NBM for critical discussion and reading.

Abbreviations

CCI, chronic constriction injury; DBI, diazepam binding inhibitor; DRG, dorsal root ganglion; GFAP, glial fibrillary acidic protein; HRP, horseradish peroxidase; Hsp27, heat shock protein 27; IBP, isoquinoline binding protein; MPTP, mitochondrial permeability transition pore; NFH, neurofilament heavy chain; P, postnatal day; SN1, spared nerve injury; SNT, sciatic nerve transection; PBR, peripheral benzodiazepine receptor; PBS, phosphate buffered saline; PK11195, [1-(2-chlorophenyl)-N-methyl-N-(1-methylpropyl)-3-isoquinoline carboxamide]; PNS, peripheral nervous system.

References

- Aldskogius, H., Arvidsson, J. & Grant, G. (1985) The reaction of primary sensory neurons to peripheral nerve injury with particular emphasis on transganglionic changes. *Brain Res.*, **357**, 27–46.
- Amsterdam, A. & Suh, B.S. (1991) An inducible functional peripheral benzodiazepine receptor in mitochondria of steroidogenic granulosa cells. *Endocrinology*, **129**, 503–510.
- Benavides, J., Quarteronnet, D., Imbault, F., Malgouris, C., Uzan, A., Renault, C., Dubroeuq, M.C., Guerey, C. & Le Fur, G. (1983) Labelling of 'peripheral-type' benzodiazepine binding sites in the rat brain by using [³H]PK 11195, an isoquinoline carboxamide derivative: kinetic studies and autoradiographic localization. *J. Neurochem.*, **41**, 1744–1750.
- Benn, S.C., Perrelet, D., Kato, A.C., Scholz, J., Decosterd, I., Mannion, R.J., Bakowska, J.C. & Woolf, C.J. (2002) Hsp27 upregulation and phosphorylation is required for injured sensory and motor neuron survival. *Neuron*, **36**, 45–56.
- Bennett, G.J. & Xie, Y.K. (1988) A peripheral mononeuropathy in rat that produces disorders of pain sensation like those seen in man. *Pain*, **33**, 87–107.
- Besman, M.J., Yanagibashi, K., Lee, T.D., Kawamura, M., Hall, P.F. & Shively, J.E. (1989) Identification of des-(Gly-Ile)-endozepine as an effector of corticotropin-dependent adrenal steroidogenesis: stimulation of cholesterol delivery is mediated by the peripheral benzodiazepine receptor. *Proc. Natl. Acad. Sci. USA*, **86**, 4897–4901.
- Bono, F., Lamarche, I., Prabonnaud, V., Le Fur, G. & Herbert, J.M. (1999) Peripheral benzodiazepine receptor agonists exhibit potent antiapoptotic activities. *Biochem. Biophys. Res. Commun.*, **265**, 457–461.
- Braestrup, C. & Squires, R.F. (1977) Specific benzodiazepine receptors in rat brain characterized by high-affinity (3H) diazepam binding. *Proc. Natl. Acad. Sci. USA*, **74**, 3805–3809.
- Braestrup, C. & Squires, R.F. (1978) Pharmacological characterization of benzodiazepine receptors in the brain. *Eur. J. Pharmacol.*, **48**, 263–270.
- Bressan, E., Farges, R.C., Ferrara, P. & Tonussi, C.R. (2003) Comparison of two PBR ligands with classical antiinflammatory drugs in LPS-induced arthritis in rats. *Life Sci.*, **72**, 2591–2601.
- Cahard, D., Canat, X., Carayon, P., Roque, C., Casellas, P. & Le Fur, G. (1994) Subcellular localization of peripheral benzodiazepine receptors on human leukocytes. *Lab. Invest.*, **70**, 23–28.
- Carayon, P., Portier, M., Dussosoy, D., Bord, A., Petitpretre, G., Canat, X., Le Fur, G. & Casellas, P. (1996) Involvement of peripheral benzodiazepine receptors in the protection of hematopoietic cells against oxygen radical damage. *Blood*, **87**, 3170–3178.
- de Chaves, E.I., Rusinol, A.E., Vance, D.E., Campenot, R.B. & Vance, J.E. (1997) Role of lipoproteins in the delivery of lipids to axons during axonal regeneration. *J. Biol. Chem.*, **272**, 30766–30773.

- Chelli, B., Falleni, A., Salvetti, F., Gremigni, V., Lucacchini, A. & Martini, C. (2001) Peripheral-type benzodiazepine receptor ligands: mitochondrial permeability transition induction in rat cardiac tissue. *Biochem. Pharmacol.*, **61**, 695–705.
- Costigan, M., Befort, K., Karchewski, L., Griffin, R.S., D'Urso, D., Allchorne, A., Sitariski, J., Mannion, J.W., Pratt, R.E. & Woolf, C.J. (2002) Replicate high-density rat genome oligonucleotide microarrays reveal hundreds of regulated genes in the dorsal root ganglion after peripheral nerve injury. *BMC Neurosci.*, **3**, 16.
- DalBo, S., Nardi, G.M., Ferrara, P., Ribeiro-do-Valle, R.M. & Farges, R.C. (2004) Antinociceptive effects of peripheral benzodiazepine receptors. *Pharmacology*, **70**, 188–194.
- Dagerlind, A., Friberg, K., Bean, A.J. & Hokfelt, T. (1992) Sensitive mRNA detection using unfixed tissue: combined radioactive and non-radioactive in situ hybridization histochemistry. *Histochemistry*, **98**, 39–49.
- Decosterd, I. & Woolf, C.J. (2000) Spared nerve injury: an animal model of persistent peripheral neuropathic pain. *Pain*, **87**, 149–158.
- DeLorey, T.M. & Olsen, J.W. (1992) Gamma-aminobutyric acidA receptor structure and function. *J. Biol. Chem.*, **267**, 16747–16750.
- Devor, M., Schonfeld, D., Seltzer, Z. & Wall, P.D. (1979) Two modes of cutaneous reinnervation following peripheral nerve injury. *J. Comp. Neurol.*, **185**, 211–220.
- Diorio, D., Welner, S.A., Butterworth, R.F., Meaney, M.J. & Suranyi-Cadotte, B.E. (1991) Peripheral benzodiazepine binding sites in Alzheimer's disease frontal and temporal cortex. *Neurobiol. Aging*, **12**, 255–258.
- Farges, R.C., Torres, S.R., Ferrara, P., Ribeiro-d. o-Valle, R.M. (2004) Involvement of steroids in anti-inflammatory effects of peripheral benzodiazepine receptor ligands. *Life Sci.*, **74**, 1387–1395.
- Ferzaz, B., Brault, E., Bourliand, G., Robert, J.P., Poughon, G., Claustre, Y., Marguet, F., Liere, P., Schumacher, M., Nowicki, J.P. *et al.* (2002) SSR180575 (7-chloro-N,N,5-trimethyl-4-oxo-3-phenyl-3,5-dihydro-4H-pyridazinol[4,5-b]indole-1-acetamide), a peripheral benzodiazepine receptor ligand, promotes neuronal survival and repair. *J. Pharmacol. Exp. Ther.*, **301**, 1067–1078.
- Gehlert, D.R., Stephenson, D.T., Schober, D.A., Rash, K. & Clemens, J.A. (1997) Increased expression of peripheral benzodiazepine receptors in the facial nucleus following motor neuron axotomy. *Neurochem. Int.*, **31**, 705–713.
- Ghoumari, A.M., Ibanez, C., El-Etr, M., Leclerc, P., Eychenne, B., O'Malley, B.W., Baulieu, E.E. & Schumacher, M. (2003) Progesterone and its metabolites increase myelin basic protein expression in organotypic slice cultures of rat cerebellum. *J. Neurochem.*, **86**, 848–859.
- Guidotti, A., Forchetti, C.M., Corda, M.G., Konkelt, D., Bennett, C.D. & Costa, E. (1983) Isolation, characterization, and purification to homogeneity of an endogenous polypeptide with agonistic action on benzodiazepine receptors. *Proc. Natl Acad. Sci. USA*, **80**, 3531–3535.
- Hasse, B., Bosse, F. & Muller, H.W. (2002) Proteins of peripheral myelin are associated with glycosphingolipid/cholesterol-enriched membranes. *J. Neurosci. Res.*, **69**, 227–232.
- Itzhak, Y., Baker, L. & Norenberg, M.D. (1993) Characterization of the peripheral-type benzodiazepine receptors in cultured astrocytes: evidence for multiplicity. *Glia*, **9**, 211–218.
- Jones, K.J. (1993) Gonadal steroids and neuronal regeneration. A therapeutic role. *Adv. Neurol.*, **59**, 227–240.
- Karchewski, L.A., Kim, F.A., Johnston, J., McKnight, R.M. & Verge, V.M. (1999) Anatomical evidence supporting the potential for modulation by multiple neurotrophins in the majority of adult lumbar sensory neurons. *J. Comp. Neurol.*, **413**, 327–341.
- Koenig, H.L., Schumacher, M., Ferzaz, B., Thi, A.N., Ressouches, A., Guennoun, R., Jung-Testas, I., Robel, P., Akwa, Y. & Baulieu, E.E. (1995) Progesterone synthesis and myelin formation by Schwann cells. *Science*, **268**, 1500–1503.
- Krueger, K.E. (1995) Molecular and functional properties of mitochondrial benzodiazepine receptors. *Biochim. Biophys. Acta*, **1241**, 453–470.
- Krueger, K.E. & Papadopoulos, V. (1990) Peripheral-type benzodiazepine receptors mediate translocation of cholesterol from outer to inner mitochondrial membranes in adrenocortical cells. *J. Biol. Chem.*, **265**, 15015–15022.
- Kuhlmann, A.C. & Guilarte, T.R. (2000) Cellular and subcellular localization of peripheral benzodiazepine receptors after trimethyltin neurotoxicity. *J. Neurochem.*, **74**, 1694–1704.
- Lacor, P., Benavides, J. & Ferzaz, B. (1996) Enhanced expression of the peripheral benzodiazepine receptor (PBR) and its endogenous ligand octadecaneuropeptide (ODN) in the regenerating adult rat sciatic nerve. *Neurosci. Lett.*, **220**, 61–65.
- Lacor, P., Gandolfo, P., Tonon, M.C., Brault, E., Dalibert, I., Schumacher, M., Benavides, J. & Ferzaz, B. (1999) Regulation of the expression of peripheral benzodiazepine receptors and their endogenous ligands during rat sciatic nerve degeneration and regeneration: a role for PBR in neurosteroidogenesis. *Brain Res.*, **815**, 70–80.
- Lawson, S.N. (2002) Phenotype and function of somatic primary afferent nociceptive neurones with C-, Adelta- or Aalpha/beta-fibres. *Exp. Physiol.*, **87**, 239–244.
- Lazzarini, R., Malucelli, B.E. & Palermo-Neto, J. (2001) Reduction of acute inflammation in rats by diazepam: role of peripheral benzodiazepine receptors and corticosterone. *Immunopharmacol. Immunotoxicol.*, **23**, 253–265.
- Le Fur, G., Perrier, M.L., Vaucher, N., Imbault, F., Flamier, A., Benavides, J., Uzan, A., Renault, C., Dubroeuq, M.C. & Guerey, C. (1983) Peripheral benzodiazepine binding sites: effect of PK 11195, 1-(2-chlorophenyl)-N-methyl-N-(1-methylpropyl)-3-isoquinolinecarboxamide. I. In vitro studies. *Life Sci.*, **32**, 1839–1847.
- Leong, D.K., Oliva, L. & Butterworth, R.F. (1996) Quantitative autoradiography using selective radioligands for central and peripheral-type benzodiazepine receptors in experimental Wernicke's encephalopathy: implications for positron emission tomography imaging. *Alcohol Clin. Exp. Res.*, **20**, 601–605.
- Lewis, S.E., Mannion, R.J., White, F.A., Coggeshall, R.E., Beggs, S., Costigan, M., Martin, J.L., Dillmann, W.H. & Woolf, C.J. (1999) A role for HSP27 in sensory neuron survival. *J. Neurosci.*, **19**, 8945–8953.
- Lieberman, A.R. (1971) The axon reaction: a review of the principal features of perikaryal responses to axon injury. *Int. Rev. Neurobiol.*, **14**, 49–124.
- Magnaghi, V., Cavarretta, I., Galbiati, M., Martini, L. & Melcangi, R.C. (2001) Neuroactive steroids and peripheral myelin proteins. *Brain Res. Brain Res. Rev.*, **37**, 360–371.
- McCauley, L.D., Park, C.H., Lan, N.C., Tomich, J.M., Shively, J.E. & Gee, K.W. (1995) Benzodiazepines and peptides stimulate pregnenolone synthesis in brain mitochondria. *Eur. J. Pharmacol.*, **276**, 145–153.
- McEnery, M.W., Dawson, T.M., Verma, A., Gurley, D., Colombini, M. & Snyder, S.H. (1993) Mitochondrial voltage-dependent anion channel. Immunochemical and immunohistochemical characterization in rat brain. *J. Biol. Chem.*, **268**, 23289–23296.
- McEnery, M.W., Snowman, A.M., Trifiletti, R.R. & Snyder, S.H. (1992) Isolation of the mitochondrial benzodiazepine receptor: association with the voltage-dependent anion channel and the adenine nucleotide carrier. *Proc. Natl. Acad. Sci. USA*, **89**, 3170–3174.
- Messmer, M.K. & Reynolds, G.P. (1998) Increased peripheral benzodiazepine binding sites in the brain of patients with Huntington's disease. *Neurosci. Lett.*, **241**, 53–56.
- Michael, G.J. & Priestley, J.V. (1999) Differential expression of the mRNA for the vanilloid receptor subtype 1 in cells of the adult rat dorsal root and nodose ganglia and its downregulation by axotomy. *J. Neurosci.*, **19**, 1844–1854.
- Miettinen, H., Kononen, J., Haapasalo, H., Helen, P., Sallinen, P., Harjuntausta, T., Helin, H. & Alho, H. (1995) Expression of peripheral-type benzodiazepine receptor and diazepam binding inhibitor in human astrocytomas: relationship to cell proliferation. *Cancer Res.*, **55**, 2691–2695.
- Moynagh, P.N., Bailey, C.J., Boyce, S.J. & Williams, D.C. (1991) Immunological studies on the rat peripheral-type benzodiazepine acceptor. *Biochem. J.*, **275**, 419–425.
- Papadopoulos, V. (1993) Peripheral-type benzodiazepine/diazepam binding inhibitor receptor: biological role in steroidogenic cell function. *Endocr. Rev.*, **14**, 222–240.
- Papadopoulos, V. & Brown, A.S. (1995) Role of the peripheral-type benzodiazepine receptor and the polypeptide diazepam binding inhibitor in steroidogenesis. *J. Steroid Biochem. Mol. Biol.*, **53**, 103–110.
- Park, C.H., Carboni, E., Wood, P.L. & Gee, K.W. (1996) Characterization of peripheral benzodiazepine type sites in a cultured murine BV-2 microglial cell line. *Glia*, **16**, 65–70.
- Schumacher, M., Akwa, Y., Guennoun, R., Robert, F., Labombarda, F., Desarnaud, F., Robel, P., De Nicola, A.F. & Baulieu, E.E. (2000) Steroid synthesis and metabolism in the nervous system: trophic and protective effects. *J. Neurocytol.*, **29**, 307–326.
- Sitte, H.H., Wanschitz, J., Budka, H. & Berger, M.L. (2001) Autoradiography with [3H]PK11195 of spinal tract degeneration in amyotrophic lateral sclerosis. *Acta Neuropathol. (Berl)*, **101**, 75–78.
- Snyder, S.H., Verma, A. & Trifiletti, R.R. (1987) The peripheral-type benzodiazepine receptor: a protein of mitochondrial outer membranes utilizing porphyrins as endogenous ligands. *FASEB J.*, **1**, 282–288.
- Stephenson, D.T., Schober, D.A., Smalstig, E.B., Mincey, R.E., Gehlert, D.R. & Clemens, J.A. (1995) Peripheral benzodiazepine receptors are colocalized

- with activated microglia following transient global forebrain ischemia in the rat. *J. Neurosci.*, **15**, 5263–5274.
- Stoebner, P.E., Carayon, P., Casellas, P., Portier, M., Lavabre-Bertrand, T., Cuq, P., Cano, J.P., Meynadier, J. & Meunier, L. (2001) Transient protection by peripheral benzodiazepine receptors during the early events of ultraviolet light-induced apoptosis. *Cell Death Diff.*, **8**, 747–753.
- Strohmeier, R., Roller, M., Sanger, N., Knecht, R. & Kuhl, H. (2002) Modulation of tamoxifen-induced apoptosis by peripheral benzodiazepine receptor ligands in breast cancer cells. *Biochem. Pharmacol.*, **64**, 99–107.
- Szabo, I., De Pinto, V. & Zoratti, M. (1993) The mitochondrial permeability transition pore may comprise VDAC molecules. II. The electrophysiological properties of VDAC are compatible with those of the mitochondrial megachannel. *FEBS Lett.*, **330**, 206–210.
- Tanimoto, Y., Onishi, Y., Sato, Y. & Kizaki, H. (1999) Benzodiazepine receptor agonists modulate thymocyte apoptosis through reduction of the mitochondrial transmembrane potential. *Jpn J. Pharmacol.*, **79**, 177–183.
- Torres, S.R., Frode, T.S., Nardi, G.M., Vita, N., Reeb, R., Ferrara, P., Ribeiro-d., o-Valle, R.M. & Farges, R.C. (2000) Anti-inflammatory effects of peripheral benzodiazepine receptor ligands in two mouse models of inflammation. *Eur. J. Pharmacol.*, **408**, 199–211.
- Trapani, G., Franco, M., Latrofa, A., Ricciardi, L., Carotti, A., Serra, M., Sanna, E., Biggio, G. & Liso, G. (1999) Novel 2-phenylimidazo[1,2-a]pyridine derivatives as potent and selective ligands for peripheral benzodiazepine receptors: synthesis, binding affinity, and in vivo studies. *J. Med. Chem.*, **42**, 3934–3941.
- Verma, A., Nye, J.S. & Snyder, S.H. (1987) Porphyrins are endogenous ligands for the mitochondrial (peripheral-type) benzodiazepine receptor. *Proc. Natl. Acad. Sci. USA*, **84**, 2256–2260.
- Vowinkel, E., Reutens, D., Becher, B., Verge, G., Evans, A., Owens, T. & Antel, J.P. (1997) PK11195 binding to the peripheral benzodiazepine receptor as a marker of microglia activation in multiple sclerosis and experimental autoimmune encephalomyelitis. *J. Neurosci. Res.*, **50**, 345–353.
- Waterfield, J.D., McGeer, E.G. & McGeer, P.L. (1999) The peripheral benzodiazepine receptor ligand PK 11195 inhibits arthritis in the MRL-lpr mouse model. *Rheumatology (Oxford)*, **38**, 1068–1073.
- Xiao, H.S., Huang, Q.H., Zhang, F.X., Bao, L., Lu, Y.J., Guo, C., Yang, L., Huang, W.J., Fu, G., Xu, S.H., Cheng, X.P., Yan, Q., Zhu, Z.D., Zhang, X., Chen, Z., Han, Z.G. & Zhang, X. (2002) Identification of gene expression profile of dorsal root ganglion in the rat peripheral axotomy model of neuropathic pain. *Proc. Natl. Acad. Sci. USA*, **99**, 8360–8365.
- Zavala, F., Taupin, V. & Descamps-Latscha, B. (1990) In vivo treatment with benzodiazepines inhibits murine phagocyte oxidative metabolism and production of interleukin 1, tumor necrosis factor and interleukin-6. *J. Pharmacol. Exp. Ther.*, **255**, 442–450.

Chapter 7

Conclusion and Outlook

At least three dichotomies are evident in the reaction of the nervous system of higher vertebrates to lesions. First, large injuries to the adult nervous system in adult mammals, including humans, cause many severe deficits with only a minor tendency to adaptive recovery, as is the case for spinal cord injury or stroke. However, the developing CNS shows strong adaptive plasticity in terms of behavioral compensation and structural rearrangements. The reaction to injuries evokes major compensation in the developing CNS and only minor adaptations in the adult. Second, there is a fundamental difference between the regenerative capacity of the adult CNS versus the adult PNS. Whereas injured axons of the PNS can re-grow along perineural sheets of connective tissue and re-innervate peripheral target structures, injured axons in the CNS usually retract and do not re-grow. Third, injury to the peripherally or centrally projecting axonal branch of DRG neurons, or more generally written, axotomy of neurons in different areas of the nervous system elicit cell body responses that vary greatly and that have been classified simply by the regulation of some growth- and regeneration-associated genes, e.g. c-Jun and GAP-43. Therefore, the dividing neuronal cell body responses are separated into two categories, one that allows for axonal regeneration and one that does not (for reviews see (Schwab and Bartholdi, 1996; Raineteau and Schwab, 2001; Fouad and Pearson, 2004).

The experiments presented in this thesis address the regulation of axonal growth after injury in the adult nervous system. Localized injury to the corticospinal tract of a rat only leads to minor morphological rearrangements of the injured neuronal system in the adult, most importantly axonal regeneration is extremely restricted. By blocking the action of Nogo-A, a major myelin-associated inhibitor of axonal growth, some of the environmental influences that prevent axonal growth can be abolished (Schnell and Schwab, 1990). We show here that the application of monoclonal antibody IN-1 leads to major structural rearrangement after unilateral transection of the corticospinal tract at the level of the medulla oblongata. The structural plasticity that we observe includes robust sprouting of corticopontine neurites. First, we show an increased innervation density of the basilar pons ipsilateral to the injury. Second, we find that sprouting axons cross the pontine midline, an axonal growth process that results in a new pontine innervation field contralateral to the injured corticospinal tract. Our detailed analysis reveals that the newly grown axons that project across the midline terminate in a topographical way that strongly resembles the unilateral somatotopic pontine innervation found in uninjured animals. A major finding is that these contralaterally projecting axons can establish physical connections with the newly innervated target cells. We show, by electron

microscopy, synapses with ultrastructural features very similar to normal corticopontine synaptic contacts. Therefore, it can be assumed that cortical neurons projecting to the pons maintain their ability to build new synapses during adulthood if provided with a permissive environment. The proof that bouton-like structures of sprouted fibers, as observed by light-microscopy, most certainly correspond to intact synapses, provides morphological support that functional recovery of forelimb movements following pyramidotomy is at least partially due to neuronal plasticity and the establishment of new neuronal circuits (Thallmair et al., 1998; Z'Graggen et al., 1998). These may compensate for some of the functions of the injured corticospinal tract. The exact physiological role of the discussed bilateral innervation following injury and treatment with IN-1 remains to be elucidated. Presumably, the new projections serve to balance and integrate motor and sensory signals in the cerebellum as a part of the cortico-ponto-cerebellar-thalamo-cortical feedback loop.

As discussed in the introduction, not only the presence of a permissive environment but also the expression of certain molecules is necessary for axon outgrowth (Plunet et al., 2002). Axonal growth responses can be induced by treatment with IN-1 but also by certain types of axonal injury (Neumann and Woolf, 1999; Buffo et al., 2000; Bareyre et al., 2002). Neurons in the central nervous system are in general embedded in an intricate structural network that makes it difficult to investigate cell body responses to axotomy of a specific population of neurons. Because of the relatively low complexity of the dorsal root ganglia (DRG), we investigate the cell body response to axotomy in DRG neurons. Additionally, this system enables us to examine differences in the cell body response following injury to centrally versus peripherally projecting neuronal processes. Using microarrays, we find that the expression of more than 100 genes is either up- or down-regulated during developmental stages when axonal growth occurs in comparison to the adult animal. Sciatic nerve transaction as well as dorsal rhizotomy is able to induce profound changes in gene expression in the adult DRG. In both cases the expression of more than 50 genes is regulated, although for many genes, only one of the injury-types is a strong enough stimulus to change the expression. Surprisingly, we find for only about one third of the regulated genes following peripheral axotomy a recapitulation of the developmental expression pattern. The hypothesis that a developmental gene expression profile is needed for successful regenerative axonal growth does not seem to be adequate. Although, among the genes that recapitulate a developmental profile, some may be crucial for the ability to regenerate. Further, we describe a common theme of injury-induced regulation. If a peripheral and a central axotomy are evoking the

regulation of a given gene, the direction of the regulation is for both injury paradigms the same. This finding gives a hint that the direct injury-related cell body response may obey more general rules than widely believed. It may, therefore, reflect different environmental influences between the peripheral and central nervous system on the neuronal cell body response. Intrinsic differences between the central and peripheral axon of DRG neurons in propagating the signal that an injury has occurred to the cell body, may also play an important role. The gene expression profile can give first ideas about the functional properties of a neuron in terms of physiological processing or induced adaptive changes.

The differential expression of glypican-1, a major heparan sulphate proteoglycan, turns out to be special in two way (for review see (Bandtlow and Zimmermann, 2000)). First, the mRNA expression of glypican-1 is high during development and induced by injury to the central as well as the peripheral branch of DRG neurons, a feature that is only shared by a few genes expressed in the DRG. In addition, we show that the initial cell body response following peripheral injury can still be intensified by a subsequent central injury. Therefore, it seems controversial whether there is a maximal cell body response following injury as it was postulated for peripheral axotomy. Second, in uninjured adult DRG neurons, glypican-1 protein is mainly localized to the nucleus. Following peripheral nerve injury, glypican-1 is distributed to the cell membrane, a change that is also seen following central injury. From these experiments we conclude that axotomy can affect, in addition to transcriptional changes, the subcellular protein localization of regulated genes. With the re-innervation of peripheral targets, glypican-1 expression is normalized. We present for the first time a detailed histological description of the mRNA expression of the slit family of repulsive guidance molecules and their receptor family, the robos, in the adult DRG and we provide evidence that glypican-1 may act as a co-receptor for the slit family or repulsive guidance molecules in uninjured as well as injured DRG neurons, since glypican-1 is co-expressed with robo-2.

Here we report the appearance of peripheral benzodiazepine receptor (PBR) mRNA following sciatic nerve transection with a concomitant increase in PBR protein from essentially undetectable levels in non-injured DRG neurons to presence in a defined subgroup of small-caliber neurons. These finding underline another aspect of injury-induced regulation. Although axons of small-, medium- and large-diameter neurons are injured, the cell body response varies between subsets of neurons. It seems likely that the differential responses of neuronal subgroups depend on intrinsic properties of a given neuron, rather than on

environmental factors. The presence of PBR protein in a conformation that is able to bind a pharmacological ligand is demonstrated in the DRG and the dorsal horn of the spinal cord following injury. These results suggest that axotomy can change the responsiveness of a given neuron to environmental factors as shown here by the induction of a previously absent receptive molecule.

In summary, this work shows that we can elicit adaptive axonal growth and the formation of new synapses in the injured adult central nervous system by counteracting Nogo-A, a major inhibitor of axonal growth. Axotomy evokes a cell body response that is to some degree dependent on environmental factors and on intrinsic properties of a given neuron itself. Injury-induced changes involve the widespread regulation of transcription, steps of post-translational modification as well as protein localization in the cell body and protein transport along the axon.

Many questions regarding the control of axonal growth remain to be asked and answered. IN-1 induced plasticity of the cortico- and rubrospinal system has been studied extensively and has been correlated to functional recovery of the forelimb (for review see (Schwab, 2002)). Less is known about plastic changes in the spinal cord induced or enhanced by IN-1 (Bareyre et al., 2002). Histological and behavioral analysis of ascending sensory fiber tracts after treatment with anti-Nogo-A antibodies is one crucial topic that we are currently working on. New antibodies recognizing specific sequences of Nogo-A are currently tested together with a method of spinal intrathecal drug delivery by miniosmotic pumps. We ask whether anti-Nogo-A treatment following spinal cord injury alters segmental termination patterns of primary sensory afferents, a process that may affect proprioceptive and nociceptive processing in the spinal cord and may account for severe maladaptive changes, such as neuropathic pain and spasticity (for reviews see (Pearson, 2000; Edgerton et al., 2004; Woolf, 2004)). This aspect is especially important regarding possible clinical application of anti-Nogo-A antibodies. Special tracing techniques including transganglionically transported molecules and a pseudorabies virus based transsynaptic tracing method may be used to describe adaptive changes in local spinal networks. The molecular mechanisms that control regenerative axonal growth are under intense investigation. Recently, a neuronal receptor for Nogo-A and some proteins involved in the downstream signaling cascade have been found. It is not clear yet, to which extent the same molecules are involved in structural plasticity. Gene regulation following treatment with IN-1 in the intact or pyramidotomized animal revealed some genes with

potential functions in axonal growth and guidance, e.g. BDNF, semaphorins, slits, STATs (Bareyre et al., 2002). Further analysis using a proteomics approach may provide additional relevant information. Based on the results of our gene chip experiments, selected genes can be studied to determine their functional role in regenerative axonal growth. One approach is to use a genetically modified viral vector with a tropism for primary sensory neurons to over-express the gene of interest in situations of neural injury (Seijffers and Woolf, 2004). In order to extend our knowledge about neuronal responses to injury, newly developed techniques such as single cell micro-dissection may be used to investigate the cell body response of subpopulations of neurons that truly lie within the central nervous system, e.g. pyramidal cells in the motor cortex.

Recently mAb IN-1 was tested in a rat stroke model. Its application after an ischemic lesion in adult rats induced strong improvements in a food pellet reaching task that tests fine hand movements, and established new cortico-fugal projections from the uninjured, opposite hemisphere. Unpublished results even demonstrated a positive effect on functional recovery after stroke if the antibody was applied with a delay of seven days following the injury (G.L. Kartje and M.E. Schwab). Preliminary results obtained from experiments with a humanized anti-Nogo-A antibody following unilateral cervical spinal cord injury in adult monkeys, revealed improved recovery of hand function (T. Wannier, E.M. Rouiller and M.E. Schwab). The present data about the action of anti-Nogo-A antibodies are very encouraging in terms of a potential clinical application in humans, primarily following spinal cord injury, with the possibility of subsequent application in stroke. Currently, preparations are under way in collaboration with Novartis and a group of clinical spinal cord injury centers for first toxicological studies in animal models and subsequently in humans.

References

- Bandtlow CE, Zimmermann DR (2000) Proteoglycans in the developing brain: new conceptual insights for old proteins. *Physiol Rev* 80:1267-1290.
- Bareyre FM, Haudenschield B, Schwab ME (2002) Long-lasting sprouting and gene expression changes induced by the monoclonal antibody IN-1 in the adult spinal cord. *J Neurosci* 22:7097-7110.
- Buffo A, Zagrebelsky M, Huber AB, Skerra A, Schwab ME, Strata P, Rossi F (2000) Application of neutralizing antibodies against NI-35/250 myelin-associated neurite growth inhibitory proteins to the adult rat cerebellum induces sprouting of uninjured purkinje cell axons. *J Neurosci* 20:2275-2286.
- Edgerton VR, Tillakaratne NJ, Bigbee AJ, de Leon RD, Roy RR (2004) Plasticity of the spinal neural circuitry after injury. *Annu Rev Neurosci* 27:145-167.
- Fouad K, Pearson K (2004) Restoring walking after spinal cord injury. *Prog Neurobiol* 73:107-126.
- Neumann S, Woolf CJ (1999) Regeneration of dorsal column fibers into and beyond the lesion site following adult spinal cord injury. *Neuron* 23:83-91.
- Pearson KG (2000) Neural adaptation in the generation of rhythmic behavior. *Annu Rev Physiol* 62:723-753.
- Plunet W, Kwon BK, Tetzlaff W (2002) Promoting axonal regeneration in the central nervous system by enhancing the cell body response to axotomy. *J Neurosci Res* 68:1-6.
- Raineteau O, Schwab ME (2001) Plasticity of motor systems after incomplete spinal cord injury. *Nat Rev Neurosci* 2:263-273.
- Schnell L, Schwab ME (1990) Axonal regeneration in the rat spinal cord produced by an antibody against myelin-associated neurite growth inhibitors. *Nature* 343:269-272.
- Schwab ME (2002) Increasing plasticity and functional recovery of the lesioned spinal cord. *Prog Brain Res* 137:351-359.
- Schwab ME, Bartholdi D (1996) Degeneration and regeneration of axons in the lesioned spinal cord. *Physiol Rev* 76:319-370.
- Seijffers R, Woolf CJ (2004) Utilization of an HSV-based amplicon vector encoding the axonal marker hPLAP to follow neurite outgrowth in cultured DRG neurons. *J Neurosci Methods* 132:169-176.

- Thallmair M, Metz GA, Z'Graggen WJ, Raineteau O, Kartje GL, Schwab ME (1998) Neurite growth inhibitors restrict plasticity and functional recovery following corticospinal tract lesions. *Nat Neurosci* 1:124-131.
- Woolf CJ (2004) Pain: moving from symptom control toward mechanism-specific pharmacologic management. *Ann Intern Med* 140:441-451.
- Z'Graggen WJ, Metz GA, Kartje GL, Thallmair M, Schwab ME (1998) Functional recovery and enhanced corticofugal plasticity after unilateral pyramidal tract lesion and blockade of myelin-associated neurite growth inhibitors in adult rats. *J Neurosci* 18:4744-4757.

Curriculum Vitae

Name Stefan Blöchlinger

Home Address Obere Briggerstrasse 24
CH-8406 Winterthur, ZH
Switzerland

Phone ++41 76 388 16 52

E-Mail bloechlinger@hifo.unizh.ch

Place of Citizenship Goldingen SG

Date of Birth 10-27-1976

Education

1983-1989	Primary School	Winterthur, Switzerland
1989-1996	Secondary School (Matura Type B)	Gymnasium Rychenberg, Winterthur, Switzerland
1996-2003	M.D. Program	University of Zürich, Switzerland
2000-present	M.D.-Ph.D. Program	University of Zürich, Switzerland
2003	Medical Diploma	University of Zürich, Switzerland

Academic Appointments

1999-2000 2003-present	Research Fellow	Brain Research Institute, University of Zürich and Department of Biology, Swiss Federal Institute of Technology Zürich
2001-2002	Research Fellow	Neural Plasticity Research Group, Department of Anesthesia & Critical Care, Massachusetts General Hospital & Harvard Medical School

Fellowships

2003	Maurice E. Müller Foundation	M.D.-Ph.D. Fellowship
------	------------------------------	-----------------------

Professional Societies

1999-2001	Medical Student Association, University of Zürich	President
-----------	--	-----------

2004-present	FMH Swiss Medical Association	Member
--------------	-------------------------------	--------

2004-present	Swiss MD-PhD Association	Member
--------------	--------------------------	--------

2004-present	VSAO Verband Schweizerischer Assistenz- und Oberärzte	Member
--------------	--	--------

Publications

Blochlinger, S., Weinmann, O., Schwab, M. E., & Thallmair, M. 2001, "Neuronal plasticity and formation of new synaptic contacts follow pyramidal lesions and neutralization of Nogo-A: a light and electron microscopic study in the pontine nuclei of adult rats", *J.Comp Neurol.*, vol. 433,no. 3, pp. 426-436.

Woolf, C. J. & Bloechlinger, S. 2002, "Neuroscience. It takes more than two to Nogo", *Science*, vol. 297,no. 5584, pp. 1132-1134.

Bloechlinger, S., Karchewski, L., Woolf, C.J. 2004, „Dynamic changes in glypican-1 expression in dorsal root ganglion neurons after peripheral and central axonal injury", *Eur J Neurosci.*, 2004 Mar;19(5):1119-32.

Karchewski, L., Bloechlinger, S., Woolf, C.J. 2004, „Axonal injury-dependent induction of the peripheral benzodiazepine receptor in small-diameter adult rat primary sensory neurons", *Eur J Neurosci.*, 2004 Aug; 20(3):617-83.

Dodd, D.A., Niederoest, B., Bloechlinger, S, Dupuis, L., Loeffler, J.-P. & Schwab, M.E. 2004, "Nogo-A, -B and -C are found on the cell surface and interact together in many different cell types", submitted in October 2004

Published abstracts

Bloechlinger, S., Karchewski, L. A., Samad, T. A., Griffin, R. S., Costigan, M., Befort, K., Fitzgerald, M., & Woolf, C. J., "An Expression Profile Analysis Using cDNA-Microarrays of Regeneration-Associated Genes.", presented at the Society for Neuroscience Annual Meeting, 2001

Ji, R. R., Bloechlinger, S. & Woolf, C. J., "Activation of MAP kinases after a spinal cord injury lesion", presented at the Society for Neuroscience Annual Meeting, 2002

Acknowledgments

My very special thanks go to Martin Schwab, for introducing me to the fascinating field of neurosciences, for being an excellent and patient supervisor during the preparation of this thesis. He was always ready to discuss ideas, and more than once he helped me focusing my thoughts on the essential aspect of a problem.

I want to thank Clifford Woolf, who gave me the unique possibility to join his lab and to experience the extraordinary environment at Harvard University and MGH. I appreciate his scientific and personal support very much.

Laurie Karchewski, thank you so much for sharing your thoughts, your theories and a lot of your time with me.

When I first started working at the Hifo, Michaela Thallmair was a wonderful supervisor and became a good friend. I want to thank her for the personal conversations and all the inspiring discussions. It was such a pleasure that we both came back to the Hifo in 2003.

In 2003 when Simone Bosshard joined the lab to do her diploma thesis under my supervision, a fruitful collaboration started. I want to thank her very much for putting so much effort in our experiments and for her enthusiasm.

Special thanks go to Irin Maier. The last year in Zürich would not have been half as interesting and entertaining if she had not been there.

Many thanks go to Lisa Schnell, Dana Dodd, Jeanette Scholl, Regula Schneider, Oli Weinmann, Silvia Kaufmann and Roland Schoeb for their help with all sorts of technical and other issues.

I thank Peter Sonderegger at the Institute of Biochemistry who volunteered to be my tutor.

For financial support in 2004 I would like to thank the Maurice E. Müller Foundation.

I am especially thankful to Olivia Jeleff for constantly letting me feel her love and strength, for her encouragement and for being patient with me.

Without the continuous support from my parents, Armin and Trudi Blöchliger, I would have never succeeded. They taught me that natural sciences and humanities evolve hand in hand. I am very grateful to them.